The Pennsylvania State University

The Graduate School

FLEXIBLE, DATA-DRIVEN PARAMETRIC DESIGN FOR BUILDING FAÇADES

A Dissertation in

Architectural Engineering

by

Laura Hinkle

Submitted in Partial Fulfillment
of the Requirements
for the Degree of

Doctor of Philosophy

August 2024

The dissertation of Laura Hinkle was reviewed and approved by the following:

Nathan Brown
Assistant Professor of Architectural Engineering
Co-Dissertation Advisor
Co-Chair of Committee

Julian Wang
Associate Professor of Architectural Engineering
Co-Dissertation Advisor
Co-Chair of Committee

Gregory Pavlak
Assistant Professor of Architectural Engineering

James Wang
Distinguished Professor of Information Sciences and Technology

James Freihaut
Professor of Architectural Engineering
Interim Head of the Department

ABSTRACT

Building façades are an important aspect of the building envelope, regulating the light, heat, and ventilation exchange from the outdoors to the indoor environment. A well-designed façade minimizes operational energy while also achieving ideal daylighting conditions and allowing for ventilation. Maintaining this balance is a challenging design task. With growing computational resources, it is now possible to simulate these behaviors and develop robust workflows to estimate the performance of building façades. However, these methods are not widespread due to the manual effort required to establish the building model, which is parametric in nature, and the challenge of analyzing data while exploring design decisions. Additionally, there is a new category of façade solutions that are dynamic, adding more complexity to the design task.

This dissertation first proposes and demonstrates two new early design methods that improve upon the accessibility and flexibility of surrogate model-based workflows. The latter half of this dissertation focuses on optimizing dynamic façades, specifically in the glazing category, in order to begin to integrate dynamic façades with traditional early design decisions. The first study addresses the issue of accessibility by proposing a new tree-based surrogate model workflow that filters a large generalizable design space, making it reusable. Three early design spaces were constructed, and using this workflow, the large pre-computed dataset can be filtered to provide specific variable importance and performance estimates across early design changes and multiple projects.

The second study demonstrates a second workflow that, instead of filtering down a generalizable design space, allows for the addition of new design variables to a custom parametric model and corresponding surrogate model with fewer simulations. It accomplishes this through the application of a tabular transfer learning approach paired with random walks

sampling. Through a building façade case study, it is shown that applying this workflow can significantly reduce the number of samples required to achieve sufficient surrogate model performance compared to classical machine learning approaches. This approach reduces the time between applying early design changes, improving the flexibility of surrogate model-based workflows. However, considering dynamic façade elements in the early design process would improve flexibility further and introduce more creative, sustainable design solutions, which are the focus of the second half of this dissertation.

The third study shifts to fundamental questions regarding dynamic façade performance, specifically in dynamic glazing. In this work, parametric energy simulations were conducted to determine the optimal dynamic glazing properties across multiple climates. This allowed for the determination of the ideal relationship between these properties, intended to guide future product development. It also identifies the ideal transition temperature for such technology and offers guidance on decoupling strategies for each climate zone.

Finally, the fourth study begins to integrate traditional early design decisions considered in the first two studies with those from the third study. A series of constrained optimization runs were conducted to demonstrate the consequences of traditional sequential early design process that considers building geometry somewhat independently of façade materials. In the unique scenario of dynamic glazing applications, it is beneficial to consider dynamic glazing variables in the early stages since they are sensitive to orientation, self-shading, and radiant heat exchange with respect to building form. This work paves the way for a fully integrated design workflow that accounts for both static and dynamic design decisions, generating more innovative façade options necessary to meet current and future sustainability goals.

TABLE OF CONTENTS

LIST OF FIGURES

LIST OF TABLES

ACKNOWLEDGEMENTS

This work would not have been possible without the guidance and support of my co-advisors, Dr. Nathan Brown and Dr. Julian Wang. I sincerely appreciate the countless hours they invested in training me. I have significantly grown as both a researcher and a person under their supervision. I am also grateful to my committee members, Dr. Gregory Pavlak and Dr. James Wang, for their continual feedback and expertise, which strengthened my research. Thanks are also due to GAAN and NSF for their funding support, which allowed me to continuously pursue this work. The findings and conclusions do not necessarily reflect the view of the funding agency.

I would like to acknowledge my labmates in the Building Design Group and ArchiLambda for providing feedback at crucial points. I equally appreciate the many laughs shared and friendships built. I would also like to thank my parents and siblings for their encouragement and understanding throughout my PhD experience. I realize many sacrifices were made for me to achieve my goals. Lastly, to my fiancé, Mahdi, for believing in me and teaching me to believe in myself. I couldn't have done it without you.

Chapter 1

Introduction

Motivation

Historically, building façades regulate light, heat, and ventilation, and also influence the visual impression of the building. While these are still the primary considerations when designing a building façade today, there are more advanced design solutions that are available in response to the need to reduce operational energy. Because building façades facilitate the light, heat, and ventilation exchange from the outdoor environment to indoors, they affect the operational energy, specifically the electricity usage from the heating, cooling, and fans (HVAC system) and lighting system, which are a substantial portion of total operational energy. These systems are necessary to meet the demands of modern work and residential environments and to ensure occupant comfort. This is an urgent issue as the building sector accounted for about 38% of US energy consumption in 2022 [6], and the building façade has a significant impact on the total operational energy of a building [7].

However, it has been demonstrated that it is possible to reduce the operational energy by optimizing the 'static' and 'dynamic' façade design elements and accounting for their interaction with the controls of the HVAC and lighting systems. The static design elements include such aspects as the window-to-wall ratio and window orientation, which should be considered in the early stages when the design is most flexible [8]. Meanwhile, the dynamic design elements include decisions like shading devices and changeable materials. The ability of designers to engage with both of these decision categories has been enhanced through the availability of computational power, which will be extensively explored in this dissertation.

Increased computational power has led to the integration of simulation software into building design workflows. It has allowed for not only the evaluation of different design configurations, but also the ability to explore the effects of design variables and balance performance objectives with other design criteria [9]. There are many approaches that range from design catalogs [10], [11] to surrogate model-based workflows [12] to formal optimization [13], [14], with varying levels of designer intervention. Surrogate model-based workflows involve generating simulation data and training a statistical or machine learning model to replace the expensive simulation during exploration. This workflow is particularly approachable with available open-source packages, and an example is demonstrated in Figure **1-1**. Regardless, these approaches enable informed, data-driven design decisions for static and dynamic façade design elements, although they are not typically designed at the same stage. However, they require significant computational and manual effort to establish a parametric model and generate data, so they are not yet widely accessible. Furthermore, when adjustments are required, as is often the case in early building design, the process must be repeated, thus making them not very flexible from a designer's perspective.

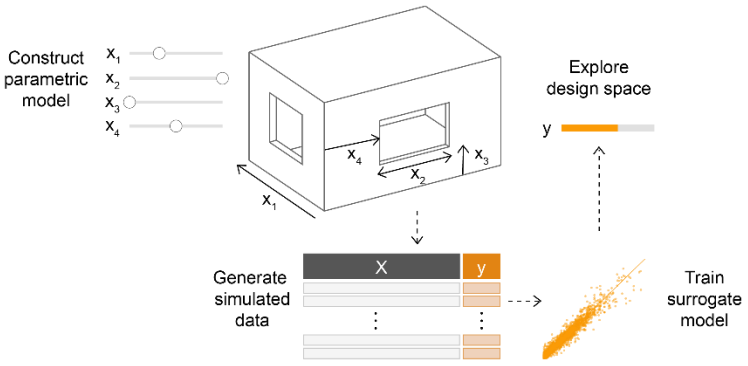

Figure **1-1**: An example of a surrogate model-based workflow.

Within the dynamic façade design element category, increased computational power has also facilitated the development and specification of new façade materials, particularly changeable materials. Changeable façade materials adjust their properties over time due to passive or active control, including opaque materials like dynamic insulation [15], as well as transparent materials such as dynamic windows [16]. Given the prevalence of glazing in modern architecture, this dissertation will focus on the impacts of dynamic windows. Dynamic windows have been demonstrated to reduce operational energy by more than 50% in terms of primary energy [17] depending on the baseline used in the calculation, the orientation, and the climate. However, it is hypothesized that further savings can be achieved by decoupling the solar heat and light properties [18], but these limits have not yet been established. On the specification side, dynamic windows are often implemented after the building façade geometry has been determined, which leaves little flexibility in the specification and tuning of the technology. It is unclear how to best integrate dynamic window considerations into the early design process and how much additional savings could be achieved.

As building electricity usage increases to offset the effects of the climate crisis [19], targeting building façade improvements is crucial to reach sustainability goals within the building sector. The work in this dissertation proposes improvements to the design of ‘static’ and ‘dynamic’ façade elements that balance the performance with practical design criteria. While considering both façade types, it also engages with two different computational methodologies: surrogate-model based design approaches, and automated optimization.

Background

Simulation-driven early stage building façade design

Building façade design requires the integration of experts in mechanical systems and daylighting, in addition to structural engineering and construction, which are beyond the scope of this dissertation. Often, there is a tradeoff between achieving ideal daylighting conditions and energy consumption. Simulation software allows designers to estimate the performance of façade design options and compare them. In collaboration with an architect, the team seeks to identify a design that balances technical objectives such as spatial daylight autonomy and energy use intensity (EUI) with other design criteria [8]. The use of data-driven decision-making can make a significant impact on sustainability goals, particularly in the early stages when the design is most flexible. However, over the past decade, designers have evolved from using simulation software solely to evaluate designs to using it to discover new design directions through parametric design [20]. Rather than manually constructing a few design options and running simulations for them, the model is constructed parametrically, and a sampling technique or optimization algorithm facilitates the generation of a dataset, which can be used to consider many more options than previously achievable.

Parametric design spaces and design space exploration

A performance-based parametric design space consists of at least one variable and one objective [21]. Once the variables and their bounds are determined by the designer, the parametric model is typically constructed in a visual programming environment such as Grasshopper [22]. Parametric models for building façades might include variables related to WWR [23], overall form [24], or shading devices [25]. Then, the design space is sampled through one of many

methods, including traditional sampling methods like grid-sampling and Latin Hypercube sampling (LHS), performance-based sampling [26], or formal optimization procedures where data is generated as a byproduct. Since simulation software is integrated into such environments, simulations are often conducted directly within it to generate a dataset. While this is a powerful workflow for façade design, managing and navigating large datasets in practice can be challenging.

In response, researchers have proposed various design space exploration techniques. The most directed is perhaps an optimization-based approach, although interactive optimization workflows [27] allow for designer interventions. However, optimization-based approaches may not be appropriate for the earliest stages of design. More open-ended approaches include design catalogs [28], performance maps [29], [30], and various performance metrics [31], which equip designers with performance information without pointing to a single solution. The basis for many of these methods is a surrogate model. With the availability of open source statistical and machine learning packages, surrogate model-based workflows are becoming increasingly accessible to designers.

Surrogate model-based workflows

A surrogate model is a statistical or machine learning model that estimates the objective function. Surrogate modeling has been widely implemented in other engineering fields, but it was only recently introduced to the building design domain as a means to reduce reliance on expensive simulations and make inferences [12], [32]. Within a parametric design context, once a parametric dataset is generated, a surrogate model can be trained to estimate the objective, effectively replacing simulation software as the design space is explored. Additionally, many surrogate models provide supplementary metrics like variable importance, enriching the design

process further. Yet, the process of constructing a parametric model, generating data, and training an appropriate surrogate model is time-consuming in practice, and in the earliest stages when the design is still changing, it is likely for some or all of these steps to be repeated.

One approach to alleviate this issue is to construct a series of generalizable parametric models that can be filtered down to apply to many projects and through early design changes [33], [34]. An example of such design spaces might include sidelit room daylighting analysis. Another approach to make surrogate models more flexible is to allow for the addition of new variables to an existing parametric model and corresponding surrogate model without starting from scratch. Both approaches require the application of new methods. The goal is to make surrogate model-based workflows more accessible and flexible for designing sustainable building façades.

Dynamic façades

While the previous sections primarily address static façade design decisions, increased computational power has also affected the development and specification of dynamic façade systems. Dynamic façades are mechanisms that change their properties in response to environmental or indoor conditions, often for the purpose of reducing the HVAC and lighting electricity usage. Although the term ‘dynamic façades’ does include mechanical devices like exterior shading structures [35], this dissertation will specifically focus on material-level dynamic façades designed for windows. Windows were selected as the focus because they are a thermal vulnerability in the façade. Additionally, they are of great interest to architects, especially considering the proliferation of glazed façades in modern architecture.

Dynamic window technologies include both passive technologies like thermochromic glazing [36], which responds to heat from incident radiation, and active technologies such as

electrochromic glazing [16], which transitions based on the applied voltage. Some technologies have been demonstrated to reduce operation energy by 5-57% [17]. However, for many of these technologies, solar and visible light transmission are coupled, and it is likely that decoupling them would yield higher savings in certain climates. Furthermore, technologies that are controlled based on incident solar radiation are highly sensitive to orientation, which is a 'static' design decision typically determined before the implementation of the technology. Since some 'static' decisions affect dynamic glazing performance, integrating dynamic glazing design considerations into the early stages may also lead to greater energy savings.

Optimization of dynamic glazing systems

The optical and thermal behavior of dynamic glazing systems can be studied through a standalone software suite consisting of WINDOW, Optics, and EnergyPlus. The impact on whole building energy usage is calculated through EnergyPlus. Within the EnergyPlus Energy Management System (EMS), different construction states made up of simple glazing materials can be modulated to mimic the behavior of dynamic glazing materials. An EMS program contains a program that incorporates various sensors and actuators. For dynamic glazing programs, the sensors are usually outdoor air temperature, incident radiation, or window surface temperature, depending on the control scheme. The actuators are the window constructions, and the program specifies the construction state switching control logic. Paired with Python or MATLAB programming environments, optimization algorithms can be implemented to determine the optimal configurations. This workflow allows us to test different technologies and control strategies, quantify energy savings, and ultimately inform product development [37].

Yet, since simplified versions have been integrated into visual programming software, as well as daylighting software, these technologies can be simulated for real-world buildings that

feature complex geometries. Many dynamic glazing technologies are affected by orientation, self-shading, and radiant heat exchange in relation to building form. Therefore, rather than following the traditional design process that establishes the geometry and then specifies materials, it may be beneficial for energy savings to consider them simultaneously.

Research objectives and questions

There are two primary objectives in this dissertation. The first objective is to apply statistical and machine learning methods to support the development of surrogate model-based workflows that are more responsive during the early stages of building façade design. This objective will focus on 'static' design decisions and is represented as the left column in Figure **1-2**. To achieve this objective, two pathways are proposed. The first pathway involves filtering down a large generalizable design space, such as a daylit room on a façade, and providing an updated surrogate model with variable importance metrics in real-time. This will enable *accessible* surrogate model-based workflows across different projects. Alternatively, the second pathway allows for the addition of new variables to an existing parametric model and corresponding surrogate model without starting from scratch. The goal of this approach is to improve the *flexibility* of surrogate model-based workflows and account for early design changes. The following questions are proposed:

1. How can a generalizable parametric design spaces be filtered down to provide useful variable information for specific problems?
2. How might we enable flexible surrogate modeling for parametric design spaces to support early building design?

The second objective relates to dynamic façade systems and is to establish the limits of dynamic glazing energy savings potential when integrated into whole building design scenarios.

The objective is shown as the right column in Figure **1-2**. First, we need to understand if uncoupling solar and visible light is necessary to achieve greater energy savings and in which climates. The next need is to demonstrate the consequences of considering dynamic glazing properties at different stages in the design process and their effect on energy savings to develop design recommendations.

3. What is the ideal range of dynamic glazing properties across different climates?
4. Is a traditional, sequential design process appropriate for optimal dynamic glazing performance?

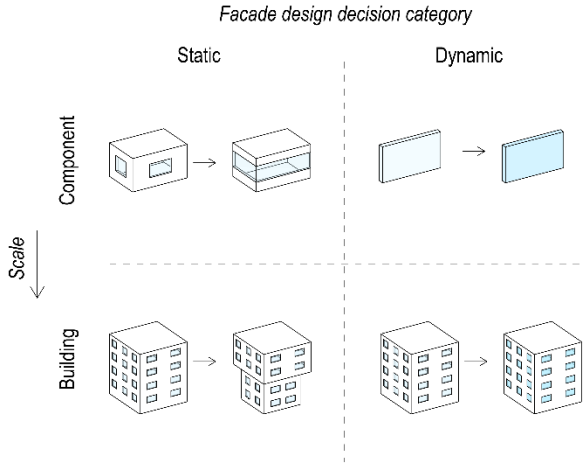

Figure **1-2**: Façade decision categories at different scales.

This research agenda improves upon the façade design process, considering both 'static' and 'dynamic' design decisions.

Organization of dissertation

This dissertation is organized based on the type of design decision, the scale of design task, and the type of technique used (Figure **1-3**). Chapters 1 and 2 consider 'static' façade design elements, beginning with generalizable design spaces at the room scale in Chapter 1, graduating

to custom design spaces at the whole building scale in Chapter 2. Both chapters leverage machine learning techniques to accomplish the research objectives. Chapter 3 begins again at the component scale, optimizing dynamic glazing, and then Chapter 4 uses real-world buildings as case studies to understand the different design decision categories through constrained optimization. Finally, the conclusion summarizes all research contributions and suggests future research directions.

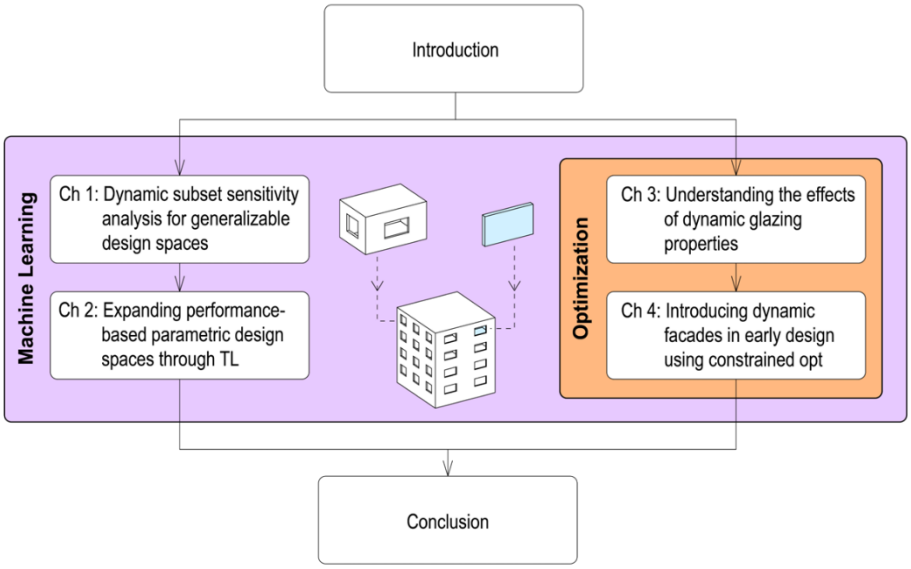

Figure **1-3**: Organization of dissertation topics.

Chapter 2

Dynamic subset sensitivity analysis for generalizable design spaces

This chapter has been published as:

L. E. Hinkle, G. Pavlak, L. Curtis, and N. C. Brown, "Implementing dynamic subset sensitivity analysis for early design datasets," *Automation in Construction*, vol. 158, 2024, doi: 10.1016/j.autcon.2023.105198.

Introduction

With the integration of simulation engines into visual programming environments, parametric modeling techniques can be easily paired with simulation data to provide performance feedback during design. This approach allows designers to quickly evaluate many potential design configurations. In practice, it is not feasible to consider every design in the parametric design space, but several methods have been developed to navigate the design space efficiently. While some methods directly point the designer towards optimal performance, including automated optimization [38]–[40] and interactive optimization [13], [27], [41], [42] workflows, others intend to more gently guide the designer towards better performing designs, offering increased flexibility and opportunities for designer preference expression. Such methods include design catalogs [10], [43], [44], surrogate-model-based workflows that enable live manipulation [32], [34], and performance maps [29]. The latter methods can be most useful in the earliest stages when many aspects of the design are flexible [45], there are competing objectives that need to be synthesized [46], or designers have mixed quantitative and qualitative criteria [47]. In particular, surrogate modeling can be used to facilitate discussions as changes are made [12] and

is accessible with modern statistical tools and libraries. However, building custom parametric models and running simulations to generate data is time-consuming, and further adjustments may be required throughout early design, requiring more effort to update the surrogate model. Design practice moves quickly, and tools get left behind if they do not provide salient information at crucial points when designers really need them. Even with newly available tools, there remains a need for responsive and accessible performance feedback from parametric design spaces.

In this vein, designers might prefer to use a general parametric model to determine which design aspects or variables tend to influence the performance before modifying the design outside a restrictive parametric framework. The general parametric model must contain many variables and configurations but have the ability to be filtered down to provide useful feedback on a specific design problem. As the design space is filtered to reflect project-specific criteria, designers can quickly discover which variables are more likely to improve performance metrics and where "good" settings tend to be for their problem. The process of determining which variables matter is a type of sensitivity analysis. Sensitivity analysis has been used for a range of building design problems, from model calibration [48] to setting up a design optimization problem [49]. While there are many existing sensitivity analysis methods appropriate for building design problems, few are suited for real-time analysis. As the general parametric model is filtered, existing sensitivity analysis methods require re-running the analysis each time, which is disruptive to the design process.

One approach to allow for real-time sensitivity analysis is to split the general parametric model design space into many regional models to be accessed during filtering. Existing regional sensitivity analysis methods have been used to develop useful qualitative feedback but encountered low accuracy in certain regions and lacked intuitive visualizations for designers [31]. Depending on the sampling technique, many regions or subsets may lack data necessary to describe the behavior [50]. For the general parametric model to be truly flexible, it must have the

ability to be filtered on any design criteria and provide sensitivity analysis of sufficient accuracy for early design. With regional models, the designer can gain intuition on how variable behavior changes in each region prior to filtering to inform the initial design. However, a new method is required to provide this information along with real-time subset sensitivity analysis.

In response, this paper extends and rigorously investigates a new method called dynamic subset sensitivity analysis [51]. The method divides a general design space into many models using a decision-tree-like training process and provides real-time variable sensitivity through interpolation techniques. This paper considers the generalizability of the method by applying it to three building design problems of different domains and scales. A comparison of the three datasets shows when the method has enough data to be successful, along which what issues may arise when trying to apply the method to future parametric datasets. By presenting the analyses side-by-side, it also demonstrates how a designer might engage with multiple objectives simultaneously or iteratively as they move between decision variables and scales. Through this work, modifications to algorithm are proposed to communicate variable behavior more accurately in certain regions of the design space, particularly when the response is nonlinear. The value of the method is evaluated for each building design problem. Finally, a set of recommendations are developed to implement the method on future datasets. The goal is to promote adoption of performance-driven parametric tools in early design, leading to more sustainable buildings.

Literature Review

Rapid feedback in early design

Parametric modeling and design space exploration are increasingly used in early design. Researchers have been attempting to improve such design approaches through design catalogs

[43], interactive and automated explorations [13], [52], and visualization techniques [30]. One of the main considerations in the development of these methods is computational time, specifically during active design exploration. General research into computation tasks shows that an interruption of more than 400ms seconds reduces productivity [53]. Building upon this finding, [54] established the roll theory, which states that "when an individual has access to the data necessary to perform the creative task at hand, when concentration is not broken by distractions, and when the individual has developed a consistent method of organizing the data, then ideas and solutions will suggest more ideas and solutions to successive steps of the creative process, in a rapid and orderly flow." Roll theory is related to the concept of creative flow [55], which has been considered while creating tools for rapid design assessment [56]. To achieve this flow, researchers have identified and tested surrogate models that approximate performance during design exploration and reduce lag [57]. Designers can explore the design space and receive rapid feedback, facilitating team discussions [58] and guiding sustainable design decisions.

While non-parametric, black-box surrogate models often achieve the highest accuracy, many researchers have implemented interpretable surrogate models with sufficient accuracy [59], [60]. Localized models such as decision-trees and piecewise models can provide granular variable sensitivity in addition to performance feedback, making them doubly advantageous if they can reach acceptable accuracy. The linear model tree utilized in this paper is an extension of the decision-tree and has been implemented in other domains such as computational fluid mechanics [61], data mining [62], and human computer interaction research [63]. The proposed method leverages the local models yielded from the linear model tree to provide real-time sensitivity analysis in early building design scenarios.

Reusable design spaces

Despite their potential benefits, many recent interactive design methods have not been widely implemented in practice due to practical considerations [64]. Building a model from scratch and running simulations is time-consuming depending on the response variable. Many researchers have shifted focus to understanding *when* and *how* building data and prediction models can be transferred from decision to decision and project to project. The idea of reusable surrogate models for engineering design is introduced in [65]. It proposes graph-based surrogate models for trusses and demonstrates its effectiveness in new design spaces via transfer learning. Several transfer learning approaches have also been proposed for building energy prediction and control [66], [67]. However, these approaches are in the early stages of development and are not yet widely used in industry. Rather than transferring data or models, another approach that is appropriate for early building design is to create a general design space that can be customized or adapted for many design problems [33], [34]. While it takes domain expertise to define a design space that balances specificity with generalizability to many projects, many design firms work repeatedly in certain geographic areas or building sectors, making this possibility feasible [68]. There are also domain-specific ways to reuse machine learning (ML) data for predicting the performance of new designs. For example, by hybridizing data modeling with physics-based modeling and/or using ML to predict the behavior of a single unit that can be aggregated to rapidly predict the performance of a full structure [69]. However, this paper focuses on the use of parametric datasets in early design.

Sensitivity analysis for building design problems

Sensitivity analysis has been widely implemented in building design problems to inform the decision-making process. It has been incorporated into model calibration procedures [48], formulating an optimization problem [49], and decision-making in design or operation [70], [71]. However, it has not yet been applied to generalizable parametric design datasets. Sensitivity analysis allocates the uncertainty in the response among the predictor variables and can be used to gauge variable importance, as well as understand variable interactions [72]. It is particularly useful in the early design stages when the designer is trying to discover which variables tend to influence the response and by how much, whether the question is related to daylight, structures, energy, acoustics, or another response variable. This process can help identify critical decisions, as well as more flexible decisions, from the onset.

There are many established methods available to perform sensitivity analysis, both with and without an accompanying regression model. Most of the widely used standalone methods are one-at-a-time (OAT), which have local and global variations that quantify the effect of each variable individually. OAT sensitivity analysis has been used to address a wide range of building design problems, ranging from improving building life cycle assessment [73] to thermal comfort [74]. Many researchers have also leveraged regression models (or surrogate models) to produce variable importance. Specifically, standardized linear regression model coefficients [75] and variable selection procedures such as stepwise regression [76] have been implemented. The main drawback of linear regression is the linearity condition, which may not be satisfied depending on the data. However, some machine learning models have their own importance metrics, such as decision trees. For example, [77] utilized the decision tree importance metric to identify which variables are most important in predicting building energy consumption patterns. Yet, the output of many machine learning models is not directly interpretable or useful to designers [78]. Finally,

variance-based approaches have also been used to quantify variable importance for building systems [79]. These methods tend to achieve higher accuracy but require a large number of samples.

The methods described above compute variable importance over the entire variable domain. As the design space is refined or filtered during early design, the initial sensitivity analysis may no longer be accurate, so the calculations must be re-run from scratch. One researcher approached this issue by retraining the underlying regression model on the restricted variable domain [80]. However, depending on how the domain was restricted, predictions were not consistently accurate. Another study leveraged Monte Carlo filtering and Regional Sensitivity Analysis (RSA) [31], but also encountered low accuracy in certain regions, and did not use detailed building performance simulation software to generate data, leading to further potential inaccuracies. Nevertheless, filtering is a valuable design space exploration technique as reusable parametric models emerge as a new research area.

Data visualization for design space exploration

Making sensitivity analysis valuable for early design also requires careful consideration of how a user might engage with the data. Building design problems are often high dimensional and thus difficult to visualize. One of the most common methods in building design is parallel and radial coordinate plots [81]. Some researchers have proposed performance maps [29] or self-organizing maps [82], [83] to preserve multivariate information and convey it to designers. Others have argued that reducing the number of variables through principal component analysis or latent space [26] can guide designers towards high-performing designs more quickly. Regardless, the manner in which the results are communicated is equally important as the underlying model [28].

Research gaps and contributions

In summary, to make use of general models in early design, a new method is required that quickly and accurately updates variable importance as the design space is refined and yields results that are easily interpretable. Although dynamic subset sensitivity analysis was initially proposed in [51] on a single dataset, the method has not yet been rigorously tested. There are many data model issues that may arise when feeding in certain datasets, such as discontinuous spaces, collinearity, a lack of significance for certain regions, or even just not having enough data to make a quality assessment of importance. In this paper, we investigate the generalizability of dynamic subset sensitivity analysis by testing it on three datasets from different domains and scales. The three datasets are based on spatial daylight autonomy of a sidelit room, energy use intensity of a residential retrofit, and embodied carbon of a tall timber structure. These design problems were selected because their datasets differ in domain and scale, but also data type, linearity, number of variables, and number of samples. They are also similar in structure to common datasets being implemented in ML-based design tools by leading firms in AEC [68], to the extent that these structures are commonly known. Based on the implementation for these three datasets, we are able to derive a set of recommendations for the method to be implemented on future datasets and propose improvements to the algorithm.

Methodology

The overall procedure is described in Figure **2-1**. First, three general design problems were identified, and corresponding datasets were generated or obtained, and then processed in preparation for training. The linear model trees were then trained, in addition to a simple linear regression model and traditional decision tree model for comparison. Next, the average variable

sensitivity was calculated in small bins to understand where in the variable domain certain variables tended to have a large influence on the response while accounting for other variables in the model. Finally, the dynamic subset sensitivity analysis was demonstrated through a few design scenarios. The quality of the leaf node models was evaluated through coefficient p-values, and modifications to the dynamic subset sensitivity analysis algorithm were implemented. Lastly, a set of recommendations was proposed for applying this method to future datasets.

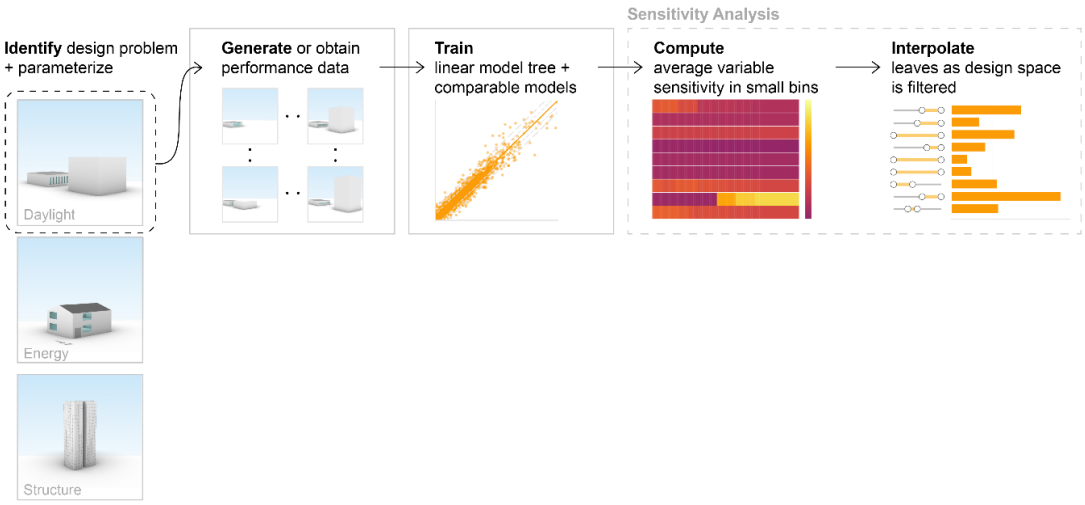

Figure **2-1**: Overall methodology with three datasets.

Problem selection

One of the goals of the proposed method was to customize a large, general dataset throughout the early design stage and across many building projects. To this purpose, three datasets were generated or selected to represent general design problems from the domains of daylighting, energy, and structure (Figure **2-2**).

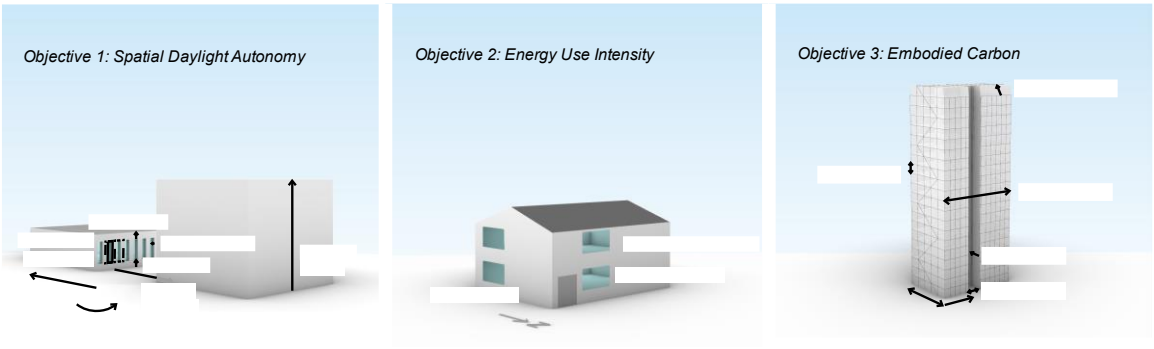

Figure **2-2**: A visualization of the geometry for the daylight, energy, and structure design spaces.

Data generation and processing

Three datasets were generated or obtained from the three design spaces described in the previous section. The following subsections provide details on data generation and processing for each dataset, and a summary of the variables and responses are provided in Table **2-1**.

Table **2-1**: Datasets summary.

Dataset	Variables	Response
Daylight	Room depth, sill height, head height, orientation, context distance, context height, number of panels, panel width, wall thickness	Spatial Daylight Autonomy (%)
Operational energy	Cooling COP, R-value, U-value	Energy Use Intensity (kWh/m^2)
Structures	Building width, building length, story height, setback, notch X position, notch X size, notch Y size	Embodied Carbon (kgCO2)

Daylighting model and dataset

A sidelit room model was developed to represent the domain of daylighting. In building practice in the United States, daylight simulations are often required to obtain LEED v4 Daylight

credits [84]. Therefore, this model could be useful across many spaces and projects. It is assumed that a designer would consult the model repeatedly for a single project as they establish the layout of rooms and the façade. First, the daylit room was modeled parametrically in Grasshopper to include nine variables: room depth, sill height, head height, orientation, context distance, context height, number of panels, panel width, and wall thickness (Figure **2-2**). All room surfaces accord with LM-83 guidelines [85]. The windows were typical double-pane low-e with 61% visible transmittance and incorporated an automated shade. The shade fabric had 7.2% visible transmittance and 6.6% permeability in accordance with LM-83. Room width and room height were 9m and 3m, respectively, although they could be incorporated as variables in the future. The variable bounds are provided in Table **2-2**. They were set to provide enough flexibility for repeated use, but still abide by modern construction standards.

Spatial daylight autonomy (sDA) at 300 lux was the response variable, or "objective" in design space terms, generated using ClimateStudio in Grasshopper. To ensure enough samples for the regression tree, 12,500 points were sampled using Latin Hypercube sampling. The simulations were conducted in Pittsburgh, PA, USA, which is often overcast and at a 40.44° N latitude. For future datasets, sky condition and latitude could be included to make the design space more flexible, but these parameters were set to demonstrate the method. While designers might in different cases design to the typical, worst-case, or average annual behavior, these assumptions would be applicable when making a reusable dataset for buildings across a given city. The sensors were spaced at 1m and the workplane was positioned 0.762m above floor finish. Within the path-tracing settings, the number of rays emitted for each sensor at each pass was 500. The Radiance parameters considered up to 6 ambient bounces before discarding a ray. The dataset was split 80/20 for training and testing, and all predictor variables were scaled from 0-1 to ensure importance was not influenced by the variables' scale.

Table **2-2**: Variables in spatial daylight autonomy dataset.

Variable	Minimum	Maximum
Room depth (m)	6.00	15.00
Sill height (m)	0.10	1.10
Head height (m)	0.10	1.10
Orientation (deg from south)	0.00	360.00
Context distance (m)	3.00	15.00
Context height (m)	0.00	15.00
Number of panels	1	20
Panel width (relative)	0.10	0.90
Wall thickness (m)	0.20	1.00

Energy model and dataset

The second dataset was based on a residential energy retrofit scenario. This dataset represents a reusable model for within a city when testing upgrades on similar residential stock. However, the model would have to be customized based on the feasible ranges of variables to consider in each individual case. An EnergyPlus model was constructed to represent a residential home considering upgrades on the cooling COP, exterior wall insulation, and window construction. Specifically, cooling COP, R-value, and U-value were included as variables (Figure **2-2**). The generic home was 331.23 m^2 and assumed to contain a DX cooling coil and an electric heating coil. The settings for each variable are provided in Table **2-3**. U-value was not controlled directly, as it typically varies with other window properties. Instead, 19 window constructions were selected and used to generate data. The U-value and solar heat gain coefficient (SHGC) were extracted during data processing to represent the window constructions in the dataset. However, because U-value and solar heat gain were highly correlated, only U-value was incorporated into the linear model tree to prevent collinearity issues (Figure **2-7**). Previous studies have also shown a correlation between U-value and SHGC among existing window constructions [86], [87]. The R-values were converted to conductivity in the exterior wall material in

EnergyPlus, and the cooling COP was accessed directly in EnergyPlus. All 6,859 permutations were simulated in Altoona, Pennsylvania, USA. The total site energy per conditioned building area was the response. Although grid sampling is not recommended for the proposed method (see limitations section), simulating 19 settings for each variable yielded high-resolution data sufficient for sensitivity analysis. The dataset was split 80/20 for training and testing, and all predictor variables were scaled from 0-1.

Table **2-3**: Variable options for energy dataset.

Variable	Options
Cooling COP	1.2, 1.4, 1.6, 1.8, 2.0, 2.2, 2.4, 2.6, 2.8, 3.0, 3.2, 3.4, 3.6, 3.8 4.0, 4.2, 4.4, 4.6, 4.8
R-value (ft^2-F-h/BTU)	12, 14, 16, 18, 20, 22, 24, 26, 28, 30, 32, 34, 36, 38, 40, 42, 44, 46, 48
U-value (W/m^2-K)	0.785, 0.992, 1.062, 1.265, 1.525, 1.624, 1.704, 1.71, 1.765, 1.772, 2.143, 2.255, 2.556, 2.72, 2.765, 3.122, 3.835, 4.513, 5.894

Structural model and dataset

The third dataset used to demonstrate the proposed method was an embodied carbon dataset initially generated by Hens et al. [88] and used to explore performance prediction for interactive parametric design in Zargar & Brown [89]. The dataset includes a wide variety of geometric configurations for a mass timber building with a post-beam-panel gravity system and a lateral system incorporating linear elements. For each geometry, a custom sizer based on timber design codes sizes each element based on applicable structural loads and fire protection criteria. Embodied carbon coefficients are then used to convert the building elements into carbon emissions equivalent values, assuming no carbon storage. The embodied carbon contributions of the elements are then summed to predict the overall embodied carbon of the entire structural system. Hens et al. [88] and Hens et al. [90] describe the methodology used to generate the

dataset in more detail. In this paper, we incorporated the independent and several partially dependent variables, including building width, building length, story height, setback, notch x position, notch x size, and notch y size into the linear model tree (Figure **2-2**). The response was embodied carbon. Because notch x position, notch x size, notch y size, and setback depend on the more fundamental variables of width and length, the linear correlations were calculated to diagnose collinearity issues before training the linear model tree (Fig. **2-7**). However, all Pearson correlation coefficients were within the acceptable range and thus incorporated into the model. Outliers were eliminated by the interquartile range (IQR) method, which resulted in 940 data points. The variable bounds are provided in Table **2-4**. The dataset was split 80/20 for training and testing, and all predictor variables were scaled from 0-1.

Table **2-4**: Variables in embodied carbon dataset.

Variable	Minimum	Maximum
Building width (normalized)	0.0005	0.9995
Building length (normalized)	0.0005	0.9995
Story height (m)	3.048	4.876
Setback (relative)	0.005	9.995
Notch X position (relative)	0.0005	0.9995
Notch X size (relative)	0.0005	0.9995
Notch Y size (relative)	0.00045	0.89955

Training the linear model tree

After preparing the datasets, the first step is to create regression trees that can eventually be used for sensitivity analysis and filtering. Figure 3 is a representation of a one-dimensional linear model tree, but a similar procedure follows for high dimensional spaces. The trees are built through recursive binary splitting, where predictor X_j is split at cutpoint s such that splitting the predictor space into the regions $\{X \mid X_j < s\}$ and $\{X \mid X_j \geq s\}$ leads to the greatest reduction in the

residual sum of squares (RSS). Splitting stops based on some threshold and each terminal node, or leaf (Figure **2-3**), contains a model that applies in the j-th region only. For traditional regression trees, the estimated response $\hat{y}_{R_j}$ is the mean response for the training observations in the j-th region. However, this is often an over-simplification of the true relationships. To address this issue, linear model trees use a linear model to estimate the response. By the end of the training process, each leaf node contains its own linear model.

$$RSS = \sum_{j=1}^{J} \sum_{i \in R_j} (y_i - \hat{y}_{R_j})^2 , \quad \text{(Equation 1)}$$

In Equation 1, the outer summation accounts for each variable and the inner summation accounts for all points in the specified region. While previous studies have achieved high accuracy with nonparametric models, it is often not possible to make inferences and inform the building design process. It was hypothesized that linear model trees could achieve sufficient accuracy for early design while allowing for dynamic interpretations about variable sensitivity because of how they are constructed. The correctness of this hypothesis is tested by comparing the results across the varying datasets.

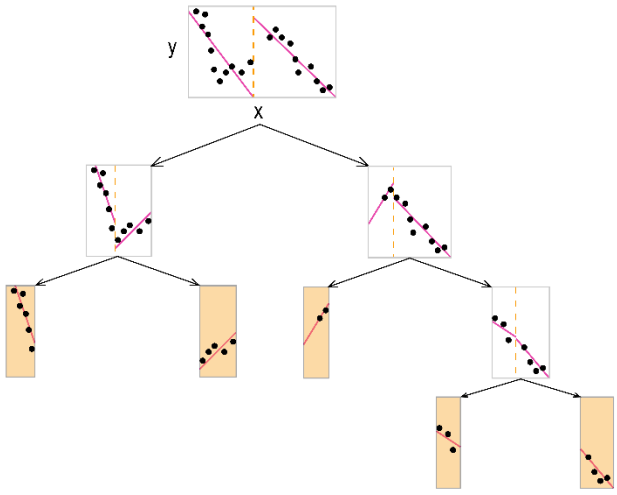

Figure **2-3**: Linear model tree with leaf nodes in orange, after [1].

The termination criteria for a linear model tree are the maximum depth and minimum number of samples per leaf, which have to be tuned for a given dataset. For all models, the maximum depth was set to 8 and minimum number of samples per leaf was set to 30. If there are 30 samples, the distribution is considered normal based on the Central Limit Theorem from statistics. The model achieved sufficient accuracy at this depth and enforcing at least 30 points per leaf ensured the model was valid. The maximum depth of 8 was selected to control training time while ensuring enough leaf nodes for interpolation. Once the linear model tree was built, the leaves were used to compute average sensitivity in small bins.

Calculating average sensitivity over the variable domain in a multi-dimensional design space

The next step is to determine how coefficients of individual leaves should be combined to indicate local variable importance. To get a sense of sensitivity over the entire variables' domain, the average linear model coefficient was computed in small bins. The domain of each variable X_j is partitioned into 100 bins of equal length. The m-th bin is denoted by $b_m \coloneqq \left[\frac{m-1}{100}, \frac{m}{100}\right)$, for $1 \leq m \leq 100$. The k-th leaf is denoted by ℓ_k and the number of samples in ℓ_k is n_k. Then, the domain of each variable X_j is constrained by $c_{j,k} \leq X_{j,k} \leq d_{j,k}$ in leaf ℓ_k. Let $\theta_{j,k}$ be the original coefficient of $X_{j,k}$ in ℓ_k. Then the weighted coefficient restricted to bin $b_{j,m}$ is shown by $\hat{\theta}_{j,k,m}$ and is given by the following formula:

$$\hat{\theta}_{j,k,m} = \theta_{j,k} * \frac{n_k}{n(b_{j,m})} * \mathbb{I}(p - value_{\ j,k} \leq 0.05), \text{ (Equation 2)}$$

where $n(b_{j,m})$ is the number of samples in the leaves that overlap $b_{j,m}$ for X_j and $\mathbb{I}(q) = \begin{cases} 1 \; if \; q \equiv True \\ 0 \; if \; q \equiv False \end{cases}$ which is normally denoted as an indicator function. This dictates that if the hypothesis test that determines if the variable linearly affects the response fails, the coefficient is

forced to zero to prevent inaccuracies in the averaging equations. Additionally, there must be at least one sample per bin. Figure **2-4** is a simple example to show the parts of the weighted coefficient equation.

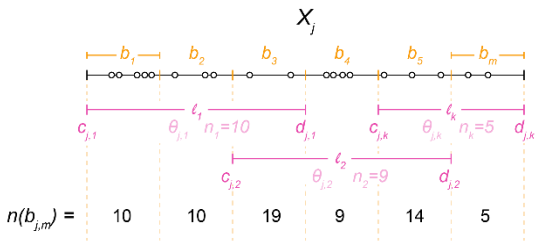

Figure **2-4**: Weighting process in the averaging scheme.

Finally, the weighted coefficient for variable X_j in b_m is given by:

$$\hat{\theta}_{j,m} = \sum_k \hat{\theta}_{j,k,m} \quad \text{(Equation 3)}$$

The result is a local sensitivity analysis over the entire domain that can be used to understand changes in the response. Next, the model leaves are used to update variable importance for user-defined intervals.

Real-time variable sensitivity via leaf model interpretation

While many machine learning methods can return importance metrics, they are often established through training, requiring retraining if the variables and their corresponding bounds are modified. By precomputing linear models in regions determined by the regression tree, the model coefficients can be interpolated to quickly return variable information without full model retraining. If the user-defined intervals correspond exactly to a pre-defined region, variable sensitivity is provided by that model. Otherwise, the model coefficients must be interpolated based on the "agreement" between the user-defined intervals and the variable domains in the leaves. The agreement of the user restricted intervals with the constraints of ℓ_k is given by:

$$\widetilde{w}_k = \left(\sum_{j=1}^{J} w_{k,j}^{\frac{1}{p}}\right)^p, \text{ (Equation 4)}$$

where $w_{k,j}$ is the amount of "agreement" of X_j in ℓ_k and $p > 1$ is a hyperparameter. Let $[a_j, b_j]$ be the user-defined interval on X_j. Then, the amount of agreement $w_{k,j}$ is defined as:

$$w_{k,j} = \frac{\min\{\mathrm{d}_{j,k}, b_j\} - \max\{\mathrm{c}_{j,k}, a_j\}}{b_j - a_j} \text{ (Equation 5)}$$

where a, b, c, and d are non-negative values. Without loss of generality, assume $\widetilde{w}_1, \widetilde{w}_2, \ldots, \widetilde{w}_t$ are the top t agreements. The total weight w_k is a function of top t agreements normalized by their sum:

$$w_k = \frac{\widetilde{w}_k}{\sum_{k=1}^{t} \widetilde{w}_k} \text{ (Equation 6)}$$

Finally, variable importance was computed using the following formula:

$$\widehat{\boldsymbol{\theta}} = \sum_{k=1}^{t} w_k \cdot abs(\boldsymbol{\theta}_k \odot \mathfrak{I}(\boldsymbol{\theta}_k)), \text{ (Equation 7)}$$

where $\boldsymbol{\theta}_k$ is the linear model coefficients at ℓ_k, $abs(\cdot)$ is element-wise absolute value of a vector, $\mathfrak{I}(\cdot)$ is element-wise $\mathbb{I}(\cdot)$ of a vector, and $\odot$ is element-wise multiplication of vectors. The procedure is presented in Algorithm 1. Note that p and t are hyperparameters that can be tuned based on the dataset. For all datasets, p and t were set to 3 and 10, respectively. For higher values of p, the contrast between the top t agreements becomes sharper. As t approaches the total number of leaves, the impact of individual leaves gets lost due to normalization. On the other hand, if $t = 1$, only one leaf is used, which might not be an accurate model of the user-defined region. Once the intervals are specified, individual predictions are made with the linear model tree itself. Single designs only fall into one leaf since the regions do not overlap. The prediction is made by the linear model in the appropriate leaf. Once this model has been established, a metric for overall variable importance and visualizations of how performance changes with variable setting modifications can both be returned to a designer without the added time of model

retraining. The results section first presents the dataset itself before showing these potential visualizations for the designer.

Ensuring model significance

The algorithm mentioned above proposed an improvement to eliminate the possibility of poor linear models in the leaf nodes affecting the interpolation calculations. While this issue did not necessarily arise for the daylight dataset in [91], it is an important consideration, as some building datasets contain highly nonlinear variables that cannot be handled during the training process due to a lack of data. The improvement consists of checking the coefficient p-values in each leaf node linear model, and if the p-value is greater than the desired level of significance (in this paper, 5%), the coefficient is forced to zero in the interpolation calculations (Step 10 in Algorithm 1). If the p-value is low, we can reject the null hypothesis, which is that the coefficient is equal to zero, therefore there is evidence that the coefficient is statistically different than zero. However, if the p-value is high, there is no evidence that the coefficient is different from zero and we cannot reject the null hypothesis. In this case, the coefficient is forced to zero instead of ignored because ignoring it would eliminate information from the region and bias the interpolation towards the other models that may or may not fully cover the region. The pseudocode for the updated interpolation algorithm is provided below in Algorithm 1.

Algorithm 1: Leaf node interpolation

Input: Linear model tree, user-defined intervals, and hyperparameters p and t
For every leaf ℓ_k:
    For every variable j:
        Compute amount of agreement $w_{k,j}$ according to Eqn 5
    Compute agreement $\widetilde{w}_k$ per Eqn 4
Pick top t leaves with the highest agreement $\widetilde{w}_k$. Let these leaves be $\ell_{1'}, \ldots, \ell_{t'}$.
Compute the normalized total weight w_k according to Eqn 6
Initialize updated coefficients $\widehat{\boldsymbol{\theta}}$ by a vector of zeros // dimension is the number of variables
Iterate through all top t leaves (Chosen in Step 5) and do the following:
    Let current leaf have index $k' \in \{1', \cdots, t'\}$
    Update the coefficient in $\widehat{\boldsymbol{\theta}}_{k'}$ by setting all the coefficients that have a *p-value* > 0.05 to zero // this describes $\boldsymbol{\theta}_k \odot \mathfrak{I}(\boldsymbol{\theta}_k)$ in Eqn 7
    Take the absolute value of the updated coefficients and multiply by the total weight w_k
    Replace $\widehat{\boldsymbol{\theta}}$ by $\widehat{\boldsymbol{\theta}} + \widehat{\boldsymbol{\theta}}_{k'}$ // output of Step 11
Return $\widehat{\boldsymbol{\theta}}$

Results

This section first presents linear model tree characteristics for each dataset before the results of the linear model tree interpolation procedures (Table **2-5**). The daylight dataset produced the highest number of leaf nodes, followed by energy and structures. The training criteria enforced 30 samples in each leaf node and maximum depth of 8, but the number of samples per leaf dictated the number of leaves for the energy and structures datasets. For the daylight dataset, the number of panels and wall thickness were split the most, followed by orientation and panel width. Although orientation was split frequently, the results in the following sections show that the slopes were small; therefore, orientation was not important in most regions. Similarly, the cooling COP and R-value were split a comparable number of times, but the cooling COP has large slopes in some regions, and the R-value does not. Finally, building width was split the most for the structures dataset, followed by building length and notch Y size, which largely corresponds with the importance results in the following sections.

Table **2-5**: Linear model tree characteristics.

	Daylight	Energy	Structures
Number of leaf nodes	144	58	18
Number of splits	Number of panels: 32 Wall thickness: 29 Orientation: 26 Panel width: 18 Context height: 13 Room depth: 12 Context distance: 5 Head height: 5 Sill height: 3	U-value: 30 Cooling COP: 14 R-value: 13	Building width: 7 Building length: 3 Notch Y size: 3 Story height: 1 Setback: 1 Notch X position: 1 Notch X size: 1

Figure **2-5** shows a set of designs across the design space to present the range of possible designs for each domain. The daylight design options face south and assume no context building. Notably, the objectives for the daylight and structural design spaces have a visual component, while the energy objective, EUI, does not.

Figure **2-5**: Range of possible design for each dataset.

Assessing model fit

The linear model tree fit was then assessed prior to performing calculations with the leaf node model coefficients to ensure the base model was reliable. For each data point in the testing dataset, the appropriate linear model makes the prediction as determined by the linear model tree. Two parametric models were trained to provide a baseline for model performance: a multiple linear regression model and a decision tree model. Figure **2-6** shows the actual (simulated) response versus the predicted response for each model for the test data. For the spatial daylight autonomy dataset, the multiple linear regression model and decision tree make accurate predictions for low sDA values. However, Figure **2-6** shows that the linear model tree captures some nonlinear behavior in the model and makes accurate predictions, even for higher values of sDA

The linear regression model for EUI predictions mostly falls within +/- 5 kWh/m^2 absolute error, which is sufficient for early building design. However, given the nature of the grid-sampled data, the decision tree predicts the response with even higher accuracy. The linear model tree improves upon the decision tree by fitting a linear model in each region instead of simply averaging the data. This results in a very accurate model with high interpretability. However, the linear regression model does not fit the embodied carbon data as well due to non-linear behaviors in the model and a smaller amount of data overall [88]. While the decision tree model is able to make predictions with about equal accuracy throughout the design space, it is still not accurate enough for early building design. The linear model tree is the most accurate of the three models. It is important to acknowledge that other non-parametric machine learning models such as neural networks could achieve higher accuracy, as in [89], [92] but such models would pose difficulty for interpretation. The information extracted from interpretable models is valuable to the design process and central to this paper.

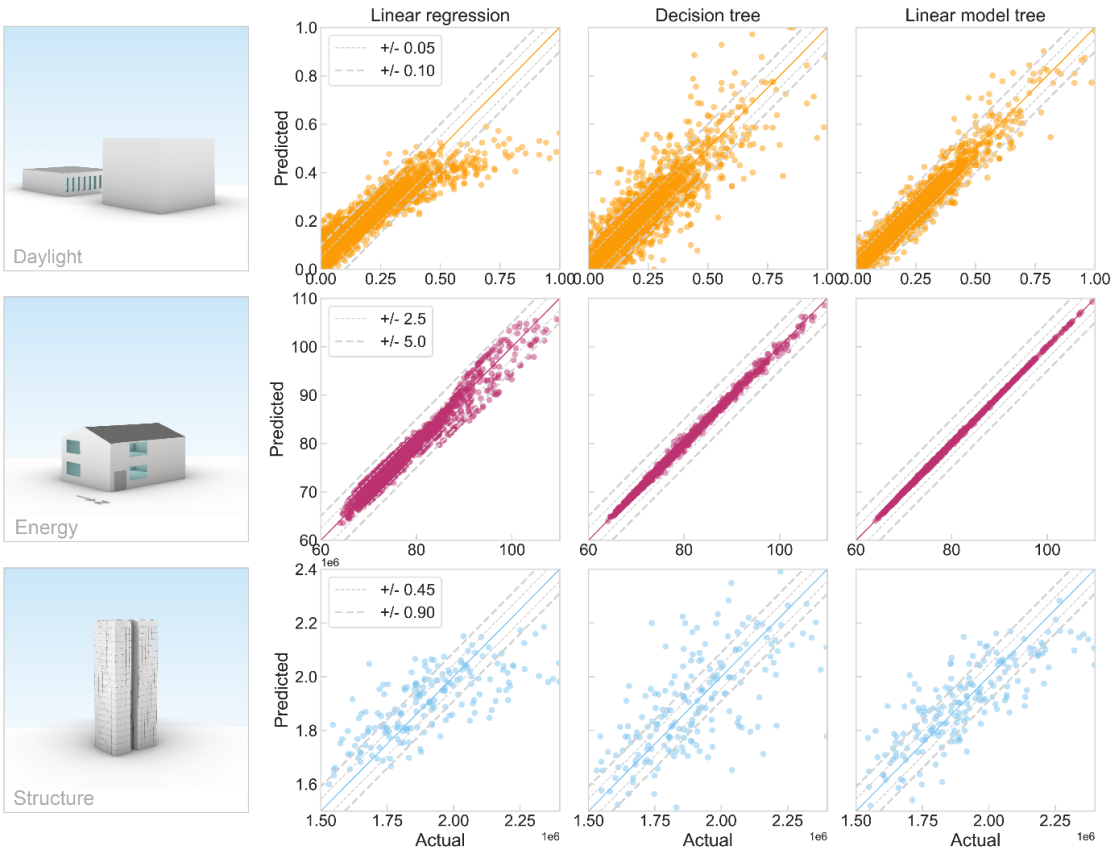

Figure **2-6**: Model fit comparison for spatial daylight autonomy (top), energy use intensity (middle), and embodied carbon (bottom).

In addition to assessing the linear model tree fit, the linear correlations among the variables were checked to ensure collinearity issues are avoided. Figure **2-7** shows correlation coefficients for each dataset, including in at least one instance where a variable was eliminated due to collinearity. While the variables in the spatial daylight autonomy are not highly correlated, the window SHGC and window U-value are highly correlated. As previously mentioned, the U-value was kept in the model over the SHGC because it had a stronger linear relationship to the EUI. Finally, although the embodied carbon variables have minor correlations, the absolute value of the Pearson correlation coefficients all fall below 0.065, which is reasonable for similar

building design problems in the literature [93]. Therefore, the linear regression assumption that all variables are independent is valid.

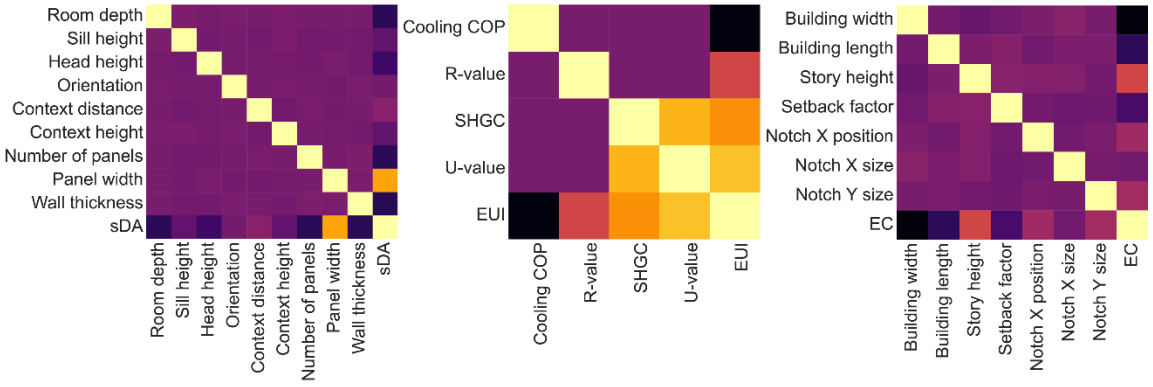

Figure **2-7**: Pearson correlation coefficients for spatial daylight autonomy (left), energy use intensity (middle) and embodied carbon (right).

Sensitivity over the variable domain in a multi-dimensional design space

Once the linear model trees were trained, the average coefficients for each variable were plotted over their domains (Figure **2-8**). This figure shows where the relationship to the response changes, considering all the variables in the model and all possible design directions. Although many of the variables in the spatial daylight autonomy dataset have the same slope throughout, room depth and panel width show noteworthy changes. On average, panel width does not significantly affect sDA until it reaches ~0.5 relative width of the panel. Designers can freely choose within 0.10-0.50 without affecting sDA. Similarly, room depth greatly influences sDA until it reaches about 8.7m; at this point, increasing the room depth does not change sDA. This is potentially useful information while designing floorplans. In order to achieve a high sDA, other variables must be adjusted if the room depth is beyond 8.7m.

For the energy retrofit model, only low values of cooling COP have a strong effect on the EUI. The simulations were conducted in ASHRAE climate Zone 5, which is heating dominated, so increasing the cooling COP beyond ~2.2 does not result in a significantly different EUI given other variables in the model. Adding insulation to the exterior walls (R-value variable) has a consistent though relatively smaller effect on the EUI throughout its domain. Similar to cooling COP, low U-values strongly affect EUI until about 3 W/m^2-K. The EUI includes HVAC, lighting, plug, and miscellaneous loads, and at some point, the HVAC portion is minimized. This explains the diminishing returns of the incremental insulation and COP. The diminishing returns of the incremental insulation and COP. The results in Figure **2-8** only consider the coefficient magnitude, but they follow domain knowledge—installing new windows with a low U-value would improve the EUI in a heating-dominated climate. Furthermore, the results in this section specify at what point increasing the variable has a negligible effect. In future sections, the coefficient sign is considered in order to better describe the relationships. Nevertheless, Figure **2-8** provides a high-level overview of changes in importance to EUI over the variable domain, assuming the other variables are present in the model.

In the embodied carbon dataset, building width is the strongest predictor, especially for very narrow building widths. For very small widths, the lateral system requires extremely large sections to carry the lateral forces from the broad building side, so building width significantly affects overall performance response in this region. Building length is the second-most important predictor; however, the slope is relatively consistent throughout. Among the independent and partially dependent variables considered in [88], building width and building length had the strongest linear relationships (Figure 13 in [88]), which supports the results in this paper. The embodied carbon design space contains more non-linearities than spatial daylight autonomy and EUI, and although the linear model tree can capture non-linear behavior through its piece-wise nature, it is restricted based on the training requirements for the number of data points per leaf

node. Nevertheless, this result provides designers with a set of ranges to design within without significantly affecting the embodied carbon.

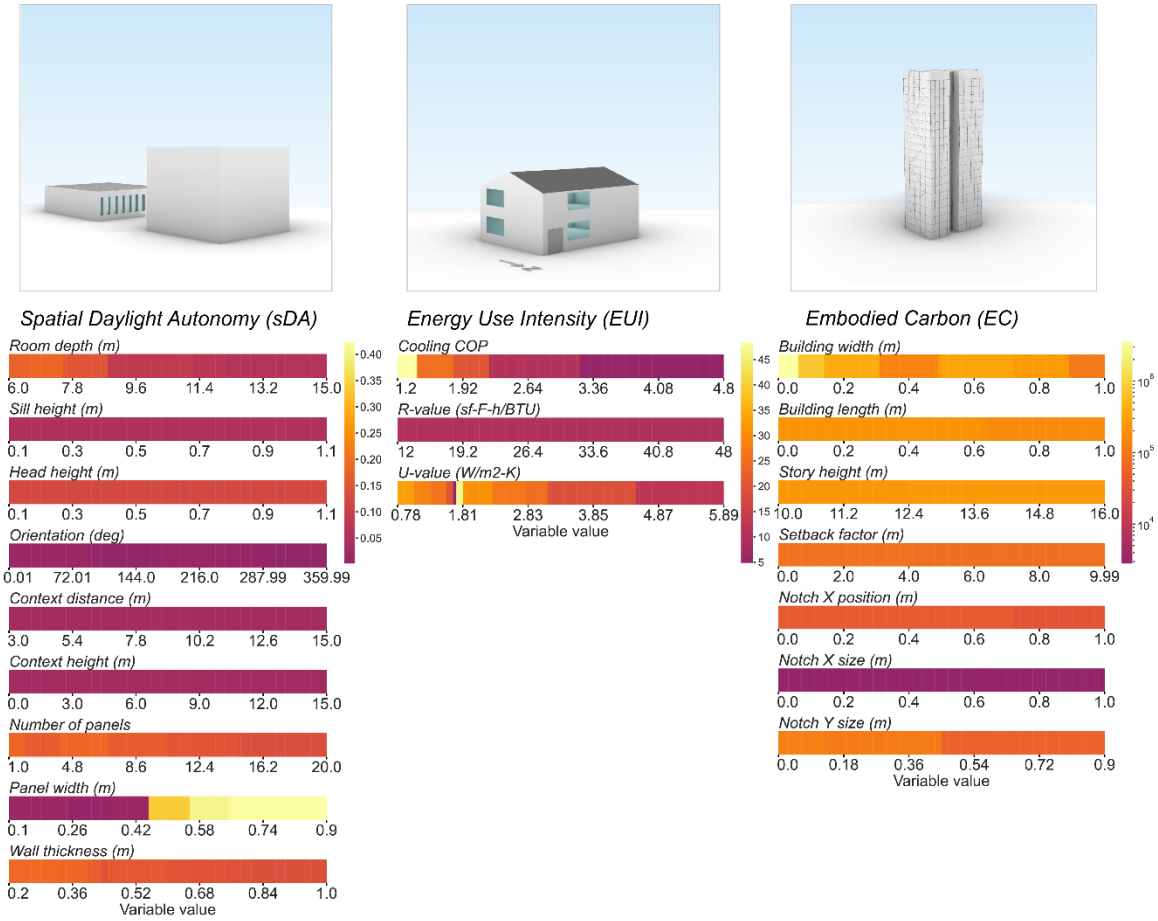

Figure **2-8**: Average sensitivity in small bins for spatial daylight autonomy (left), EUI (middle), and embodied carbon (right).

To understand the relationships on a more granular level, Figure **2-9** shows the raw output of the procedure described in the calculating average sensitivity over the variable domain in a multi-dimensional design space section. The gray line represents the linear model coefficient from the overall linear regression model (shown in Fig. **2-6**) for comparison. While Figure **2-8** shows the absolute value or "importance," Figure **2-9** shows the sign of the coefficient, which indicates the variables' tendency to increase or decrease the response in each bin or region of the

domain. Comparing the two models shows similar but more detailed trends for important variables such as panel width and room depth for daylight and building width for structure. These results can also be interpreted in light of the overall model characteristics. For example, the R-value variable in the energy dataset was split the fewest number of times, so the coefficient was relatively consistent throughout the design space and very similar to the overall linear regression model. The U-value variable shows discontinuous behavior near 2 W/m^2-K because many of window constructions in the dataset had a U-value around this value but differing SHGC and other properties. While the behavior in this region is unstable, it indicates to the designer that there are many potential solutions in this region. This is a result of the real-world, discretely sampled energy variables, as well as the elimination of SHGC due to high correlation.

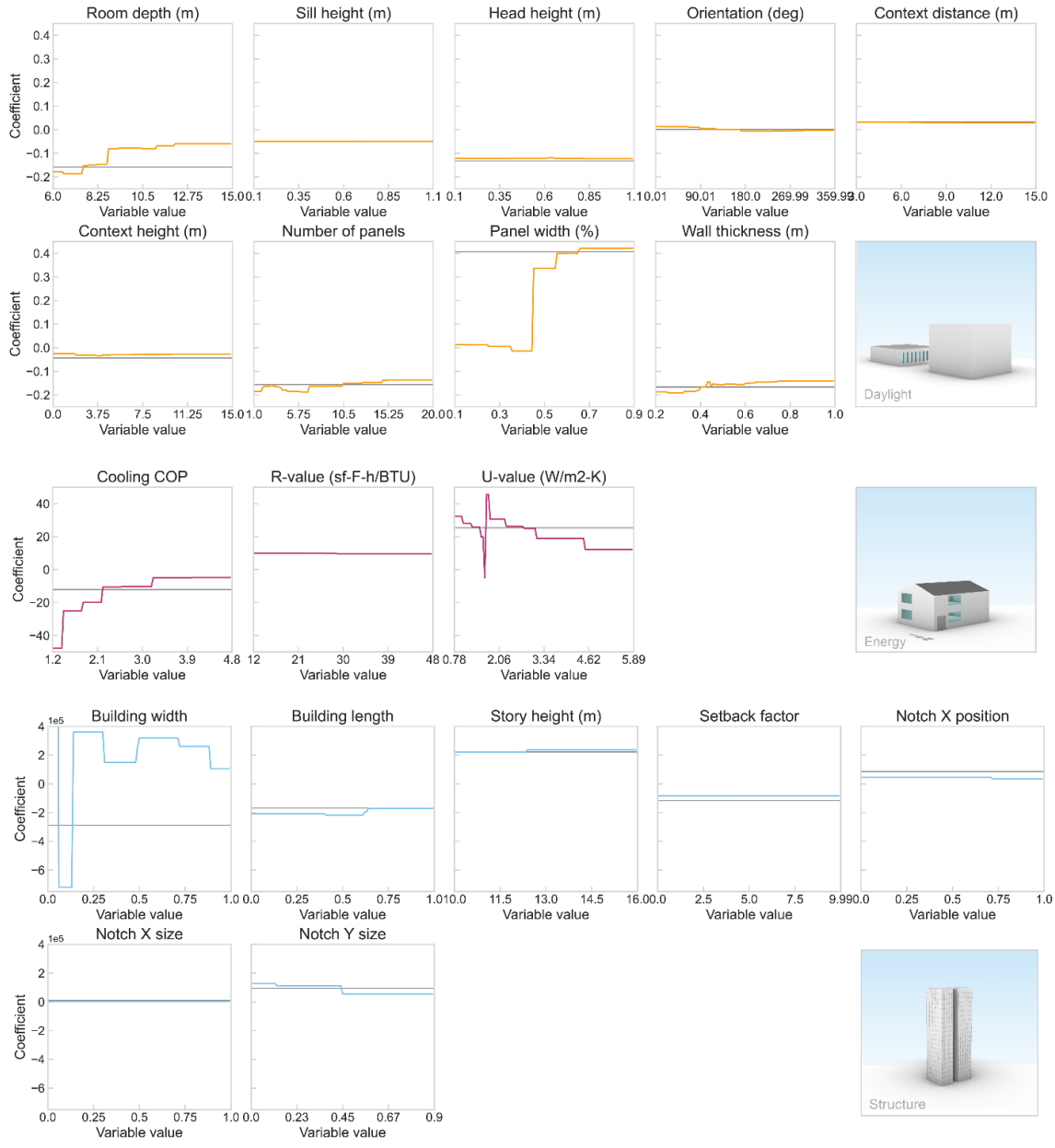

Figure **2-9**: Average coefficient in small bins for spatial daylight autonomy (top), EUI (middle), and embodied carbon (bottom).

These results so far explain how the models were trained, how accurate they are for prediction, and how the linear model coefficients can guide designers on an expected performance response in a certain region of the design space. The following results demonstrate how these models can be aggregated to provide variable importance as designers change the

possible ranges of decisions without full model retraining, since relative importance can change significantly in different regions of the design space.

Dynamic subset sensitivity analysis

Real-time variable importance

Data-driven parametric design often involves setting variable domains, generating data, and fitting a prediction model. As the design is refined, variable domains are narrowed until one value is ultimately selected. Previously, the prediction model needed to be re-trained on the subset of data to provide accurate variable importance and support decisions. We instead achieve subset sensitivity analysis by precomputing linear regression models in regions determined by the tree and then interpolating between regions to estimate the variable importance in the subset. Two examples per design problem are shown in Figure **2-10**, which includes a slider for each variable, the user-defined intervals, and variable importance, presenting a potential visualization for a design tool. It is important to note that a series of visualizations presented to the designer should show both (1) *which* variables deserve attention (by virtue of producing a large effect on performance, regardless of direction) and (2) *how* such variables tend to affect performance along their domains (where the variable makes the performance trend up or down). There is some loss of precision due to the averaging in the simpler graphics, but they are intended for rapid feedback for designers that can be explored in more detail if desired. To give an indication of speed, updating the variable importance from design scenario 1 to design scenario 2 for the daylight design space takes 0.003 seconds on a desktop computer with 32 GB RAM and an Intel Core i7 2.6 GHz processor. The speed also depends on the size of the tree, but this example uses the largest tree among the three datasets. If the method were fully incorporated into an interactive

tool, possibly as a plug-in to parametric design software, the rendering speed would depend on the software and would likely be more substantial than the importance calculation.

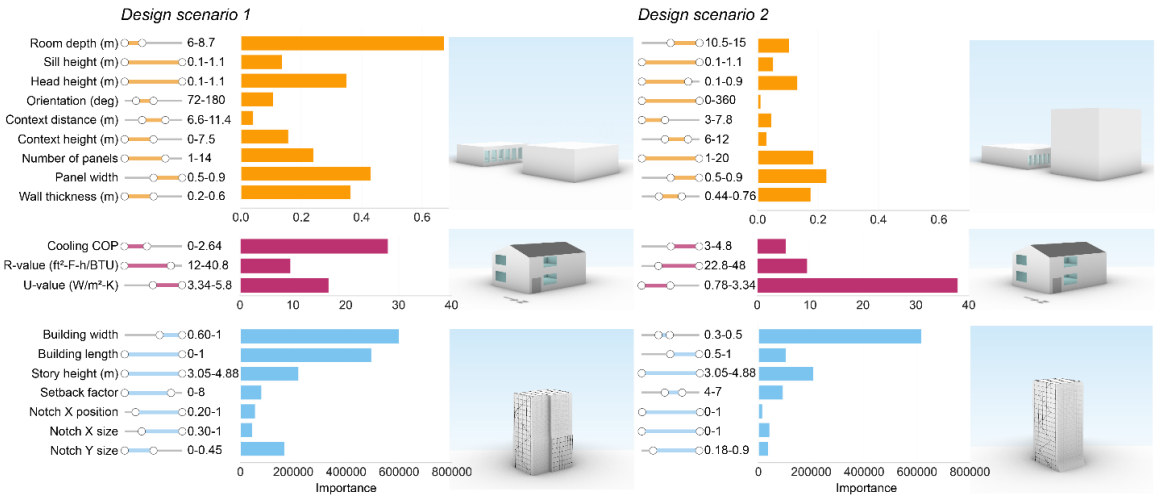

Figure **2-10**: Dynamic subset sensitivity analysis for 2 design scenarios per dataset.

Figure **2-10** shows two sets of design criteria imposed on each design space. Design scenario 1 for spatial daylight autonomy restricts room depth, and thus it is very sensitive in this region. With different restrictions on panel width and number of panels in design scenario 2, room depth is the most important variable. In the second design scenario, with different ranges for room depth, panel width becomes the most important variable. Similar changes are seen in the different design scenarios for energy, as Cooling COP or U-value can become the most important in different regions. In the structure dataset, building width is almost always the most important variable, but in certain scenarios other variables can approach its magnitude of importance to influencing embodied carbon.

Significance in leaf nodes

Although all variables are assigned a coefficient during the linear model fitting step of the linear model tree training procedure, it is possible that some of the variables do not significantly affect the response in certain regions of the design space. To determine if a variable affects the response, a hypothesis test is conducted where the null hypothesis is that the coefficient is equal to zero, which implies that there is no effect. If the p-value is less than 0.05 (5% level of significance), the null hypothesis is rejected and the relationship between the variable and the response is deemed statistically significant. Once the linear model tree was fitted, the coefficients with p-values higher than 0.05 were reset to zero from the calculations described in the methodology. This avoids biasing the results towards coefficients that are not statistically significant.

Figure **2-11** illustrates how consideration of significance affects each model in this paper, as the blurred heatmap cells contain coefficients that were not statistically significant. The blurred heatmap cells have a translucent mask to represent that the coefficient p-value was higher than 0.05. The y-axis is leaf node model index and the x-axis is variables; the color represents the linear model coefficient. It was important to take coefficient p-values into account to eliminate the possibility of a high magnitude coefficient that is not statistically significant greatly influencing the calculations. For example, in the structure dataset leaf node model 30 has a high magnitude coefficient for the width variable, but it is not statistically significant, so it must be excluded to avoid inaccurately representing the behavior in this region of the domain. The coefficients of notch X position, notch X size, and notch Y size were not statistically significant for many leaf node models and were thus ignored. This is consistent with the initial variable assessment in [88], which does not show a clear relationship to embodied carbon throughout the domain. In contrast, the energy dataset variables have a statistically significant relationship to the

response in all regions of the design space. Piece-wise linear relationships were observed in the initial data exploration, and all three variables are well-known retrofit strategies, leading to this expected result. Finally, the daylight dataset shows a mix of significant and non-significant leaf nodes, which seems to be most present for orientation, context distance, and context height.

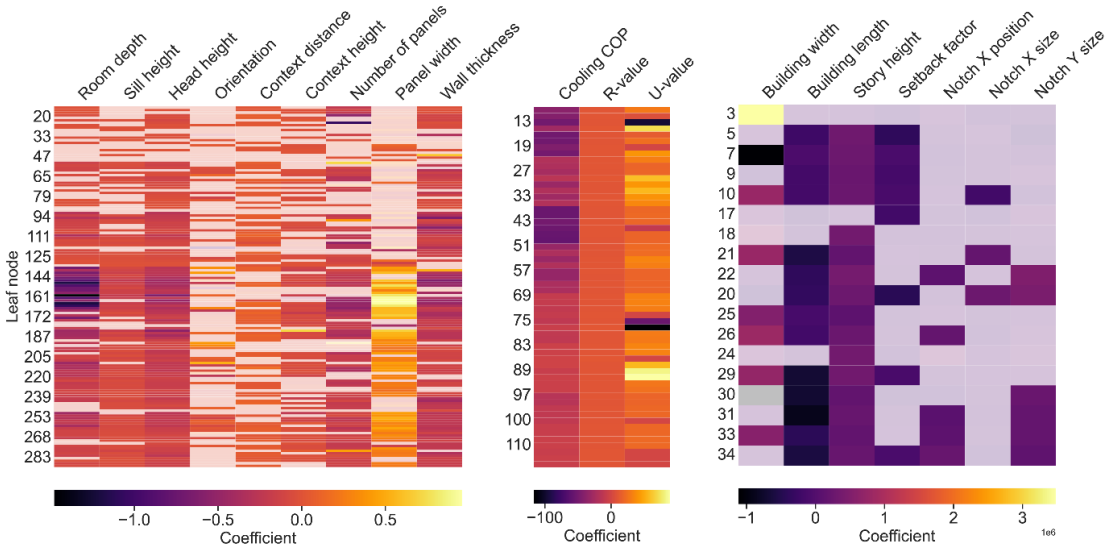

Figure **2-11**: Linear model coefficients for each variable in each leaf node model, with a translucent mask on coefficients that do not have a statistically significant p-value.

Discussion: recommendations for future datasets

Comparing the application of dynamic subset sensitivity analysis to several general datasets in the architectural engineering domain reveals several benefits and potential pitfalls. Resulting discussion points are included as recommendations for what could be changed or customized for use on future datasets:

- **Sampling technique**: Choose as continuous of a sampling technique as possible to ensure sufficient coverage of the design space for interpolation. If a grid-sampling technique was used to generate the data, it is possible that the variables are split at each option during the

training process. At this point, the variables would no longer be treated as variables in the leaf node models. Therefore, if grid-sampling is used to generate the data, it is important to make sure the grid is fine enough. It is recommended to use Latin Hypercube sampling or similar to avoid this problem.

- **P-values in leaf nodes**: It is important to check the variable p-values in the leaf nodes, and if the p-values fall below the desired level of significance, the corresponding coefficient should be forced to zero in order to accurately represent variable importance.
- **Hyperparameters**: The hyperparameters determine the sensitivity of the interpolation calculations. Increasing the power p hyperparameter puts more emphasis on the leaf nodes with a higher agreement. For a design setting, it is recommended to keep the power low to proportionally account for the behavior in the leaf nodes, even those with a lower agreement. When choosing the appropriate number of leaf nodes in the calculations, hyperparameter t, it is important to consider the size of the dataset. The maximum t value is the total number of leaf nodes in the linear model tree, which depends on the size of the dataset and the training requirements.
- **Leaf node model fit**: It is recommended to calculate the R^2 values for the leaf node models and to assign the leaf node models with a low R^2 value a lower weight in the interpolation calculations. These models could also be useful information to the designer, as these regions are highly nonlinear and could not be handled by the linear model tree. The trends or tradeoffs in these regions may differ from the surrounding regions.
- **Traditional decision tree importance metric**: The typical decision tree has an importance metric based on how much the error metric was reduced by each split. However, this only indicates which variables are highly nonlinear, not which variables have the steepest slopes or highest importance. The metrics in this paper were developed to capture this.

- **Normalization among leaf node models:** The coefficients from all the leaf node models could be normalized, but then the method would not provide "how much" the variables matter, just a relative ranking of variable importance.
- **Number of samples**: In order to produce reliable linear models in each node, the algorithm enforces a specified number of data points per leaf node. In this paper, it was assumed the number of data points required per leaf node was 30 data points. The structural dataset contained 7 variables and 940 data points, which resulted in only eighteen leaf node models. During the interpolation process described in the real-time variable sensitivity via leaf model interpretation section, there were only 18 models to consider, versus the spatial daylight autonomy dataset which had 144 leaf node models to consider.

As demonstrated in the assessing model fit section, it is also necessary to reduce collinearity among variables. Collinearity can be assessed by calculating the Pearson correlation coefficients. For example, the energy dataset in this paper had two variables, SHGC and U-Value, that were highly correlated, and it was necessary to eliminate one to prevent model instability issues. Because U-value showed a stronger linear relationship to the response EUI, SHGC was eliminated. Variable selection can be conducted in many other ways including stepwise selection, forward selection, and backward elimination. It is ultimately up to the designer to determine which variables to include in the model.

Conclusion

Summary of contributions

This work presents a method for dynamic subset sensitivity analysis that includes a new procedure for ensuring coefficient significance. It then demonstrates the method's generalizability

on three building design problems. This method updates variable importance in real-time as design criteria emerge, aiding discussion for new design directions. It also determines where in the variables' domain it tends to influence the response, which provides ranges to design within and supports design freedom.

Limitations and future work

Some aspects of this specific approach depend on having linear model coefficients. The model tree could include quadratic or cubic terms in the linear regression models to produce local polynomial models. Additionally, it is possible to implement the model tree with other node model types such as neural networks or SVM. However, linear models were selected in this method to utilize the coefficients to develop importance metrics, as well as to reduce training time. To implement the model tree with other model types, additional importance metrics must be developed, especially for nonparametric models. It is likely the training time would also increase. Another limitation for the daylight and energy datasets is using a single location. In future iterations, latitude and cloud condition could be included as variables to make it more flexible. Finally, it could be argued that the size of the embodied carbon dataset was not large enough for a model tree given the nonlinear nature of many of the variables, compared to energy [94]. However, this example was chosen to demonstrate the method on an existing dataset that was not developed directly for this method. Future general datasets in the domain of structures should be based on a larger dataset.

Concluding remarks

In this work, we investigate a new method called dynamic subset sensitivity analysis across three domains. Many factors on the dataset affect the effectiveness of the method, specifically the sampling technique and the number of samples. Considering the quality of the leaf node models through the coefficient p-value and R^2 improve the reliability of the interpolated variable importance. In the future, this work could be combined with recent work on training design agents to learn generalizable design behavior [95]. If implemented more widely, methods such as dynamic subset sensitivity analysis could track with design practice to make the greatest impact without requiring computation specialists to generate a custom parametric model and simulation data for each project.

This research is supported in part by the National Science Foundation under Grant #2033332. Any opinions, findings, and conclusions or recommendations expressed in this material are those of the authors and do not necessarily reflect the views of the NSF.

Chapter 3

Expanding performance-based parametric design spaces through transfer learning

This chapter is under review for publication in an academic journal.

Introduction

Combining parametric models with simulation software enables designers to generate datasets that can be used to train surrogate models. Surrogate models can then replace the simulations in a design workflow by approximating the objective function, alleviating simulation wait time and facilitating exploration within the parametric design space. These faster models can serve as a valuable tool in collaborative decision-making by offering live performance feedback [32], [33]. However, despite their benefits, surrogate model workflows may unintentionally restrict creativity. This limitation arises from the substantial effort needed to adjust the parametric model and generate new data, potentially leading to premature design fixation [96], [97]. In the early stages of design, where many aspects are still flexible and decisions greatly influence building performance [45], this restriction becomes more apparent. Adding more variables to the initial parametric model complicates the updating of its corresponding surrogate model, necessitating the regeneration of simulated datasets with current tools--essentially starting from scratch. This wastes resources, as the source (initial design space) and target (updated design space) tasks are highly related.

Ideally, the initial dataset could be leveraged to reduce the number of new simulations with both original and new variables required to update the surrogate model. Recent

developments in machine learning have shown instances where a model for a specific task can inform the model of a related task with limited data. This learning approach is known as transfer learning (TL) [98]. However, most existing TL methods are intended for image or text data, rather than the tabular data typical of many design space datasets. Tabular data is highly structured, which makes it more challenging to identify variables and patterns that generalize across tasks. This challenge is particularly pertinent in fields like medicine, where tabular datasets are common, and generating datasets is both difficult and expensive. These datasets often lack consistency, with variations in the inclusion of variables or columns.

To address this limitation in existing TL approaches, a recent paper has introduced a relaxed-table TL method [4]. In our paper, we apply their method in the domain of parametric design to utilize an initial dataset, which only contains a subset of variables present in the updated dataset, to update the surrogate model. While this tabular tokenization-embedding method originated in another field, introducing it within early parametric building design introduces new research questions. In typical transfer learning scenarios, the challenge is that the target dataset is limited, and the objective is to leverage a dataset from the same domain or a similar task from a different domain to improve the model. However, in our case, we generate a target dataset with the knowledge that we already have a similar dataset (the original dataset). Thus, we must test the applicability of the method overall while determining an effective approach to sample from the new design space.

The basic idea is visualized in Fig. **3-1**. Our initial dataset is created with a parametric model of a building façade's geometry, while the updated dataset includes additional variables for geometric flexibility, which might have been implemented by an architect or engineer after exploring the results of the initial model. The surrogate model is used for classification to predict whether designs will be "good", "fine", or "poor" based on simulated Annual Sun Exposure

(ASE). By incorporating the initial dataset through tokenization and embedding, fewer simulations from the updated dataset are required to adequately update the surrogate model.

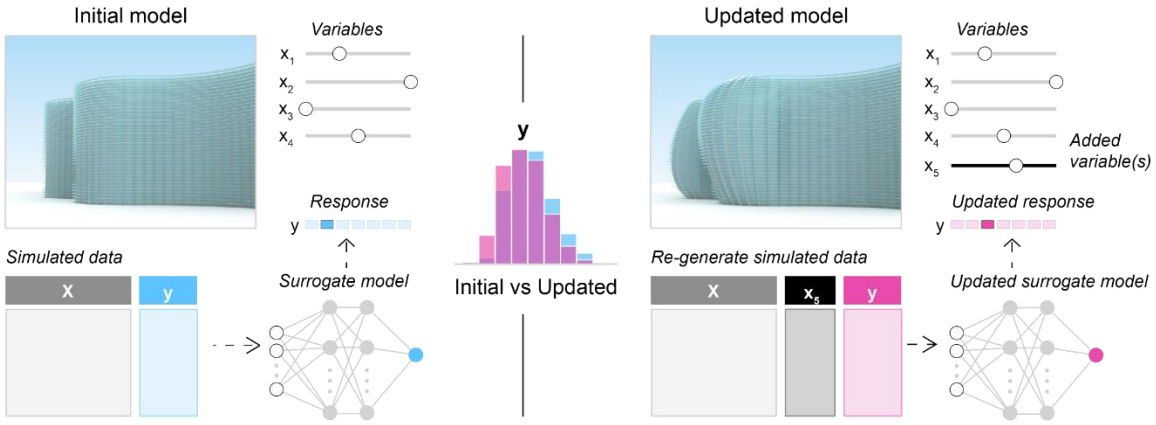

Figure **3-1**: A summary of the performance-driven parametric design scenario.

As we consider the potential benefits of this new TL approach, we compare it to classical machine learning methods for two reasons. First, we acknowledge that the interpretability of some classical methods can be valuable to the design process. Interpretable machine learning methods provide designers with information on variable importance and interactions that can be used to as an initial step in decision-making [99]. Given that the new method reduces interpretability, we also evaluate the performance of classical machine learning methods trained on limited data from the updated design space.

Second, we recognize that the data sampling technique can affect model performance and is of critical importance in situations with very few samples. To try to ensure class representation in the limited dataset from the updated design space, we introduce a random walks sampling technique that efficiently incorporates data from the updated design space and we thoroughly test the hyperparameters, providing valuable guidance for future applications.

Throughout this paper, we thus assess the effectiveness of TL in this specific early design setting paired with a random walk sampling technique and compare it to classical machine

learning models. We use both random walks sampling, which is suited for very small sample sizes, as well as Latin Hypercube sampling, which is more common in the architectural engineering field. The overall goal is to enhance the flexibility and responsiveness of performance-based parametric design in the early design process. While we demonstrate and rigorously test this new workflow on a realistic façade design problem, the method may be of future use to other design scenarios in which surrogate models are built for design exploration with tabular data.

Literature review

Performance-based parametric design

Parametric modeling allows architects and engineers to rapidly investigate design aspects through manipulating variables. With the integration of simulation software in visual programming environments, it is common to evaluate designs with respect to performance objectives, such as daylight [25], [100], [101], visual comfort [102], operational energy [103], [104], thermal comfort [105], [106] and embodied carbon [88], [107]. For example, [25] used a parametric approach to design a solar screen in desert climates, where the variables included the number of louvers, louvers tilt angle, screen depth ratio, and screen reflectivity, and the objectives were spatial daylight autonomy (sDA) and annual sunlight exposure (ASE). In [102], Tabadkani et al. designed an origami-based dynamic façade to improve visual comfort using a parametric design workflow. However, in practice, setting up a parametric model and generating simulations can be time-intensive, even with recent advancements in simulation software. It is not always feasible to run extensive simulations between design iterations. Thus, researchers have developed

approaches to incorporate performance feedback in decision-making, usually involving some computation prior to exploring design options.

Researchers have found it is often useful to sample the design space to generate a representative dataset, through a prescribed method like Latin Hypercube sampling [108] or performance-driven sampling [109], and filter through design options [110]. Yet, in some complex cases, it might be necessary to resort to optimization [111], [112]. Another way to decrease the negative impacts of computation on the design process is to reduce high dimensional spaces through methods such as principal component analysis or canonical correlation analysis [99]. Regardless of how they are created, these methods yield a synthetic dataset that can be used to train a surrogate model, which permits real-time performance estimations [92]. Moreover, surrogate modeling is particularly accessible as open-source machine learning packages have become readily available. However, choosing the best surrogate model depends on many factors, including the nature of the function, size of the dataset, evaluation metric, among others [113].

Surrogate models in building design

Many types of surrogate models have been tested in different building design domains with varying performance and interpretability [12]. Although there is no formal mathematical definition for interpretability [114], [115], a surrogate model is generally considered interpretable if designers understand the reason for the predictions. These models usually provide designers confidence while also providing additional information such as variable importance. In this work, we study a classification task, but regression is also applicable when the objective is continuous. For some design objectives, interpretable surrogate models such as linear regression, logistic regression, Naïve Bayes, or decision trees can achieve sufficient fit and provide designers with some intuition. Esteghamati and Flint compared the performance of 5 surrogate models to predict

multiple objectives related to seismic vulnerability and showed that a linear regression model was sufficient to estimate the seismic-induced embodied carbon emission [116]. However, depending on the nature of the underlying function, a more complex model may be required, including an ensemble method or a neural network. Neural networks are often used to predict building energy [117]. Nevertheless, all of these models are considered classical machine learning methods that require a fixed column table, i.e., all datasets involved have the same variables.

While this workflow is helpful for making performance-driven design decisions, it is not flexible from a designers' perspective. The variables must be defined prior to establishing the design space and exploring it, which inherently limits the number of possible designs. Gero and Maher expressed similar concerns in the infancy of computer-aided design, stating that in routine design, where all decision variables are known a priori, "the designer operates within a defined, closed state space" [118]. They emphasize that "creative design occurs when new design variables are introduced in the process of designing" [118]. Furthermore, not only must the parametric model be programmed in a flexible way, but each time variables are added or adjusted, the simulation data must be re-generated. A new model is needed because classical machine learning methods require all variables (columns) be present for all samples, which is the focus of this paper. This might prevent designers from incorporating new design directions, which can lead to design fixation. This is common in digital design environments as a whole [119]. However, it is likely that for many design problems, the added variables cause only a minor shift in the objective distribution. To address problems like this, TL has recently demonstrated many instances in which a model of a particular task can be leveraged to inform the model of a related task with limited data. The next section will introduce TL, its current applications in building design, and how it could be used to add new variables to an existing surrogate model compared to starting from scratch with classical methods.

Transfer learning and current engineering applications

TL is a class of techniques used to improve the model performance of a task by leveraging the model of a related task. The data-based interpretation of TL approaches in [98] is most relevant for this work. According to [98], there are two main strategies for data-based approaches: instance weighting and feature transformation. Instance weighting assigns different weights to individual samples to emphasize certain samples that are more useful for the target task [120]. Because our application involves overlapping but different feature spaces, we instead focused on strategies in the feature transformation category. The feature transformation category includes feature mapping, feature clustering, feature selection, and feature encoding [98]. Feature encoding has been previously applied to building design applications in the form of autoencoders [121]. The tabular TL method implemented in this work also falls within this category.

Research efforts in TL have been primarily focused on applications in computer vision and natural language processing (NLP). Image data and text data are considered unstructured, and pre-trained models in deep learning can learn general representations that are transferable across tasks [122]. In contrast, tabular data is highly structured, which makes it difficult to select variables and patterns that generalize across tasks. Although several building domains utilize graphs [65] and images [123] to analyze performance, many building datasets are tabular, particularly in practice. Currently there are some tabular approaches that involve training the source neural network and then copying the first n layers to the target network, by either fine-tuning them or freezing them [124]. This has been shown to reduce prediction error in short-term energy prediction applications [124], [125] and HVAC control [66] and annual building energy consumption [126]. However, the TL methods applied in these works require a fixed column table.

Outside of buildings, there has been research attention on developing tabular TL techniques for medical applications since the data is often tabular [127]. Deep models have become more competitive with classical machine learning for such tabular datasets [122]. Medical datasets are a good candidate for TL because they are difficult and expensive to produce. However, they often contain inconsistencies. The naïve approach would be to only use datasets with identical columns or drop non-overlapping columns, which would waste resources and potentially negatively impact the model. This was the motivation for a TL method called TransTab [4], which relaxes the fixed column requirement through feature encoding. In early design parametric modeling scenarios, adding a new variable and generating simulated data from scratch is also computationally expensive, and the updated design space has overlapping columns with the initial design space. In this work, we apply the TransTab TL method to reduce the number of simulations required to update the surrogate model.

Gaps and response

In summary, parametric models and surrogate models are powerful when paired together, but they are potentially restrictive, especially in the early stages of building design. To our knowledge, it is often difficult and computationally expensive to add variables to the parametric model and update the corresponding surrogate model with currently implemented methods. Designers must start from scratch when rebuilding their surrogate models, which discourages them from expanding the design space and discovering new directions. In this work, we adapt a tabular TL method [4] to leverage the initial data and limit the amount of new data needed to update the surrogate model as variables are added. This includes a novel random walks sampling technique to aid in class representation within the added samples. We acknowledge benefits to classical interpretable methods, and we thus compare their performance trained on the added data,

using both random walks sampling and a more conventional sampling technique, to identify instances when TL is useful in an early design setting. By implementing and testing TL in this setting, this application prevents designers from fixating on the initial design space by requiring fewer simulations to update it with adequate performance. The goal of the proposed workflow is to make performance-based parametric design more flexible and encourage designers to explore more designs, potentially leading to more sustainable design solutions.

Methodology

To demonstrate and test the method, an initial parametric design space was first constructed in the visual programming environment Grasshopper [22]. The model included 8 variables, which were sampled using Latin Hypercube sampling at a rate of $n = 500$. Annual daylight simulations were conducted using Climate Studio [128] to generate the objective: annual sunlight exposure (ASE). Next, ASE was binned into 3 classes to create the initial simulated dataset. These three classes represent a geometry that is “good”, “fine”, or “poor” from the perspective of desired ASE, which is an appropriate resolution at such an early design stage. The initial classifiers were trained and tested (training/testing split 80/20), including selected interpretable models and a TransTab transformer model.

Once the initial classifiers were trained, 4 variables were added to the parametric design space. Additional data was generated in chunks, where the initial variables were sampled using a random walks algorithm and the new variables were generated using random sampling. ASE was binned based on the same criteria as the initial dataset. Each chunk of additional data was used in combination with the original encoded data through the tabular TL method [4]. Additionally, the new chunks of data were used to train the interpretable classifiers. This procedure was repeated 10 times, and then repeated for different numbers of random walks and step sizes. The updated

parametric design space was sampled using Latin Hypercube sampling at a rate of $n = 500$ to represent starting from scratch, and this dataset acted as the ground truth for classifier evaluation.

The entire methodology was then repeated with a second combination of initial variables, and these results are included in the discussion section. The whole procedure is shown in Figure **3-2**. Following the main simulation experiment, LHS sampling of the updated design space was also conducted incrementally to compare as larger amounts of samples were added. This was done because random walks sampling was selected specifically to generate very small additional datasets, while traditional sampling would likely be better with more new samples. Finally, TL effectiveness and class representation were checked to present a more comprehensive overview of model performance.

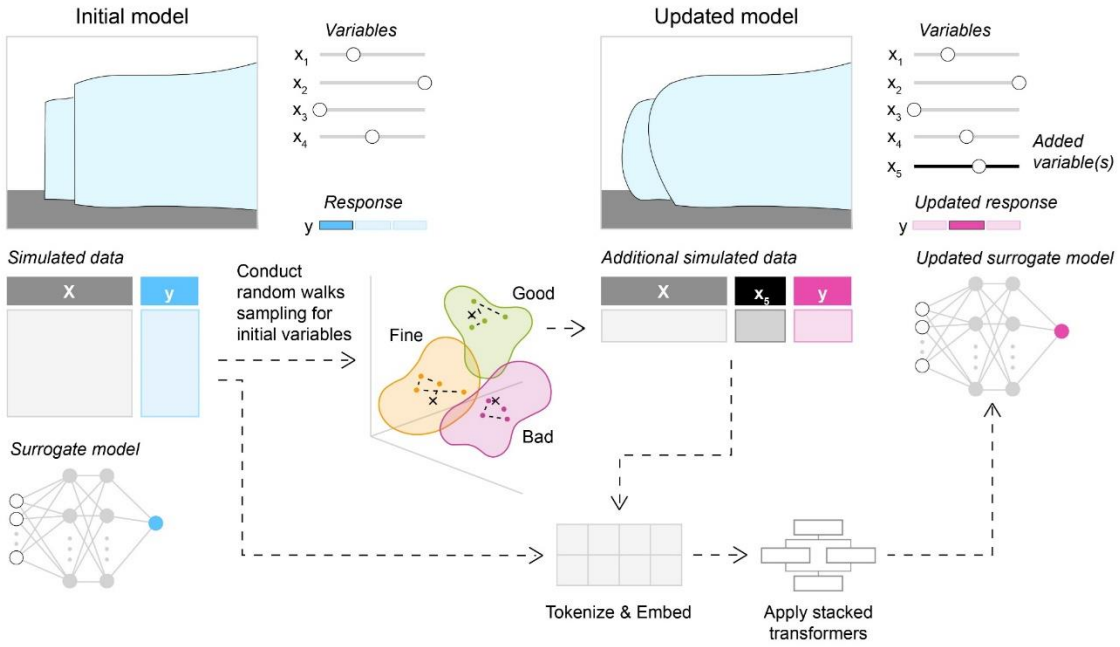

Figure **3-2**: Overall methodology for updating the performance-based parametric design space.

Design space formulation

The case study in this paper is meant to demonstrate the effectiveness of tabular TL in an early building performance-based parametric design setting. The design example is inspired by The National Art Center in Tokyo, Japan [129]. We focused on the lobby space, which features a curved curtain wall façade facing south and contains two round, concrete blocks. The top level of the blocks can be occupied as cafes or galleries. Although some glare can be tolerated in transition areas such as lobbies, it is still a concern given the curtain wall façade. Exterior and interior images of the lobby are shown in Figure **3-3**.

Figure **3-3**: Inspiration building: National Art Center Tokyo. Exterior on the left [2] and Interior lobby on the right [3].

The initial design space included 8 variables that were hypothesized to affect glare conditions and at the same time provide designers with a wide range of geometric design options. The first 4 variables related to the location of the blocks, including the location of the large block in the x-direction, distance between the two blocks, and the relative locations of the large and small blocks in the y-direction. The remaining initial variables included the blocks' height and the ratio of the blocks' top radius to lower radius, essentially modulating the blocks from cones to cylinders. Since this work intends to address real-world design scenarios, the added variables were based on a hypothetical design scenario in which the designer wants to add 3-dimensional

variables to the two façade bumps in front of the blocks. Such an expansion of variables could be the result of an initial architectural design meeting after parametrically exploring the first model. Figure **3-4** (right) shows the four added variables, which allow for the adjustment of the peak location on the curve used to construct the façade bumps in both the y- and z-directions. These variables affect the position of the block in the y-direction. A summary of all variables is provided in Table **3-1**. All variables were normalized from 0-1 prior to training.

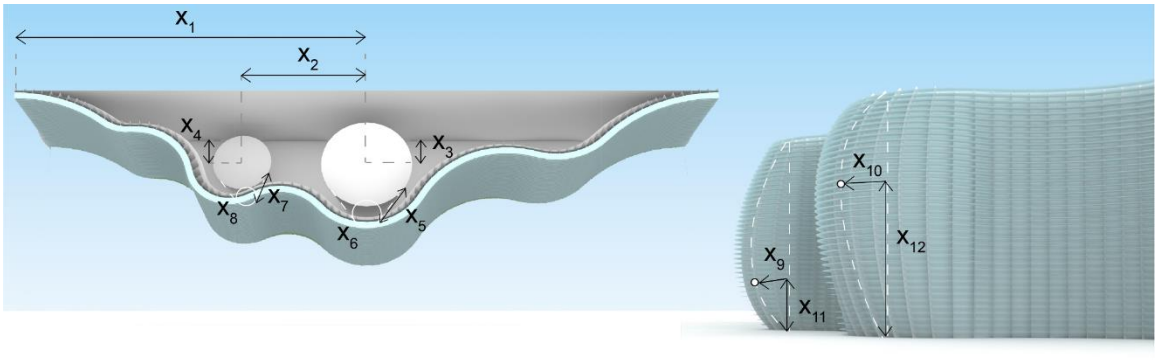

Figure **3-4**: Labeled diagram of initial variables (left) and added variables (right).

Table **3-1**: Variable details.

Variable	Description	Stage added	Minimum	Maximum
x_1	Large block x coordinate (m from origin)	Initial	-5	5
x_2	Distance between blocks (m)	Initial	1	9
x_3	Large block y location (relative)	Initial	0	1
x_4	Small block y location (relative)	Initial	0	1
x_5	Large block height (m)	Initial	8	12
x_6	Large block radii ratio (relative)	Initial	0.5	1
x_7	Small block height (m)	Initial	5	9
x_8	Small block radii ratio (relative)	Initial	0.5	1
x_9	Small block bump y coordinate (m)	Updated	0	1.5
x_{10}	Large block bump y coordinate (m)	Updated	0	1.5
x_{11}	Small block bump z coordinate (m)	Updated	1	13
x_{12}	Large block bump z coordinate (m)	Updated	1	13

The objective function for this case study was Annual Sunlight Exposure (ASE), which is the percentage of the regularly occupied floor area that receives direct sunlight (>1000 lux from the solar disc) for more than 250 occupied hours [85]. ASE was simulated using Climate Studio

aided by the Design Space Exploration toolbox [130]. All opaque surfaces including the ground were assigned according to LM-83 guidelines. The curtain wall glass was low-E double pane with 61% visible transmittance and the visible transmittance of the exterior horizontal glass shades was 43.7%. The radiance parameters were "-ab 6 -lw 0.01 -ad 1" and there were 500 samples per sensor. Since many details are uncertain in the early stages of design, the ASE output was binned into three classes and treated as a classification problem, where "good" is <0.45 ASE, "fine" is 0.45<0.60 ASE, and "poor" is 0.60> ASE. Figure **3-5** shows a range of potential designs in the updated design space in catalog format. The shading structure was removed for visualization purposes, but it was included in the simulations.

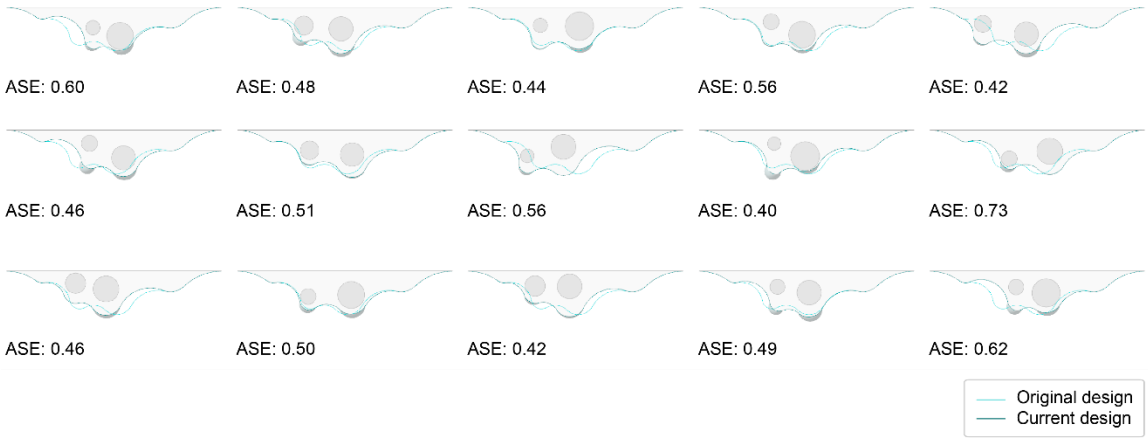

Figure **3-5**: Catalog of design options. The light blue line is the original design.

Tabular transfer learning

The selected tabular TL method is called TransTab [7]. To incorporate multiple tables with overlapping but inconsistent columns, TransTab assigns semantic meaning to the tabular data through column descriptions. This allows for the conversion of tabular data into sequences, similar to sentences, to train a transformer model adapted from NLP [51]. This way, knowledge

can be retained from the source dataset to the target dataset, regardless of whether all input columns are the same. A summary of the procedure is shown in Figure **3-6**. First, the raw data is tokenized and converted into sequences using the column name or description to assign meaning to each cell. Then, the sequence of tokens is converted into numerical vectors through an embedding layer. To align all the embeddings into the same space, the embeddings are passed through layer normalization. Finally, the input processing is completed by concatenating the classification embedding [CLS], which is a token that will facilitate sequence classification.

Next, the processed inputs are further encoded through the gated tabular transformer that was based on the classical transformer from NLP [131]. The gated transformer contains a multi-head self-attention layer and gated feedforward layers. The multi-head self-attention mechanism and gated feedforward layers determine which features to focus on by reallocating attention among tokens during the training process [4]. The embedding produced at the last layer of this process is passed to the classifier for making predictions. Further details and equations are provided in [4]. TransTab is useful for several learning applications including TL.

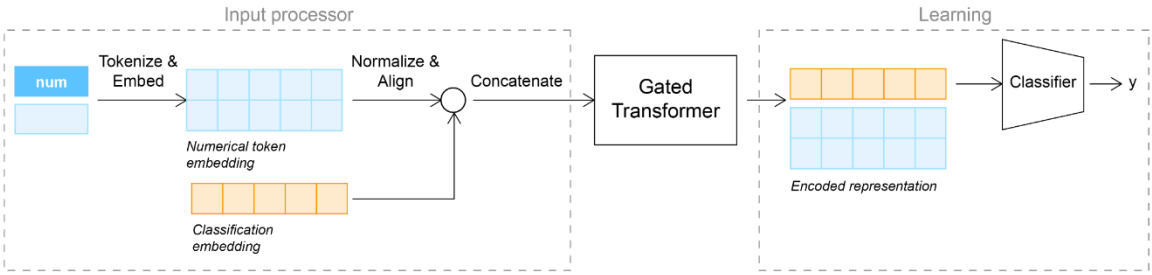

Figure **3-6**: TransTab methodology, after [4].

The TL approach was implemented in Python using the TransTab package [4]. Most of the TransTab defaults were maintained. The classifier included 2 transformer layers in the encoder and the dimension of the hidden embedding was 128. The attention module had 8 heads and the dimension of the feed-forward layer was 256. ReLU activations were used, and dropout

was not activated. A patience of 5 was kept for early stopping and the number of epochs was 100. The TransTab model was trained using the ADAM optimizer [132]. Weight decay was set to 2e-4 for regularization. The default learning rate of 1e-4 was used in the initial classifier training; however, it was increased for the updated classifier training to 2e-4 as the updated datasets were small compared to the initial dataset. Additionally, the batch size was set to 20 for the initial classifier training and reduced to 15 for the updated classifier training.

Random walks sampling

This TL procedure requires new data to demonstrate the method, which in a design scenario would be generated by a designer with some expectation about its similarity to the original dataset. The sampling technique of the updated design space is important because the goal is to add as few samples as possible to update the classifier, while making sure there is representation for each class in the added data. It is not possible to guarantee class representation because we do not know how the objective function has changed. However, we assume that the new distribution is reasonably similar, in which case it makes sense to start sampling near the centroid of each class in the initial data. From there, we propose adopting a random walks approach. We start by calculating the centroid of each class in the initial data (Eqn. 1), where $\boldsymbol{c} \in \mathbb{R}^m$ is the centroid of the class, m is the number of features, $\boldsymbol{x}_i \in \mathbb{R}^m$ represents sample $i \in \{1, 2, \dots, n\}$, and n is the number of samples in the class.

$$\boldsymbol{c} = \frac{1}{n}\sum_{i=1}^{n} \boldsymbol{x}_i \text{ (Equation 1)}$$

Next, we initiate random walks beginning from the centroid of each class (Eqn. 3). Let $\boldsymbol{t}_j \in \mathbb{R}^m$ be the position after step j for $j \in \{0, 1, \dots, k\}$, where $\boldsymbol{t}_0$ is the starting position which is the centroid. Let $U: \mathbb{R}^2 \to \mathbb{R}$ be a function that generates a uniformly distributed random value in

the given interval (a, b). Then, to generate a step vector $\boldsymbol{s_j} \in \mathbb{R}^m$, we apply $U(.,.)$ in each dimension as follows:

$$\boldsymbol{s_j} = \big(U(a_1, b_1), U(a_2, b_2), \dots, U(a_m, b_m)\big), \forall\, j \in \{1, 2, \dots, k\}. \text{ (Equation 2)}$$

Finally, we update the position vector $\boldsymbol{t_j}$ using the previous position and the new step:

$$\boldsymbol{t_j} = \boldsymbol{t_{j-1}} + \boldsymbol{s_j} \text{ (Equation 3)}$$

The number of walks that are initiated dictates how many samples are added per step. For example, if we have 3 classes and 2 walks, we add 6 samples per step. If the data has shifted significantly, it is best to take larger steps, and if the designer thinks it is very similar, the steps should be smaller. Since we do not have any information about the added variables, they are randomly sampled within their bounds. This is designed to help mitigate class imbalance and prevent the designer from adding more data just to achieve class representation.

Interpretable classical classifiers for comparison

Choosing a transformer model as a surrogate model allows for TL, but it sacrifices interpretability. In an early design setting, it might be useful to understand the predictions from the surrogate model while also gaining insight on variable importance and gradients. This paper tests what is gained in performance with low number of samples against what is lost in interpretability by comparing the TL method to classical methods. In this section, we identified classical classifiers that 1) are interpretable and 2) have low variance out of the box. This is because the added dataset from the updated design space will be limited, thus the models will be prone to overfitting.

Logistic regression (LR) is considered interpretable because it is a generalized linear model. Each feature is assigned a coefficient that can be interpreted to understand its effect on the prediction. To lower variance, a shrinkage penalty can be added which aids in regularization.

Support vector classifiers (SVC) using linear kernels also produce coefficients that can be interpreted. SVC overfitting can be prevented through the budget parameter, which controls the strength of the penalty. Alternatively, Naïve Bayes (NB) operates on Bayes' Theorem and can be interpreted through conditional probabilities [114]. NB trades off increased bias for lower variance by assuming feature independence within classes [133]. Linear discriminant analysis (LDA), also Bayes-based, can be interpreted through the coefficients assigned to each feature in the discriminant functions [134]. Similar to previous methods, LDA employs a shrinkage penalty to decrease variance. Decision trees (DT) are considered interpretable, offering insights into variable importance by quantifying the features' contribution to criterion reduction [114]. However, decision trees tend to overfit (high variance), necessitating pruning, which requires a large enough dataset, or ensemble methods, which sacrifices interpretability. Thus, LR, SVC with a linear kernel, NB, and LDA were chosen as interpretable classifiers for comparison. These classifiers and their hyperparameters are shown in Table **3-2**.

The Python library Scikit-learn [135] was used for all interpretable, classical classifiers. The parameters used to generate results for each model are provided below. Overall, the default parameters were maintained unless the model trained with the initial data did not converge or needed to be adjusted for a multi-class problem. The same hyperparameters were used for the initial model and updated models, as the designers in our assumed application would not have access to ground truth. It is important to acknowledge that TL can be a broader concept for classical learning, which would include stacking and ensemble methods, but they lose their interpretability. For this reason, these methods were excluded from this work.

Table **3-2**: Classical classifier hyperparameters. An asterisk indicates the parameter was changed from the default.

Model	Parameters
Logistic Regression (LR)	Penalty: L2 (default) Dual: False (default) Tolerance: 1e-4 (default)

	Inverse of regularization strength (C): 1.0 (default) Fit intercept: True (default) Intercept scaling: 1.0 (default) Class weight: None (default) Solver: Newton-cg* Max iterations: 500* Multi-class: Auto (default) Warm start: False (default)
Support Vector Classifier (SVC)	Regularization parameter (C): 1.0 (default) Kernel: Linear* Shrinking heuristic: True (default) Probability bool: True* (required for multi-class) Tolerance: 1e-3 (default) Cache size: 200 MB (default) Class weight: None (default) Max iterations: No limit (default) Decision function shape: one-vs-rest (default) Break ties: False (default)
Naïve Bayes (NB)	Priors: None (default) Variance smoothing: 1e-9 (default)
Linear discriminant analysis (LDA)	Solver: Singular value decomposition (default) Shrinkage: None (default) Priors: None (default) Number of components: False (default) Tolerance: 1e-4 (default) Covariance estimator: None (default)

Classifier evaluation

The models were evaluted using the One-vs-Rest area under the reciever operating characteristic (AUROC) curve. The ROC curve is a graph that shows the trade-off between the true positive rate and the false positive rate for different decision thresholds for a binary classifier [136]. ROC curve for each class $i \in \{1, 2, \ldots, k\}$ is constructed by assigning positive labels to the samples of class i and negative labels to the samples of all other classes. Then, the AUROC is calculated for the ROC curve of each class. Finally, the average AUROC is computed by taking the mean of the AUROC scores over all classes (Eqn. 4).

$$average\ AUROC = \frac{1}{k}\sum_{i=1}^{k} AUROC_i \text{ (Equation 4)},$$

where $average\ AUROC$ is the overall multiclass AUROC score, $AUROC_i$ is the AUROC score for class i, and k is the number of classes. This is to adopt it from its original use for binary classification problems. It aims to evaluate the model's performance in distinguishing between multiple classes.

Results

To determine if TL is suitable for an early design setting, we examine 1) the performance compared to classical interpretable classifiers for incrementally added samples using two sampling techniques, 2) the effectiveness of transfer learning, and 3) the effectiveness of random walks sampling of the initial design space. We also explore classifier robustness, because in a real design scenario, the designer will not have access to ground truth. These aspects are measured and discussed in the remainder of the paper.

Comparing transfer learning to classical interpretable classifiers

Model performance depends on the quality of the target dataset. Therefore, the hyperparameters of the random walks sampling were rigorously tested to fairly compare the models, in addition to generating LHS datasets that will be discussed later in this section. Figure **3-7** shows the average multiclass AUROC and standard deviation for samples incrementally added to the updated design space dataset. The two main hyperparameters in the random walks sampling were tested: number of random walks and step size. These influence the number of samples added at each iteration and the size of the step interval, respectively. For each combination and number of samples, the random walk sampling was repeated 10 times. The

classifiers were tested on the scratch dataset, which was generated by sampling the updated design space at a rate of $n = 500$ using Latin Hypercube sampling. This measures how well the classifier generalized trained on limited data from the updated design space. The TL results include the initial data and the updated data, while the classical interpretable classifiers include only the updated data.

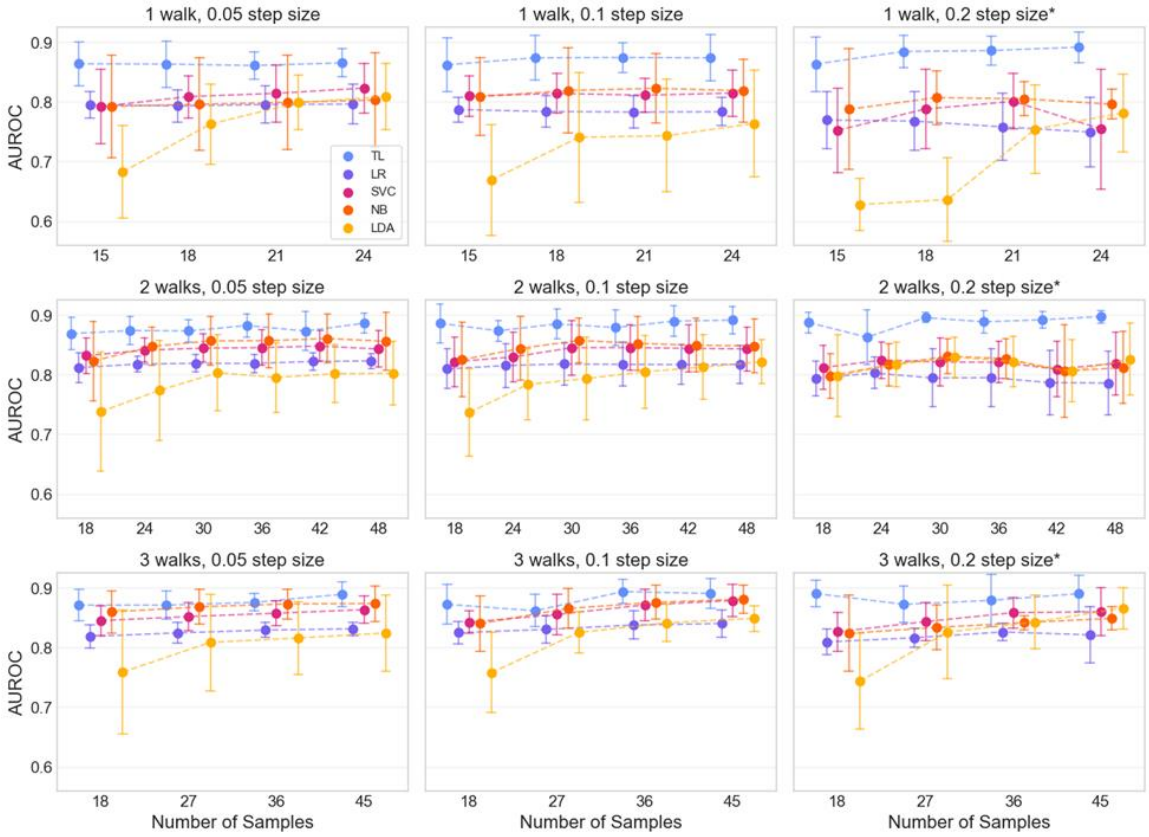

Figure **3-7**: The mean and standard deviation for each model type across 9 experiments. An asterisk indicates that some of the experiment results were not included due to lack of class representation. These datasets can be identified in Figure 9.

The results of all combinations show the TL classifier yields higher multiclass AUROC on average. As more walks were added, the classical interpretable classifiers' performance were more comparable, particularly the Naïve Bayes classifier. However, including more walks requires more samples to be added at each iteration, which is a disadvantage for designers. The

TL classifier is also more robust against random walks sampling hyperparameters, as shown by its stable average AUROC across all experiments. This is important because even if the designer does not tune the hyperparameters optimally, the TL method will yield an adequate performing classifier compared to the classical interpretable methods. The TL method is also less sensitive to the number of added samples, which is better for designers.

In addition to the average performance, the standard deviation was plotted to understand variability over 10 repetitions. A small standard deviation indicates the classifier is more reliable which is important because the designer will not have access to ground truth (scratch dataset) as we do in a research setting. Over the repeated experiments, the TL method demonstrates low standard deviation across all combinations compared to the classical interpretable methods where the standard deviation depends on the random walks sampling hyperparameters and is frequently high. This is further evidence that the TL method is more robust than classical interpretable methods.

The recommended hyperparameters for this case study are 1 walk, 0.1 step size, for two reasons. First, the TL method performance is adequate for 1 walk compared to the 2 and 3 walk experiments, and 1 walk allows the designer to add the fewest number of samples per iteration. Second, of the three 1 walk case studies, 0.1 step size shows the best class representation, which is discussed further in a later section. The initial dataset and results from the recommended random walk hyperparameters are provided in Table **3-3**. This table also provides an equivalent number of new LHC samples required for each classical method to reach the TL performance at a small number of new samples (18), which will be explained next.

Table **3-3**: Initial and scratch multiclass AUROC for each classifier and average updated multiclass AUROC for 1 walk, 0.1 step size.

				AUROC				
Model	Description	Initial samples (x_1-x_8)	New samples (x_1-x_{12})	TL	LR	SVC	NB	LDA

Initial	Data from initial design space	500	-	**.9821**	.9520	.9495	.9579	.9665
Updated	Initial data (TL only) + limited data from new design space	500	15	**0.8614**	-	-	-	-
		-	15		0.7866	0.8090	0.8082	0.6686
		500	18	**0.8732**	-	-	-	-
		-	18	**-**	0.7833	0.8136	0.8184	0.7402
		500	21	**0.8736**	-	-	-	-
		-	21	**-**	0.7824	0.8106	0.8221	0.7429
		500	24	**0.8731**	-	-	-	-
		-	24	**-**	0.7829	0.8140	0.8180	0.7633
Equivalent	Number of LHS samples required to meet or exceed TL performance at 18 random walks samples				90+	**~72**	~90	**~72**

Although the random walks sampling was necessary for achieving class representation when generating very small datasets from the updated design space, other prescribed sampling techniques may yield better results for higher numbers of added samples. Figure **3-8** shows the model performances for the recommended 0.1 step size up to 90 added samples (with a faded circle), as well as for LHS sampling at the shared number of additional samples (with a bold X) across the three walks. The LHS sampling begins at 36 samples because class representation was not achieved at 18 samples, which would have prevented proper model training. The result shows that classical interpretable methods, specifically LDA for this dataset, can achieve the same or higher AUROC as TL with 18 samples at approximately 54 samples. However, TL still performs better at 54 samples, so it is still useful at that point. Once 72 samples are reached, LDA with LHS outperforms TL, making TL no longer valuable past this point. This result also suggests that fewer than 500 samples were needed to achieve near peak performance for the initial dataset. Additional considerations concerning sample size for both original and new sampling are discussed in the discussion section.

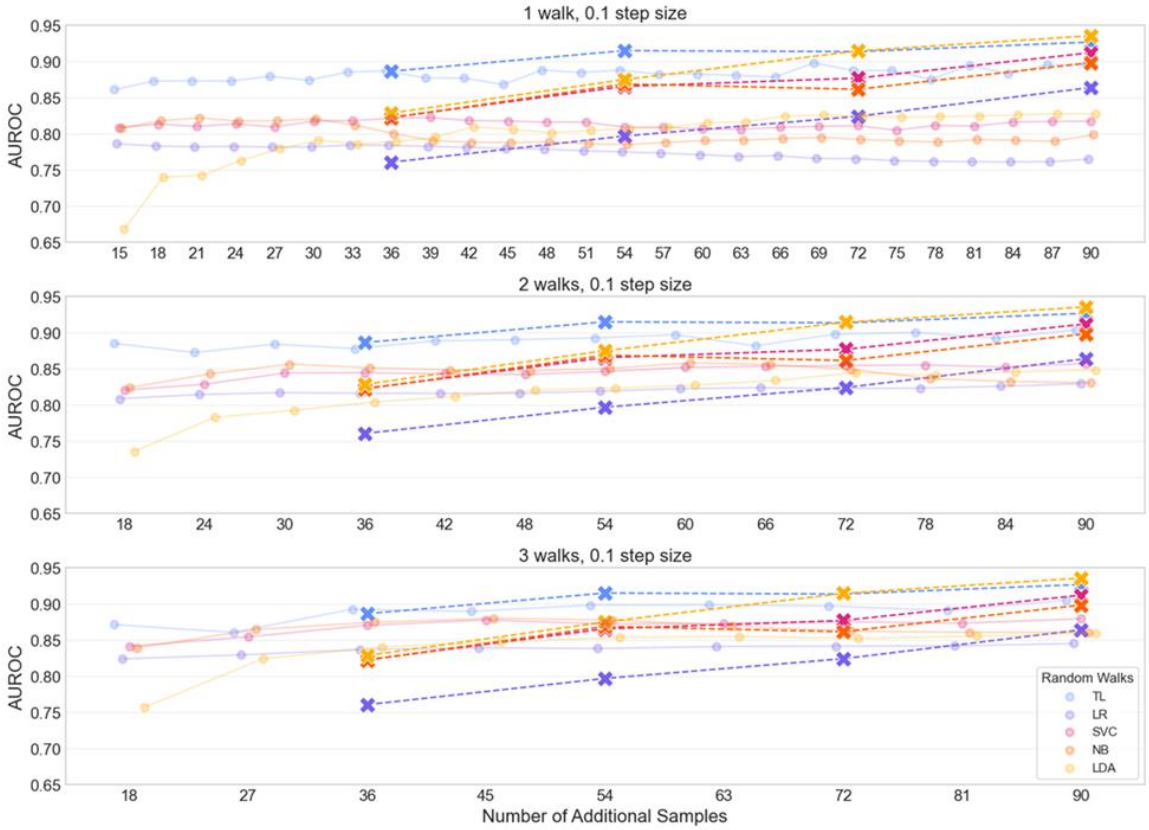

Figure **3-8**: Latin Hypercube sampling at shared number of additional samples across three walks compared to random walks sampling up to 90 added samples.

Transfer learning effectiveness

With any TL application, there is the possibility that the updated classifier performs worse than if it were trained on the target data only. This usually happens if the tasks are too different. In this case study, the source data is the initial design space dataset, and the target data is the updated design space dataset. Given the nature of the case study problem, it was assumed the source data behaved similarly to the target data. However, the TL method and a neural network trained only on the target data were compared to verify our assumption (Figure **3-9**). Figure **3-9** demonstrates a significant increase in performance across all sampling experiments,

indicating that it is beneficial to leverage the initial model data to improve the performance of the updated classifier that has limited data from the updated design space. In some experiments, the transformer model trained on only the target data performance decreased as data was incrementally added, which is likely due to overfitting. Regardless, the TL method maintains high performance.

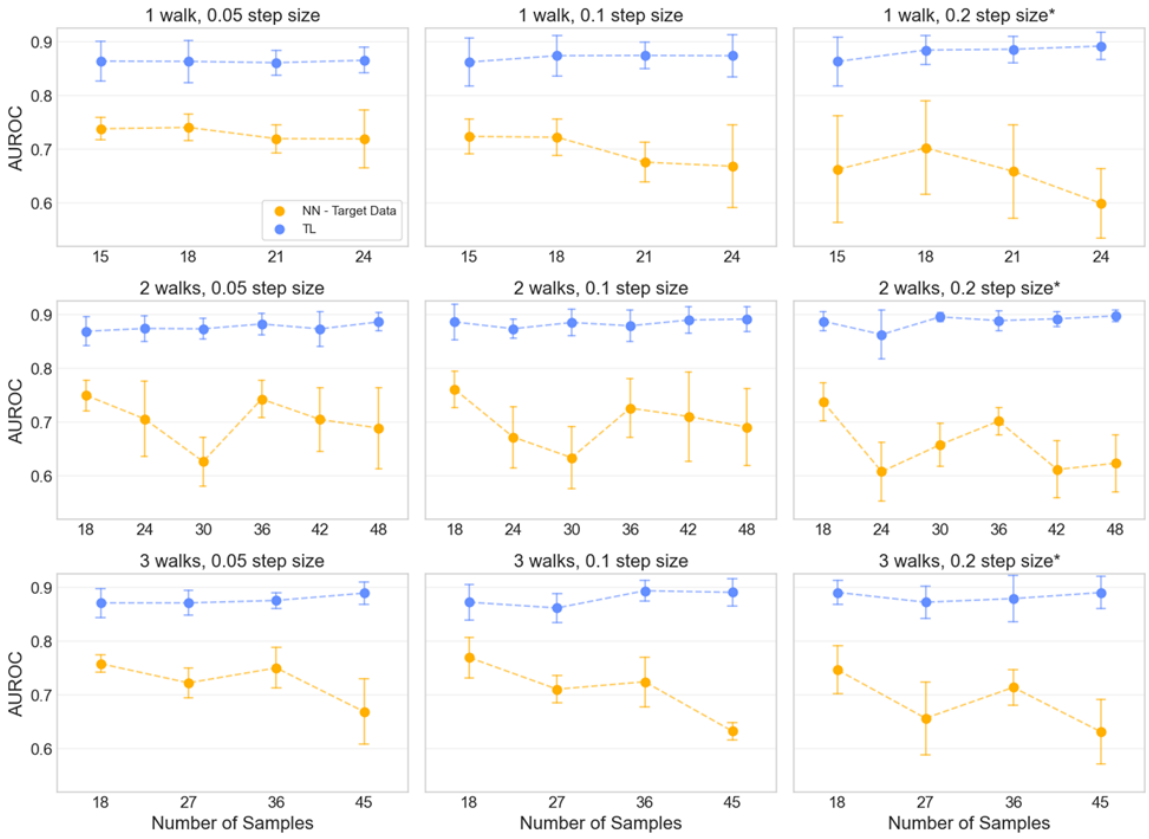

Figure **3-9**: Transformer model trained only on target data compared to TL approach leveraging source data and target data.

Class representation through random walks sampling

The random walks sampling for the initial variables was implemented to address the issue of class representation in the updated design space dataset. Figure **3-10** shows the class

representation for each random walks hyperparameter combination. As the step size increases, it becomes more difficult to attain class representation, particularly for the poor performing class (ASE >0.60). This is likely because the initial poor performing class is smaller than the other two classes, or fewer designs fall into the poor performing class with the introduction of new features. The objective class distribution shift is discussed further in the discussion section. While the results presented in this section are specific to one case study, class representation is a potential issue that must be considered when applying tabular TL in a performance-based parametric design setting.

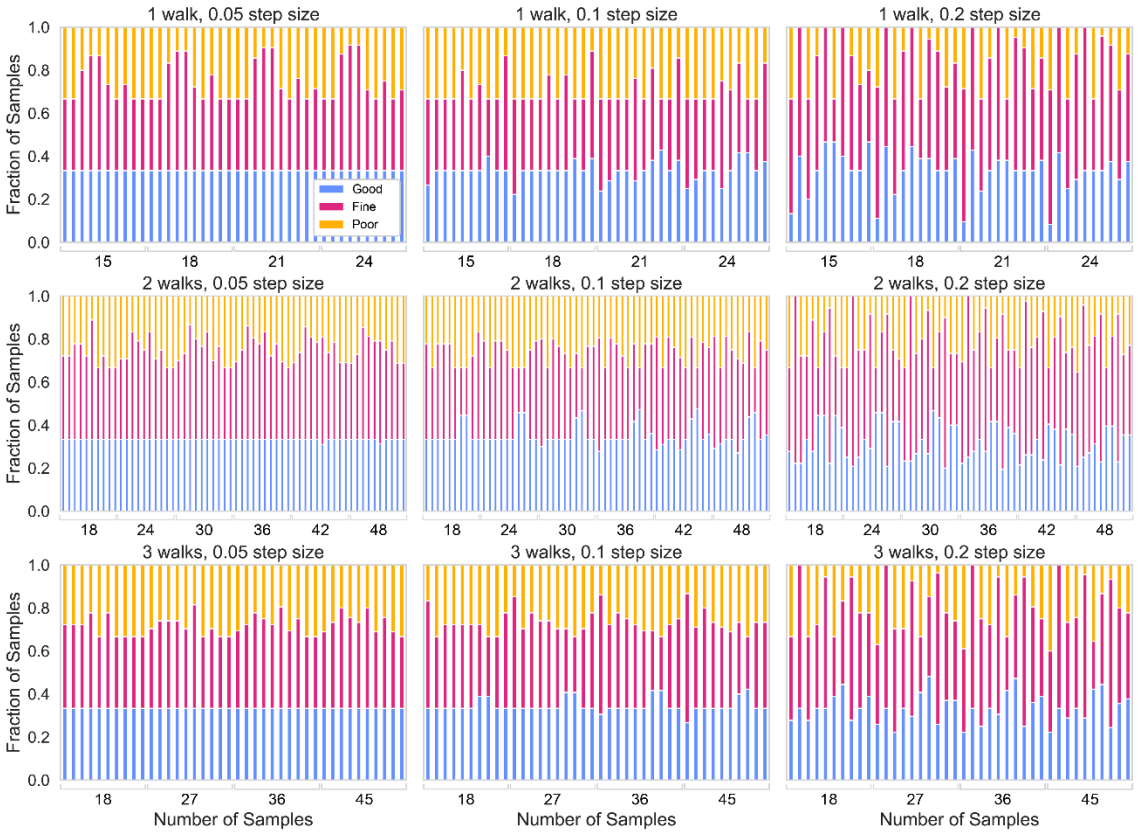

Figure **3-10**: Class representation across all experiments. In the right column, there are datasets that do not contain samples in class "poor" and were not included in Figure 3-7 and 3-9.

Discussion

Overall, the tabular TL approach paired with the random walks sampling of the initial design space yielded higher multiclass AUROC on average compared to the classical interpretable classifiers for very few additional samples. Regardless of random walks sampling hyperparameters, the TL method was able to achieve adequate multiclass AUROC (>0.85) with only 18 samples. As more samples were added, the classical interpretable methods performed comparably or better with LHS sampling; therefore, classifier selection depends on the amount of time the designer is willing to wait to update the surrogate model. However, some classical interpretable methods demonstrated large standard deviations and were not reliable for this case study. It is recommended to choose the TL method if very few samples are to be added, with a few considerations:

- Number of classes: If the initial dataset has more classes, then more samples must be added at each iteration. Reduce the number of classes to add fewer samples at each iteration.
- Number of walks: Fewer number of walks allows for fewer samples to be added per iteration. However, initializing only one walk may not fully capture the behavior in each class.
- Step size: The step size should be determined based on the size of the classes and feature magnitudes. In some cases, it may be appropriate to set different step sizes for each class. It is recommended to normalize the features prior to determination to simplify the selection.
- Initial features sampling technique: If the designer suspects the distribution has only slightly shifted, random walks sampling is recommended. However, if there is a large shift, it may be appropriate to choose a different sampling technique.

Tabular TL proved effective for this case study, primarily because the problems were similar. It is difficult to measure the similarity between the initial and scratch datasets given the feature spaces are different—i.e., the initial feature space is 8-dimensional and the updated feature space is 12-dimensional. However, because of how the features were constructed in Grasshopper, we can say that the marginal distribution according to the initial features is the same. Additionally, we can evaluate the class distribution between the initial and updated datasets, which is shown in Figure **3-11**. Most designs fall into the fine performance class for both datasets, with more designs in the good performance class with the addition of the new variables.

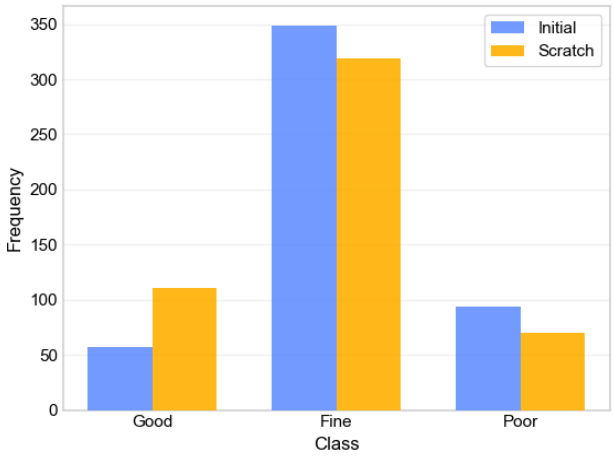

Figure **3-11**: Comparison of class distribution in the initial design space dataset and the updated design space dataset (scratch dataset).

Further research is required to measure the similarity between datasets with overlapping feature spaces in building design problems [137]. Of course, if the datasets are too different, TL would not be effective and result in negative transfer. Then, it would be necessary to start from scratch. Nevertheless, this work demonstrates a novel workflow for applying a new tabular TL method and sets the stage for future implementations.

Alternate design scenario

It is important to acknowledge that the initial variables included in the model influence the performance of the classifiers. In the main design scenario (adding variables related to the 3D façade), knowledge was successfully transferred, however, if the objective distribution were changed entirely, the designer would need to start from scratch. While it is not necessarily possible to determine how the objective function will shift, we can demonstrate another design scenario starting with a different set of initial variables to begin to understand the generalizability of the TL method. Figure **3-12** shows the classifiers' performance if the initial variables were the location of the blocks variables (x_1 - x_4) and the 3D façade variables (x_9 - x_{12}), and the added variables were those related to the shape of the blocks (x_5 - x_8) (Table **3-1**).

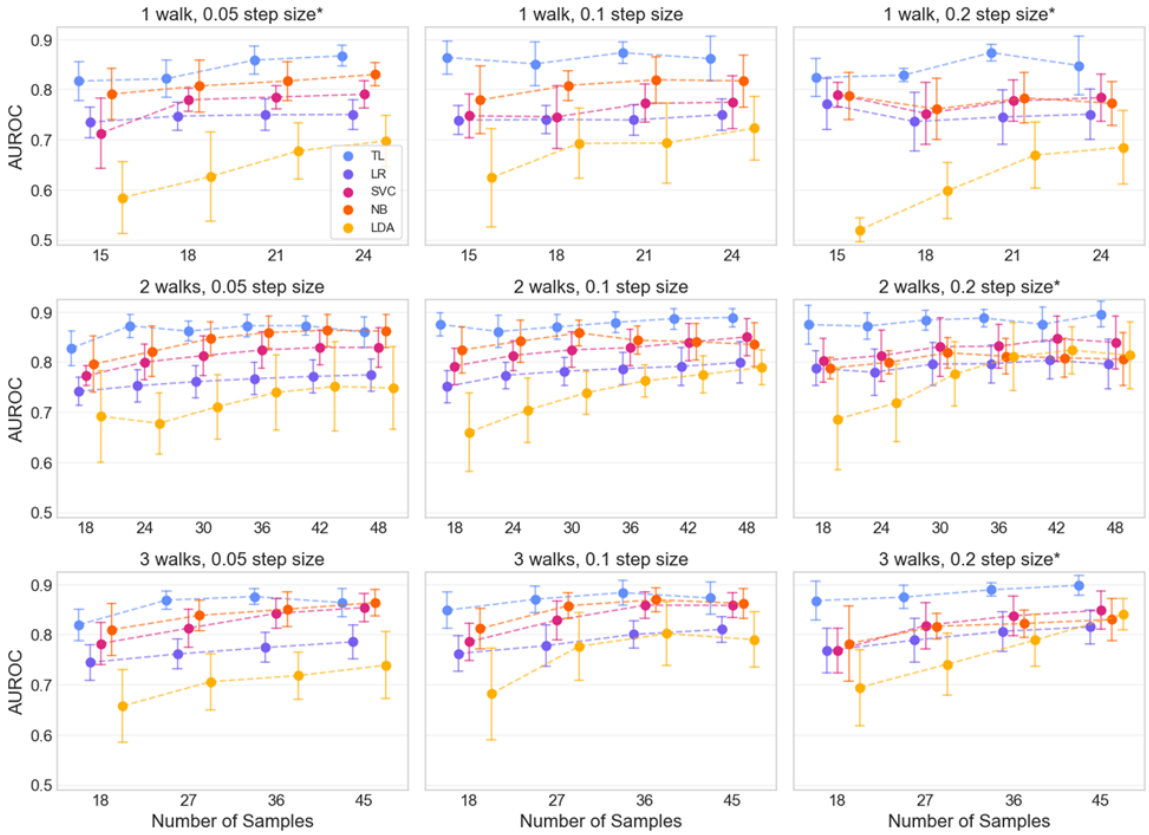

Figure **3-12**: The mean and standard deviation for each model type across 9 experiments. An asterisk indicates that some of the experiments were not included due to lack of class

representation.

Overall, the TL method performs the best on average, with two exceptions: 2 walks, 0.1 step size, 30 samples and 2 walks, 0.05 step size, 48 samples. Additionally, in this scenario, another experiment encountered issues with class representation (1 walk, 0.05 step size), unlike the main design scenario, which only experienced them with the 0.2 step size experiments. Nevertheless, this exercise shows that while the initial variables influence the effectiveness of TL, if the underlying behavior is largely maintained, it successfully reduces the number of samples required to update the surrogate model.

Limitations

While this work demonstrates the application of TL in an early design setting, it presents several limitations. One main limitation of applying TL techniques in early design settings is that many methods are intended for classification tasks. This is primarily because more of the real-world data and current problems being studied lend themselves to classification over regression. However, regression is more ubiquitous in building design datasets [138], as a continuous objective provides more information. Nonetheless, we contend that classification remains useful, especially in the early stages when there is uncertainty. Instead of knowing the exact percentage of ASE, we only discern if it is ‘good,’ ‘fine,’ or ‘poor.’ We argue that this uncertainty is typical in the early design stage and serves to buffer the problem until details are sorted out. Another limitation, specific to this work, is that only one case study is examined. The behavior of the objective function in this study may not be replicated in other datasets. For instance, if a variable is added that drastically changes the objective, such as adding a large shading device, it is likely that the designer would have to start from scratch, as discussed in previous sections.

Conclusion

This paper implemented a tabular TL method on an early building design problem to quickly preserve performance feedback in a parametric model when the variables are updated. It compared the performance of the TL method to classical methods across several sampling situations. The selected tabular TL method, paired with random walks sampling, is useful when very few samples are to be added to quickly update the surrogate model. In this case study, 'very few samples' meant 18 samples. However, if the designer could generate approximately 54-72 samples, interpretable classifiers achieved the same performance and also provided the benefit of interpretability. In the scenario that very few samples are to be added, we demonstrated that the number of simulations required to update the surrogate model can be reduced through applying the proposed workflow with higher confidence than classical interpretable classifiers. Additionally, the TL method proved more robust against sampling randomness and hyperparameters. This workflow could also be useful for design problems with even more costly simulations such as computational fluid dynamics or earthquake simulations. However, depending on the designer's goals, it may be worth sacrificing performance to gain insights on the variables' interactions and importance, or generating additional samples to achieve comparable performance.

Further research is required to establish a metric to measure the similarity between parametric datasets with overlapping feature spaces and shared label spaces. Additionally, the tabular TL method implemented in this work and future approaches should be tested on other problems in building design domains. This is the case for TL in general, as it has recently been introduced to the field [137]. Finally, it is important to note that for a parametric model to accommodate new variables, it must be programmed in a flexible way. This can be accomplished through modeling in visual programming platforms like Grasshopper, or through the implementation of modeling

methodologies that allow for reusability [139]. Since many designers already work this way, this application of TL can help make performance-based parametric models more flexible, allowing for new, creative design directions that meet sustainability goals.

Chapter 4

An exhaustive search for the optimal dynamic window properties to minimize building energy

This chapter is to be submitted for publication in an academic journal.

Introduction

There is an increasing need to reduce building energy consumption, as the building sector accounts for 36% of final global energy use [140]. Electricity demand is expected to continue growing to combat climate change effects [19]. To reduce the energy consumption within the building sector, it is important to continue to improve not only system efficiencies but also the quality of building envelopes. Building windows are of particular interest because they are the thermal weak point and impact potential electric lighting savings and occupant satisfaction. One effective approach to reduce energy consumption is to implement double-pane windows with low-emissivity (low-e) coating [141], which works by reflecting infrared (IR) light. Beyond high performance static windows, dynamic glazing systems have been identified as a viable option to improve window performance [142], [143]. Dynamic glazing systems modulate their optical and thermal properties to adjust the visible transmittance (VT) and solar heat gain coefficient (SHGC) to either accept or block solar heat gains depending on outdoor conditions. These technologies have been demonstrated to be highly effective in certain climates, saving approximately 17% compared to a static baseline [144].

However, while manipulating solar gains depending on outdoor environmental conditions is an effective strategy to reduce HVAC electricity usage, because solar light and heat are often

controlled together, it can have a negative effect on lighting electricity usage and produce an undesirable window appearance, which may prevent widespread adoption. For these reasons, there is recent interest in decoupling solar light and heat. Although it is not possible to achieve very low SHGC and very high VT due to inherent limitations in the definition of SHGC, it has been shown to be possible to achieve decoupling in the near infrared (NIR) region, which enables somewhat independent control of SHGC. A few such technologies have been proposed including a dual-band electrochromic glazing [145] and a reversible photothermal window [18]. Assuming we can decouple solar heat and light within physical restrictions, it is unclear what the optimal range of SHGC and VT is to minimize annual energy consumption in diverse climates.

In this work, we exhaustively test the VT and SHGC for a two-state dynamic glazing system, considering feasibility constraints, to determine the optimal configuration across multiple climates. The optimal states reveal the ideal relationship and determine the strategy for decoupling in each climate. Once the optimal configuration is identified, the savings are calculated against ASHRAE standard glazing and the switching behavior is evaluated to compare climates. Furthermore, a sensitivity analysis is conducted to understand the importance of tuning the transition temperature for mixed and cold climates. This work will establish goals for future product development within the dynamic glazing space.

Literature review

Current dynamic window technologies

Dynamic window technologies modulate their thermal and optical properties to reduce HVAC and lighting electricity usage. They reduce HVAC electricity usage by increasing solar heat transmission during cold conditions and decreasing it during warm conditions. From a

lighting perspective, dynamic windows can reduce electricity usage by increasing visible light transmission. This modulation has also been shown to affect thermal and visual comfort [146], [147]. It can be accomplished through a variety of mechanisms, including passive technologies such as thermochromic glazing [36], [148], and active technologies, for example, suspended particle devices [149], [150], polymer dispersed liquid crystals [151], [152], and electrochromic glazing [16], [153]. Passive technologies are controlled by environmental changes, typically solar radiation or temperature, whereas active technologies are controlled by a program that involves environmental measurements, system measurements such as cooling/heating load or illuminance, or some combination. One of the most widely adopted technologies is electrochromic glazing, which modulates its solar and visible light transmission through tuning the applied electrical voltage.

Lee, Jeong, and Chae used a search algorithm to determine the optimal control parameter for electrochromic glazing and demonstrated 17.4% annual heating and cooling energy decrease on average compared to a static window over six locations, with outdoor air temperature as the control parameter [144]. Chambers et al used a Monte Carlo model to estimate the performance of electrochromic glazing on office buildings in Switzerland and found an average of 11% energy savings on the cooling and lighting loads [154]. The savings also depend on orientation. For example, Tavares et al showed the greatest savings from EC on the west façade in mediterranean climates [155]. Favoino, Overend, and Jin identified the optimal thermal and optical properties for general dynamic glazing that transitions on a daily and monthly basis and found between 5-57% savings depending on climate and orientation [17]. However, this also included u-value modulations. Additionally, they also showed that energy savings is sensitive to the transition time scale, which is higher for current technologies. Warwick, Ridley, and Binions investigated the ideal transitioning for thermochromic glazing and found that with sharp transitions and a low transition temperature, 17.7% energy savings are achievable compared to standard glazing

systems [156]. While the building characteristics, climate, and baseline for comparison vary across studies, it is evident that maximizing dynamic glazing performance involves optimizing the transition/control parameters, switching resolution, and the properties of the glazing itself.

In whole building energy simulations, the modulations are measured through visible light transmittance (VT) and solar heat gain coefficient (SHGC). SHGC is calculated based on the full light spectrum, including the visible portion. Therefore, it is impossible to achieve very high VT and very low SHGC simultaneously, but it is possible to decouple them beyond certain bounds. This is of current interest among researchers, as it is often desirable to maintain somewhat high VT to reduce light electricity usage or at least control it independently, with some potential to improve glare conditions or visual comfort [157]–[159]. One of the remaining issues with electrochromic glazing is that the visible and infrared (IR) light transmittance are highly dependent [160], meaning that VT and SHGC change together and in fact have a roughly linear relationship, as shown in Fig. 1 in [161]. This results in two or more states that range from a 'tinted' state, with low SHGC and low VT, to a 'clear' state, with high SHGC and high VT. It is likely that improving the light-to-solar-gain (LSG) ratio, VT/SHGC, in the tinted state will lead to further electric light and HVAC electricity usage savings [142]. The most viable path thus far has been to decouple visible and NIR transmission, which will be discussed in the following sections.

Decoupling solar heat and light

Several researchers have proposed dynamic materials that manage to decouple solar heat and light by targeting the switching of specific regions within the light spectrum, specifically in the NIR region [162], [163]. There are three components of solar light that can be manipulated: transmission, absorption, and reflection. DeForest et al demonstrates a dual-band electrochromic glazing made from tungsten oxide nanocrystals that modulates between three main dynamic

glazing states: a tinted state that has low transmittance in the visible and NIR regions (low VT, low SHGC), a clear state that has low transmittance in the NIR region and high transmittance in the visible region (high VT, moderate SHGC), and a third clear state that has high transmittance in both the NIR and visible regions (high VT, high SHGC) [145]. Their dual-band dynamic glazing outperformed other dynamic glazing technologies and high-performance static glazing across multiple climates [145]. Jahid et al proposed a reversible photothermal window with plasmonic nanofilms that absorbs NIR [18]. During the summer, the plasmonic nanofilm is on the outer layer, and in the winter, it is reversed such that the nanofilm is on the inner layer. Paired with the central air layer that has localized heating and insulation qualities, NIR is released into the indoor environment. They demonstrated over 18% energy savings in mixed climates [18] compared to standard energy-efficient windows.

Research gaps

As more viable paths are identified to decouple solar heat and light, the ideal dynamic glazing properties is once again in question. It is unclear what the relationship between SHGC and VT should be to minimize energy consumption across diverse climates, assuming a hypothetical perspective that solar heat and light can be decoupled within physical limitations. In this work, we identify the optimal range of VT and SHGC and transition temperature across multiple climates through exhaustive grid sampling with constraints. The switching behaviors are investigated, and savings calculated to determine which climates benefit from such innovative dynamic glazing technologies. Furthermore, a sensitivity analysis is conducted to demonstrate the importance of the transition temperature parameter in cold and mixed climates. These contributions will inform the future development of dynamic glazing technologies.

Methodology

The optimal two-state dynamic glazing system was determined through a constrained grid sampling approach (Figure **4-1**). The variable search space consisted of five variables: state 1 SHGC, state 1 VT, state 2 SHGC, state 2 VT, and the transition temperature. After all variables were discretized and all combinations computed, configurations that violated physical limitations and domain knowledge were eliminated. These constraints are detailed in further sections. Next, annual electricity usage across end uses was calculated through conducting EnergyPlus simulations. This step was accelerated via parallel computing. Then, the optimal solution was identified based on the lowest combined annual heating, cooling, interior lighting, and fan electricity usage. The savings were calculated and switching behavior verified. The baseline for energy savings was static ASHRAE standard glazing. Finally, a one-at-a-time sensitivity analysis was conducted to understand the effect of the transition temperature parameter in cold and mixed climates. Lastly, the tradeoff between electricity consumption and thermal comfort was measured by finding the pareto front. The entire process was conducted for seven ASHRAE climate zones and the results were compared across climates.

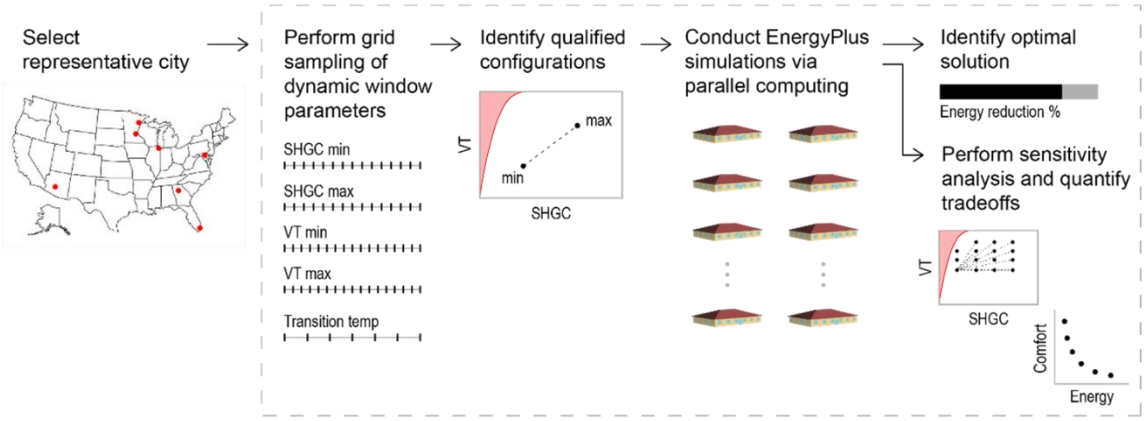

Figure **4-1**: Overall methodology.

Case study

The DOE small office prototypical model was selected as the case study building (Figure **4-2**). It comprises of one level with one core zone and four perimeter zones. The HVAC system consists of a constant volume unitary heat pump system with constant speed compressors and no economizer. The window-to-wall ratio (WWR) for all orientations is 19.8%, excluding the glazed door on the south orientation, which was not included as a dynamic window. However, all windows were included as dynamic windows in the simulations. The simulations were conducted for an annual run period at a 10-minute resolution (timestep=6). Seven US cities were selected to represent the ASHRAE climate zones: Chicago, Phoenix, Baltimore, Atlanta, Miami, Duluth, and Minneapolis. Chicago, Duluth, and Minneapolis are heating-dominated climates, while Phoenix, Atlanta, and Miami are cooling-dominated, and Baltimore is mixed. All representative cities are classified as humid except Phoenix which is dry.

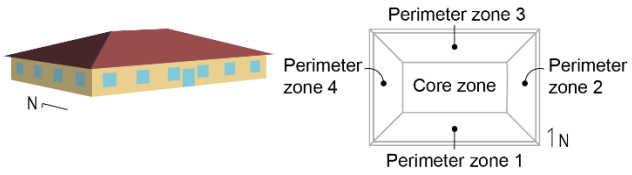

Figure **4-2**: Case study building.

The baseline for comparison was the default window construction included in the prototypical model (Table **4-1**) that follows ASHRAE standards. The U-value was kept the same for all models in each climate zone, since we only wanted to measure the effect of modulating VT and SHGC.

Table **4-1**: Baseline window parameters.

Climate zone	Description	City	SHGC	VT	U-value (W/m^2-K)
1A	Very hot humid	Miami, FL	0.23	0.25	2.86
2B	Hot dry	Phoenix, AZ	0.25	0.27	2.58

3A	Warm humid	Atlanta, GA	0.25	0.27	2.41
4A	Mixed humid	Baltimore, MD	0.36	0.39	2.06
5A	Cool humid	Chicago, IL	0.38	0.42	2.06
6A	Cold humid	Minneapolis, MN	0.38	0.42	1.94
7	Very cold	Duluth, MN	0.40	0.44	1.66

Grid sampling with constraints

A grid sampling approach was adopted to exhaustively search the variable design space. The variables included the SHGC and VT for states 1 and 2, as well as the transition temperature (Table **4-2**). The bounds for SHGC and VT were determined through surveying commercially available double and triple pane windows in the LBNL glazing database. Next, the variables were discretized and grid sampled to consider all combinations. Then, two constraints were imposed to ensure only feasible configurations were simulated. The first constraint dealt with the physical limitation of achieving high VT and low SHGC. Because SHGC accounts for the full light spectrum, including the visible portion, it is not physically possible to achieve very low SHGC and high VT simultaneously. This regions is known as the 'forbidden region' and it is visualized in red in Figure **4-3**. The second constraint was imposed to ensure that when the transition temperature was reached, a lower SHGC was adopted. This was interpreted as eliminating any combinations that produced a negative slope $\frac{(y_2-y_1)}{(x_2-x_1)}$ in Figure **4-3**. After eliminating the infeasible combinations, 110,922 configurations were simulated for each climate zone using EnergyPlus.

Table **4-2**: Variable details.

Variable	Min	Max	Range	Step	No. Options
SHGC state 1	0.1	0.8	0.7	0.05	15
SHGC state 2	0.1	0.8	0.7	0.05	15
VT state 1	0.05	0.8	0.75	0.05	16
VT state 2	0.05	0.8	0.75	0.05	16

Transition temperature (°C)	0	30	30	5	7

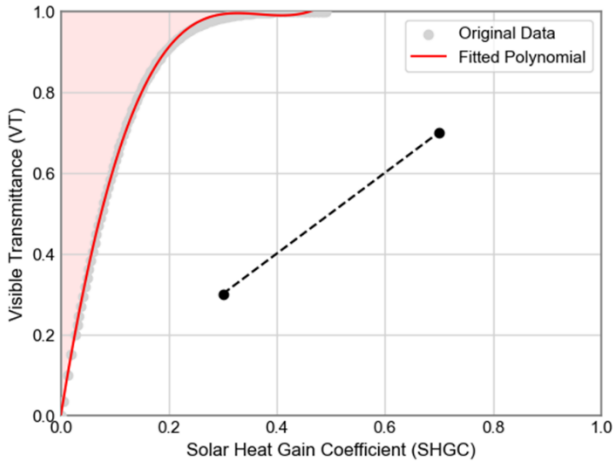

Figure **4-3**: Fitted polynomial to represent the forbidden zone. The goal is to find the ideal two-state dynamic glazing that minimizes electricity usage without violating the forbidden zone constraint.

Data generation

The two-state dynamic glazing was modeled using the EnergyPlus Energy Management System (EMS). An EMS program was developed for each window to control independently based on the window surface temperature. Since the windows were controlled based on the window surface temperature, the sensor used was 'Surface Outside Face Temperature' and the actuator used was 'Construction State'. The program was written such that if the sensor detected a value greater than the transition temperature, window construction state 1 was adopted, otherwise, window construction state 2 was adopted. The EnergyPlus model calling point was 'Begin Timestep Before Predictor,' which means that the programs were called prior to calculating zone loads. To generate the IDF files, the simple glazing system objects were modified for states 1 and 2, as well as the transition temperature which was a compact schedule object. These were

accessed using the Eppy library [164] in Python. After all the IDF files were written and the infeasible configurations eliminated, the simulations were conducted via parallel computing. The simulations were batched, and each batch ran on 20 cores with 32 GB RAM memory.

Results

Optimal solution and savings

The optimal solution was determined by identifying the configuration that yielded the greatest reduction in the combined annual heating, cooling, lighting, and fan electricity usage (Figure **4-4**). The facility electricity usage also includes the interior equipment, exterior equipment, and water system, which were constant for each climate. For Chicago (cool humid), Baltimore (mixed humid), Atlanta (warm humid), Duluth (very cold), and Minneapolis (cold humid) optimal configuration required a wide range of SHGC with the minimum SHGC at 0.1 and maximum at 0.8. However, the optimal configuration for Phoenix (hot dry) called for a minimum SHGC of 0.1 and maximum SHGC of only 0.2. Similarly, for Miami, the minimum SHGC was 0.1 and the maximum 0.15. All climates preferred a high visible transmittance, with a minimum VT of 0.6 and maximum of 0.8 or 0.75. Nevertheless, the LSG for state 1 is 6, suggesting that for all climates, decoupling SHGC and VT is important to reduce electricity usage. For state 2 in the hotter climates, the LSG remains between 4-5. However, in mixed and colder climates, the LSG is 1, which can be achieved with current products. Finally, the optimal transition temperature for all climates was 15 C.

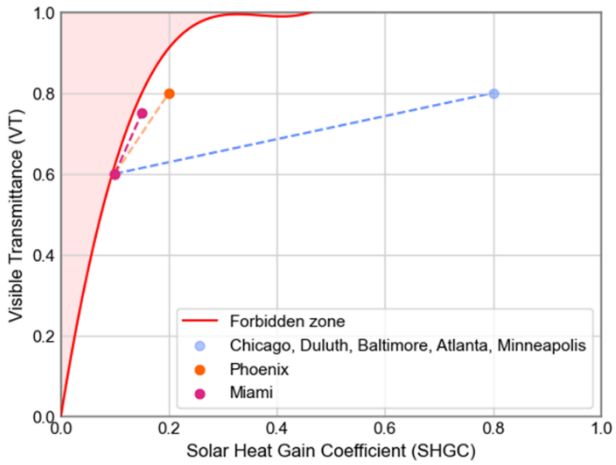

Figure **4-4**: The optimal two-state dynamic glazing for each climate zone.

The implementation of the optimal dynamic glazing system led to a reduction in combined annual heating, cooling, lighting, and fan electricity usage of 17.40%, 9.30%, 15.48%, 10.37%, 7.16%, 18.81%, and 17.91% for Chicago, Phoenix, Baltimore, Atlanta, Miami, Duluth, and Minneapolis, respectively (Figure **4-5**). The savings in Phoenix were lower because the baseline SHGC was 0.25 and the optimal states' SHGC was close at 0.1 and 0.2. Likewise, in Miami, the savings were also low with the baseline SHGC at 0.23. It also suggests that static glazing with high LSG may suffice in these climates. The percentage-wise reduction in each end use category varied per climate (Figure **4-5**). In Baltimore and Atlanta, the heating electricity usage was reduced the greatest, whereas in Chicago, Phoenix, Duluth, and Minneapolis, the cooling electricity usage was reduced the most, and in Miami, the fans electricity usage was reduced the most. For all climates, the lighting usage was reduced only a small amount (<5%), as the baseline model already implemented continuous dimming control and low wattage lighting (6.18 W/m^2).

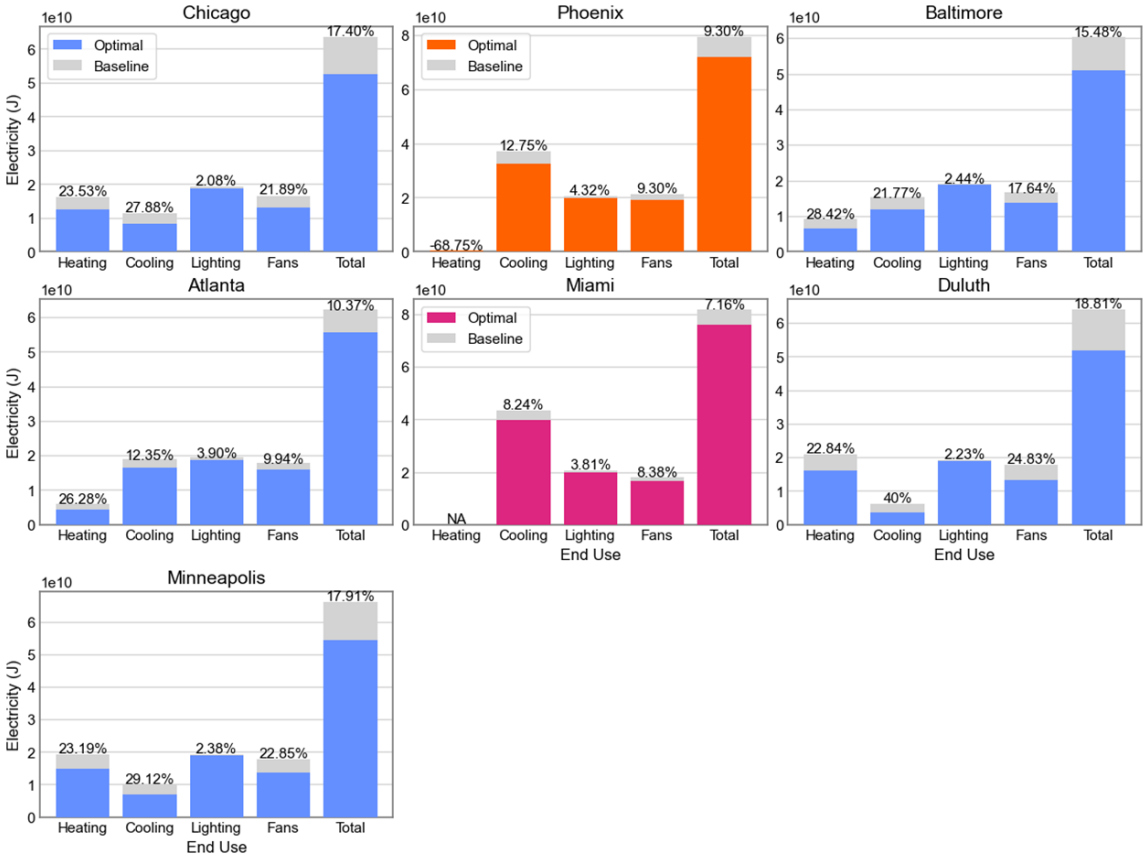

Figure **4-5**: Reduction across end use categories for all cities. The percentage decrease for each category is displayed above the corresponding bar.

To understand the frequency of switching between glazing states, the behavior of one south-facing window from the optimal configuration was plotted in Figure **4-6**. Figure **4-6** shows the window surface temperature (in gray) and the LSG at 10-minute intervals over the year. The optimal transition temperature for all climates was 15 C despite different window properties. In Chicago and Minneapolis, the window state transitioned most frequently during the shoulder months. Baltimore and Atlanta followed a similar pattern, with a larger gap during the summer months. On the other hand, Duluth, as a very cold climate, benefited from switching states in the summer months. Meanwhile, Phoenix consistently transitioned between states during the winter and spring, but not at all during the summer and fall, as the window surface temperature did not fall below 15 C. Miami demonstrated very little switching between states.

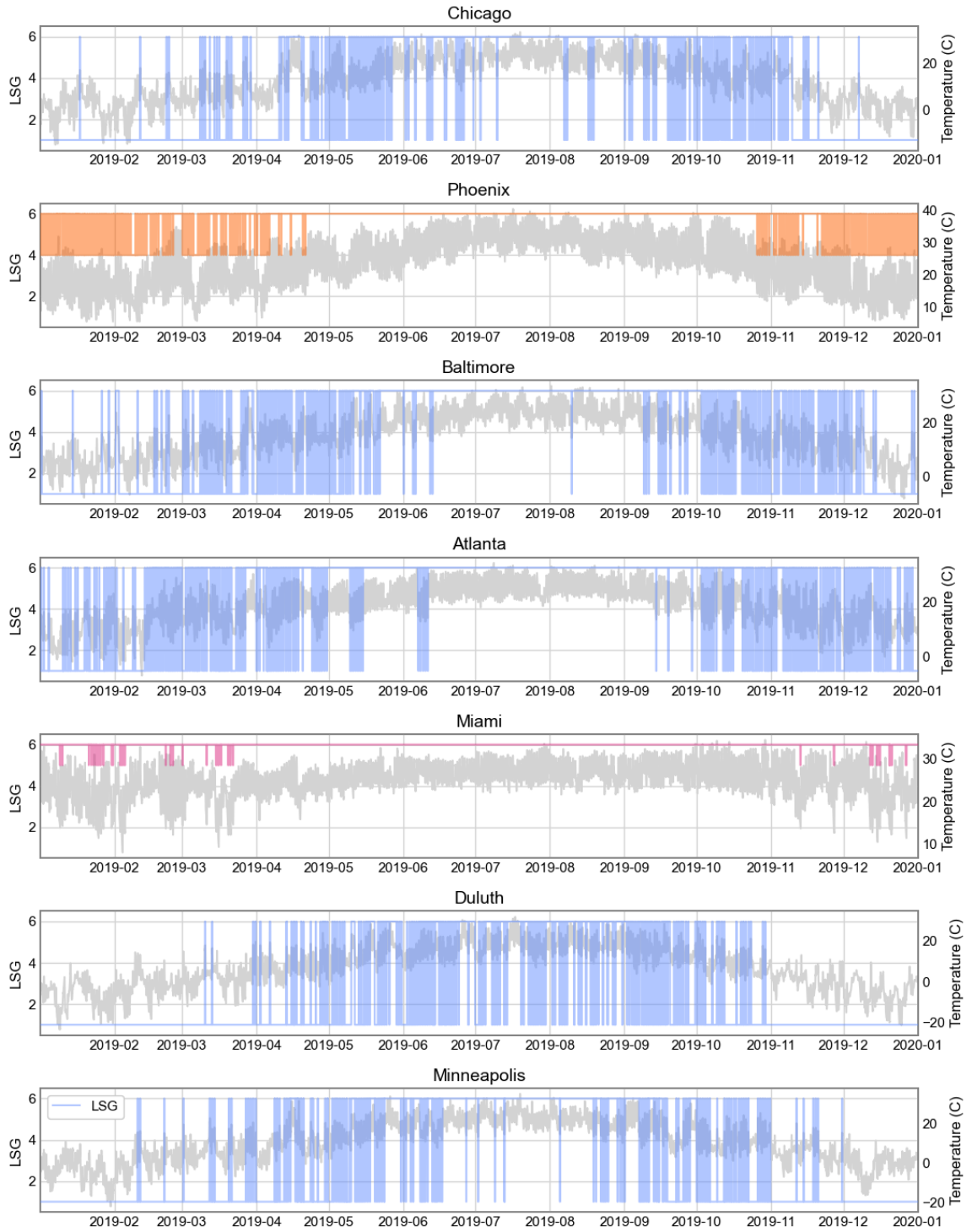

Figure **4-6**: Switching behavior for a south-facing window. The left axis plots the LSG and the right axis plots the window surface temperature in gray.

Next, to understand if there is a benefit to controlling each window independently, one window was plotted for each orientation for one day on or near the autumnal equinox, vernal equinox, or winter solstice, depending on which day was near the transition temperature for each climate (Figure **4-7**). It appears that there is little difference when the transition temperature is reached among the orientations, with the exception of a few morning hours where the east and south orientations reach the transition temperature before the east and north orientations, as well as in the afternoon where the west orientation returns to the transition temperature later.

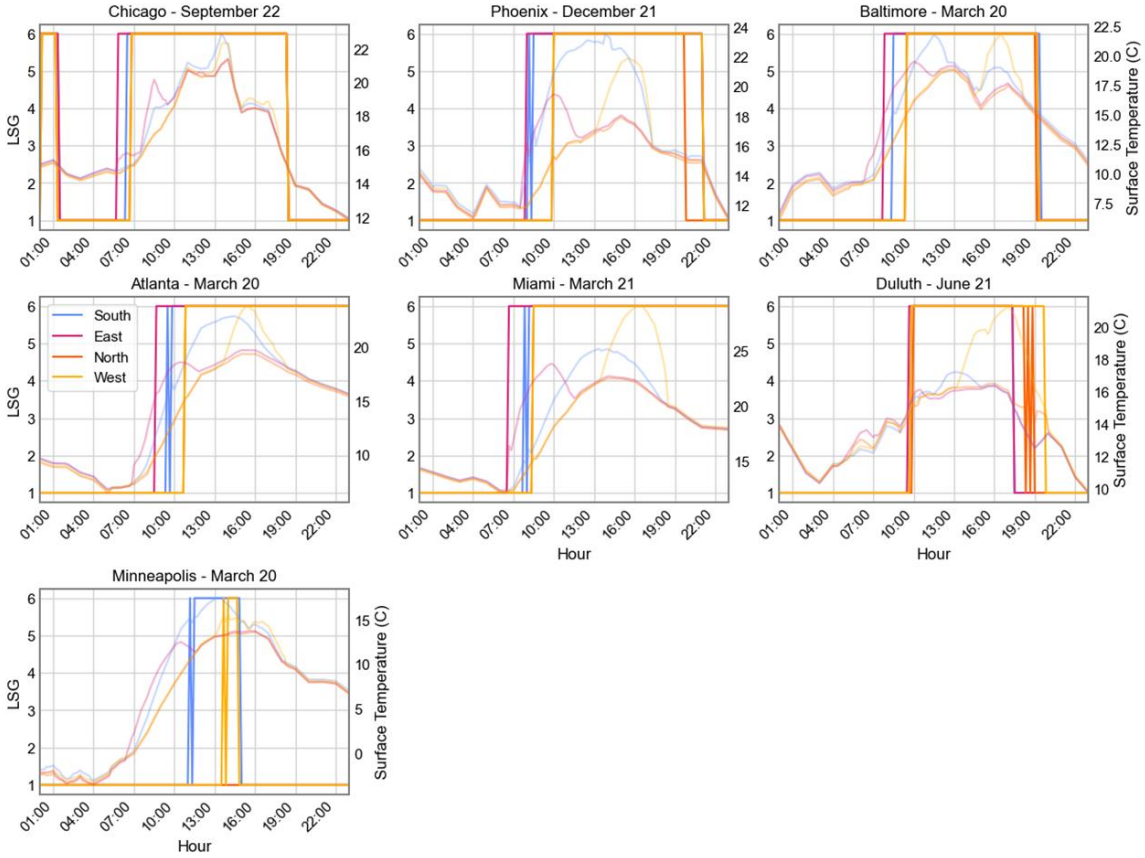

Figure **4-7**: Representative days to demonstrate differences across orientations.

Tradeoffs and sensitivities

In order to understand the importance of selecting the optimal transition temperature, particularly for the cold and mixed climates, a one-at-a-time type sensitivity analysis was conducted. Since all the cold and mixed climates selected the same dynamic window configuration, the data was filtered for this configuration, and then all transition temperatures were plotted in Figure **4-8** to quantify the difference in energy savings. It shows that the optimal transition temperature is near 15 C, and if the transition temperature is too high, the savings become negative, meaning that more energy is consumed than the baseline. This result demonstrates that transition temperature is also an important parameter to tune when specifying dynamic glazing technology.

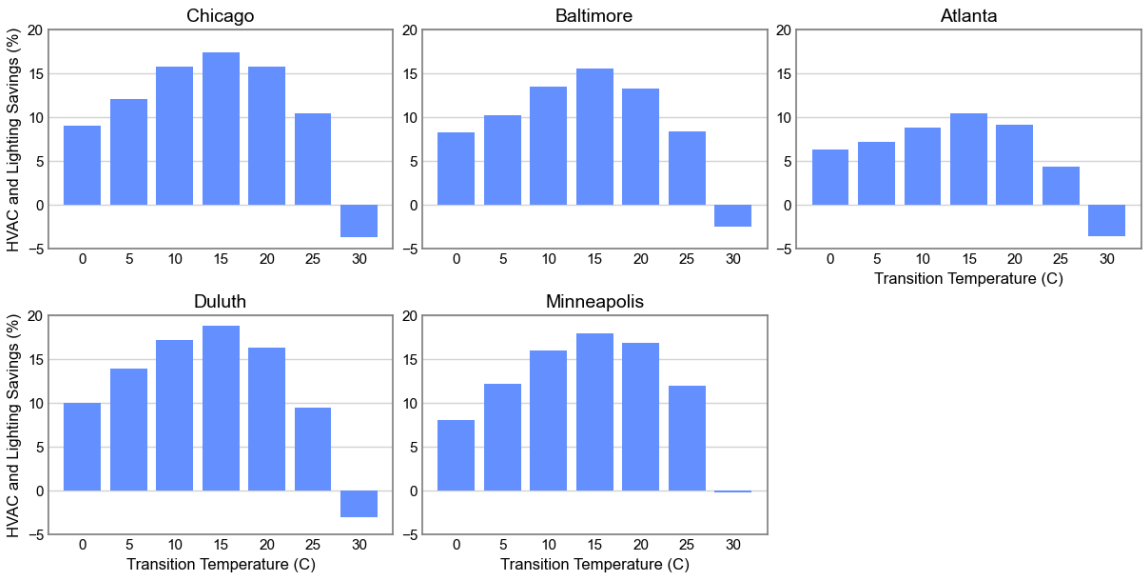

Figure **4-8**: Transition temperature sensitivity analysis for cold and mixed climates.

As mentioned previously, there has been several studies demonstrating the tradeoff between building energy savings and thermal comfort [146], [147]. To investigate if the optimal configuration sacrifices or improves thermal comfort, the facility electricity usage was plotted against the ASHRAE 55 simple model thermal comfort that measures the number of hours

summer or winter clothes are not comfortable (Figure **4-9**). Then, the pareto front was determined which represents the non-dominated solutions, and it is highlighted in Figure **4-9**. The optimal configuration for Chicago and Miami sacrifices thermal comfort, but there are other viable solutions along the pareto front. The optimal configuration for Phoenix, Baltimore, Atlanta, Duluth, and Minneapolis improve thermal comfort.

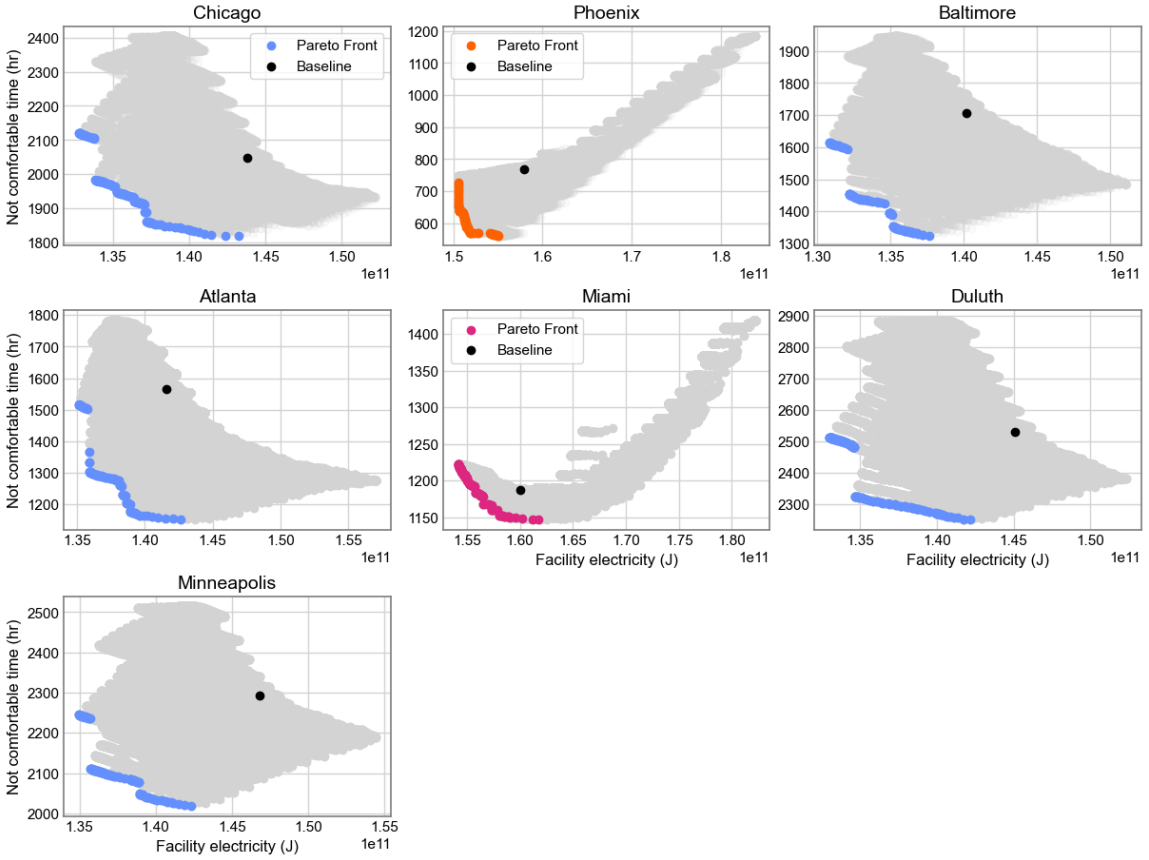

Figure **4-9**: Tradeoff between thermal comfort and facility electricity usage.

Discussion

Through exhaustive sampling, we identified the optimal two-state dynamic glazing system across multiple climates, revealing the ideal ranges for SHGC and VT and relationship between them. In climate zone 1 (Miami) and 2 (Phoenix), both SHGC and VT varied very little producing small ranges and achieving fewer energy savings. This suggests that a high-performance static glazing with very high LSG may be the most effective approach in these climates, rather than dynamic glazing technologies. However, in order to achieve very high VT (0.6) and low SHGC (0.1-0.2), solar light and heat must be decoupled. Such products in development include the use of silver nanoroads to achieve luminous transmittance greater than 50% and blockage of solar radiation by approximately 80% [165] and fluidic windows with luminous transmittance greater than 40% and SHGC 0.24-0.26 [166].

In the remaining cold and mixed climates (climates 4-7), implementing dynamic glazing technology with a high SHGC range and overall high VT would be most effective. The results demonstrate that in order to maximize energy savings, it is necessary to manipulate SHGC independently of VT, maintaining a relatively light VT while modulating SHGC from very low (0.1) to very high (0.8). This allows for minimal HVAC and lighting electricity usage. It appears dynamic glazing with decoupled SHGC and VT would be most effective in climate zone 5-7 which are considered cool and mixed, achieving up to ~19% combined HVAC and lighting energy savings. Even though dynamic glazing reduces the cooling load most percentage wise, climates with heating and cooling loads yield the highest total energy savings. Across all the climates, the optimal transition temperature was 15 C. A previous study on thermochromic glazing similarly found that the optimal transition temperature was 25 C across all climates tested [167], although the dynamic glazing properties were different.

While the results in this work serve as a guide for future product development, there were a few limitations. Firstly, the variables could have been discretized further to include more options, however, it would have led to significantly more simulations due to the exhaustive approach. Additionally, the simulations were only conducted for climates in the US, and future work should include more dry climates. Lastly, it has been previously shown that WWR influences energy savings [168], therefore it would be worthwhile to test on other building types with varied WWR.

Conclusion

This work exhaustively tested a two-state dynamic glazing system to determine the optimal range for VT and SHGC and ultimately identify which strategies of decoupling are viable for different climates. In cold or mixed climates, a dynamic glazing system with a large range in SHGC (0.1-0.8) and little variation, but overall high VT, is necessary to achieve maximum energy savings, which were over 17% in ASHRAE climate zone 5a. However, in hot climates, less variation is needed for SHGC and VT, instead static window products with very high LSG are perhaps most appropriate. In both cases, it is clear that decoupling solar heat and light to achieve high VT and low SHGC is necessary to maximize energy savings. Additionally, although cooling load is most effectively reduced through dynamic glazing, the highest overall savings were in mixed or cold climates that also had heating requirements. While such a dynamic glazing technology could be achieved in different fashions, this work identifies the optimal ranges to target for VT and SHGC switching.

Chapter 5

Introducing dynamic façades in early design using constrained optimization

This chapter has been published as:

L. E. Hinkle, J. Wang, and N. C. Brown, "Quantifying potential dynamic façade energy savings in early design using constrained optimization," *Building and Environment*, vol. 221, Aug. 2022, doi: 10.1016/J.BUILDENV.2022.109265.

Introduction

Buildings consume around 40% of primary energy around the world [140], which creates both a challenge and a set of opportunities for designers. With the introduction of parametric design and rapid simulation, computational tools are increasingly leveraged during early design to iteratively explore features or configurations that can mitigate or offset building energy loads. Researchers have experimented with design approaches ranging from optioneering to automated optimization to produce low-energy buildings. While optimization can be implemented with varying degrees of user input [13], [42], [169], it can quickly direct designers towards high-performance solutions within a design space. Within the emerging research field surrounding dynamic building envelope materials, including thermochromic- and electrochromic-based glazing [144], [153], [170], [171] and PCMs [15], [172], [173], optimization has been used to maximize energy savings. Dynamic building façade characteristics open the possibility of variation at high-resolution time intervals for external stimuli such as solar radiation, wind availability, and heatwaves, as well as long-term changes such as an evolving climate or new buildings constructed nearby that can occur years or decades into the lifetime of a building.

Existing studies show the performance of dynamic façade materials is highly sensitive to orientation, self-shading, and radiant heat exchange in relation to building shape. However, the dynamic material properties are often determined after the early-stage architectural design is established.

Due to limitations in simulation tools and the novelty of many dynamic technologies, the interplay of geometric and material design decisions and their joint effects on energy performance have not been extensively explored using computational tools. Additionally, the steps of the traditional building design are often sequential, which can limit opportunity for early integration [45], [174], [175]. The traditional building design process for commercial buildings first establishes a building form, and then develops the floorplan and façade construction, which can separate decisions about geometry and materials [176]. Yet the façade plays a key role in regulating the indoor thermal environment, and materials selection heavily influences energy performance. It is unlikely that sequentially optimizing a building's massing and glazing placement, and then its floorplan for that set geometry, and finally the façade construction will lead to the best overall result, since geometry, program, and materials all affect one another.

Overall, these divergences necessitate a platform to explore complex building geometries and emerging dynamic building envelope materials taking both optical and thermal properties into account. In response, this paper first quantifies simulated energy saving across different optimization-based building design procedures for dynamic glazing materials via two office building case studies in separate climates. A comparison between approaches can evaluate the current sequential design process as it applies to dynamic materials and reveal the importance of design decisions related to dynamic materials on energy savings. Only glazing was modeled as dynamic rather than other opaque façade elements, due to the proliferation of highly glazed contemporary office buildings and the current outlook of advanced glazing technologies.

Following these analyses, this paper proposes a new building design process to determine the optimal material-geometric configuration.

In summary, this study presents three unique contributions:

1) it establishes a new optimization-driven framework with parametric modeling and simulation methods at the early design stage for taking both geometry and dynamic material (thermal and optical) properties into account.

2) it increases understanding of the relationship between these two categories (geometry and material) of design variables towards building energy performance, especially in the context of intrinsic dynamic material limitations, while establishing the potential benefits of joint exploration; and

3) it quantitively illustrates the architectural and performance implications of using such an approach in early design. It does this for a suburban commercial case study in a heating-dominated climate and an urban commercial case study in a cooling-dominated climate, providing new information for two building types most likely to be designed using computational tools.

Literature review

Simulation in early design

Computational tools are currently a vital part of building design, helping to visualize or automate many intricate tasks. They are utilized in all phases of design, from design ideation to construction documentation. In the AEC industry, one important computational area for early design is parametric design, which allows for the generation of numerous design iterations without significant manual effort [20], [21], [177]. Parametric design is often implemented

through visual coding platforms such as Grasshopper [22] or Dynamo [178] in which users develop dynamic design variables to explore combinations of these variables and ultimately investigate interrelated design goals. During early design, designers also make assumptions about building systems and occupant behavior to simulate and predict how a constructed building will perform.

Creating combinations of the variables forms a “design space”, and mapping these designs to metrics that describe their performance, whether related to structure, energy, or daylighting, generates an “objective space” [130]. The goal is often to explore the design space with reference to the objective space in an effective and systematic manner. It has been shown that utilizing design space exploration methods allows designers to develop and select high performance design concepts for gradual refinement throughout later stages [21], [179], [180]. Since simulation engines across multiple domains are now accessible within a shared environment, research towards dynamic façade systems in buildings has taken advantage of these software environments used by designers today. However, there is limited existing literature that applies parametric design for both geometrically and materially flexible design decisions to understand the energy implications of designing with dynamic building materials.

Quantifying potential dynamic façades energy savings

Many researchers claim dynamic façades are necessary to achieve nearly net zero buildings (nNEB) [181]. Dynamic façades alter their form or function repeatedly and reversibly over time in response to environmental conditions or human controls [182]. Dynamic façade technologies refer to both micro-scale properties of façade materials, including thermochromic glazing [17], memory shape polymers [183], and phase-change materials [15], [173], [184], [185], and physical-scale elements such as kinetic shading devices [186], [187]. While a variety

of technologies are possible, this paper focuses on the micro-scale, specifically adaptive glazing technologies. Existing studies have demonstrated whole building energy savings of using dynamic façade technologies range from 8-46% [188], [189], [190], even compared with static high-performance envelopes. While electrochromic glazing is perhaps the most mature and widely implemented example, material scientists are working in coordination with architectural engineers to improve the thermal and optical capabilities of dynamic glazing [188]. Existing electrochromic glazing operates from state-to-state, where there is a strict tradeoff between visible transmittance (VT) and solar heat gain coefficient (SHGC). Adaptive u-value may be achieved through switchable insulation elements [191], thermochromic technologies that change emissivity [192], or other future technologies. However, several researchers have explored the optimization of adaptive glazing properties to justify further development of the technology.

Several previous studies have investigated dynamic glazing technologies across multiple climates, on different resolutions (e.g., monthly, daily, hourly), and with various control strategies. Wang et al. [190] used EnergyPlus EMS to alternate both opaque assemblies and window construction and achieved an average of 46% energy savings across multiple climate zones. Favoino [17] investigated an inverse performance-oriented approach to optimize visible transmittance (VT), g-value, and U-value to minimize primary building energy. Using an office reference room with 40% window-to-wall ratio (WWR) and four cardinal orientations tested in multiple climates, the study showed high energy savings are achievable by adapting the transparent part of the building envelope alone, the largest factor being cooling energy demand. Since dynamic façade systems respond to outdoor climatic conditions, results varied per orientation and location, with the highest achievable savings 55% for an east-facing zone in Rome, Italy. Similarly, Tavares [193] recommended electrochromic glazing for cooling-dominated climates and found the largest savings on the east and west façades, rather than the south. As mentioned previously, these findings suggest dynamic façade materials are highly

sensitive to their immediate environment, which is dictated by the geometry of the building. This notion introduces the possibility of early design intervention, which is explored throughout this study.

While many researchers have focused on simulating existing or theoretical dynamic envelope materials, others have focused on the control algorithms themselves, which have a large influence over performance [194]. Hoon Lee [144] investigated various control parameters, including outdoor air temperature, room air temperature, solar radiation incident on windows, and global horizontal irradiance to develop an algorithm for optimal electrochromic performance. Using ASHRAE 90.1 prototype for a medium office building as a reference, the size of the cooling equipment was reduced by up to 20%. It was acknowledged additional savings could be achieved by integrating controls with air handling units, lighting controls, and shading systems; most importantly, the study concluded that future studies should utilize real building data. In additional efforts to develop a control strategy, Wang et. al [87] performed a multiple regression analysis of window factors based on a large database of existing windows and incorporated the model into an EnergyPlus simulation-based optimization study. Though this model was developed to optimize on an annual basis (static), it could be used to investigate optimization on a daily or monthly resolution, and it is indeed incorporated into the methodology of this paper. As in previous studies, the ASHRAE prototype model was assumed and used as a reference in comparing energy savings. Although this model acts as the standard, it does not capture the potentially complex geometries of contemporary office building architecture.

Building geometry optimization

In early design stages, there are opportunities to conduct optimization on building form and fenestration configuration [195]. For most climates, the ratio between the external surface of

a building and its volume most strongly correlates to energy demand, meaning that simplified models can be adequate [196]. However, some researchers have demonstrated exceptions. For example, Granaderio et al. [197] used a case study in Lisbon, Portugal to show that the surface area to volume building shape coefficient was not strongly correlated to energy demand. Similarly, while Depecker et al. [198] found a strong correlation between shape coefficient and energy consumption for a case study in Paris, France, there was no clear correlation for the case study in Carpentras, France. Further, building geometry optimization results differ depending on the formulation of the design space. Fang [40] performed multi-objective optimization on nine geometric variables for a small single-story building, reducing Energy Use Index (EUI) by up to 20% while increasing Useful Daylight Index (UDI) by 39%. Jin and Jeong [24] used a genetic algorithm to optimize a free-form building shape, including geometric parameters such as top polygon type, top length, and tilt angle, and were able to reduce annual heat gain/loss by up 60.4% in certain climates. While these case studies exist in specific climates and design spaces, they demonstrate that geometric considerations can affect building energy consumption, often in complex ways.

Other researchers have approached this problem by determining the most influential geometric characteristics for predicting energy. Samuelson et al. [23] conducted a sensitivity analysis on various early design building characteristics, including WWR, glass type (static), building rotation, shading, and shape, and determined that, across three major cities, WWR was the most sensitive variable, followed by glass type and rotation. There have been several additional studies exploring the relationship between building geometry and building energy consumption, but the few that have [41] included dynamic characteristics investigated prototypical building types, not potentially self-shading or otherwise complex geometry. Thus, it is difficult to estimate the effects of dynamic façades, both in terms of energy savings and effects on the building design process.

Upon reviewing the sensitivity analysis literature above, there is a further opportunity to implement optimization techniques instead of exhaustive search methods, since optimization can more quickly find the best possible designs within a space and present those for consideration to the designer. However, to fully address the relationship between geometric changes under the direction of an architect and potential dynamic façade properties, realistic case studies must be developed, along with constraints that avoid architecturally infeasible solutions. If incorporating dynamic variables and using non-reference building geometry, an optimization procedure can begin to quantify the potential savings limits of modifying different variable types.

Methodology

The methodology investigates optimization-driven, rapid parametric modeling approaches for early building design in practice. As such, it required the creation of parametric models with realistic design variables, constraints, and model resolution that would be considered at this stage of design. Two case studies with different contexts and climates were modeled and analyzed to compare the effects of modifying building geometry and dynamic façade materials on building energy consumption, in sequences and combinations allowed by current simulation-integrated design tools. The procedure for testing the case studies included developing a parametric design space in Grasshopper, establishing an analytical daylighting constraint, simulating energy performance using EnergyPlus [199] through ClimateStudio [128], using a local derivative-free constrained optimization algorithm to find the best performing designs for different sequences, and analyzing the data against multiple baselines (Figure **5-1**). This section first describes the optimization sequences before detailing the case studies themselves.

Figure **5-1**: General framework for optimization procedures.

Rather than a design space exploration or "catalog" approach, which generates options and presents them for consideration, this paper uses optimization to drive towards the best energy performing designs. Obtaining optimization results establishes limits for how much energy could potentially be saved using parametric methods, even if designers might use data generated during optimization only to inform decisions rather than fully automate them. The data in this paper were generated through eight constrained optimization runs and subsequent combinations of variable settings, described in Table **5-1**. For each case study, this includes an optimization of geometric variables (Geo) and dependent dynamic glazing variables based on typical behavior (DG-E). The dynamic existing runs (DG-E) relied on a regression relationship between material properties U-value, SHGC, and VT based on current material databases [87], representing a realistic configuration possible with current technologies.

The optimal settings for each optimization (geometric and glazing) are then combined, replicating a sequential process in which the designer first optimizes one category and then optimizes the other category (Geo → DG-E and DG-E → Geo). Finally, to estimate the importance of each variable type for energy savings directly and compare with the overall optimization procedures, a random forest regression model was built to calculate feature importance. Figure **5-2** summarizes relationships between the different optimization runs and combinations, listing run numbers for case study 1; the same sequence is repeated for case study 2.

Table **5-1**: Optimization run specifications.

Run	Description	Case study		Dynamic glazing optimization	Geometry optimization
		1	2		

1	Geo	x			x
2	DG-E	x		x	
3	Geo → DG-E	x		x	
4	DG-E → Geo	x			x
5	Geo		x		x
6	DG-E		x	x	
7	Geo → DG-E		x	x	
8	DG-E → Geo		x		x

It was hypothesized that such a sequential process may not reach the full savings potential, and that simultaneous optimization of both variable types is the most effective strategy. However, limitations in current design and simulation tools contain barriers to simultaneous optimization of dynamic properties at high resolution—platforms that enable fully flexible modeling of geometry and platforms that enable fully flexible modeling of dynamic properties (as opposed to existing technologies) are not fully integrated. While future possibilities for simultaneous optimization with full flexibility are discussed in later sections, this paper makes contributions by first considering both geometry and dynamic properties using available design methods and corresponding sequences and timescales.

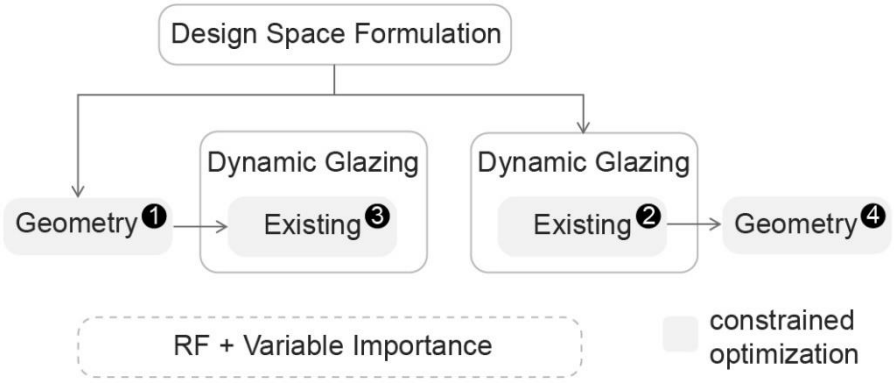

Figure **5-2**: Flowchart explaining the constrained optimization runs where the run numbers correspond to Table 5-1.

Case study selection

Figure **5-3**: Case study 1 (left) and 2 (right) location and site.

This study focuses on commercial buildings, which are frequently designed with computational approaches. Two case study sites were selected to represent common office building typologies (Figure **5-3**). Commonalities between archetype characterization methods in building energy modeling include climate, population classification (urban, suburban, rural), fenestration specifications, and building height [200]. Given the density of large office buildings, this paper considers urban and suburban cases. Case study 1 was inspired by Lake Trust Credit Union Headquarters in central Michigan [201], which is a mid-rise suburban office building with ribbon windows. This building features a curved north façade, providing ample opportunity for geometric exploration including glazing placement as well as overall orientation and shape in plan. Case study 2 was inspired by 1603 Broadway in San Antonio, Texas [202]. This building is a high-rise with a curtain wall construction and a more compact footprint for an urban setting, which limits some potential geometric interventions. Dimensions, layouts, and model settings were approximated using Grasshopper plug-in Elk [203]. Additional information about each case study is provided in Table **5-2**.

Table **5-2**: General case study assumptions.

	Case study 1	Case study 2
Inspiration building	Lake Trust Credit Union Headquarters	1603 Broadway
Location	Brighton, Michigan	San Antonio, Texas
Gross building area (m^2)	9290	58530
ASHRAE climate zone	5	2
Population classification	suburban	urban
Window-to-wall ratio	0.4	0.4
Number of floors	3	15
Floor-to-floor height (m)	4.6	4.6

Design space formulation

In contrast to previous studies using static benchmark geometry, a design space was established containing flexible form, orientation, and fenestration to accurately represent early design, in which alternatives are considered but some affinity to an original design concept is maintained. This was done to quantify the energy savings potential of architect-designed office buildings and understand the gaps in the traditional design process that may prevent widespread implementation of dynamic façade materials. Parametric variables are described in Tables **5-3** and **5-4** and visualized in Figure **5-4**. In each design, three fenestration variables were extrapolated: sill height, head height, and the percentage of opaque panels. The façades were panelized into linear sections, and the percentage of opaque panels dictated how many panels were assigned opaque construction versus glazing. Case study 1 also included three control points along the curved façade, building rotation, and a variable that transitions between a linear and L-shaped form (v_8). Case study 2 allows for variation of floor area distribution between the tower and podium building volumes, adjustments in length-width aspect ratios, and tower location. Additionally, because Case study 2 is located in an urban setting with surrounding obstructions,

the entire building can move around on the site (v_4, v_5). By incorporating the unique aspects of each building geometry, such as the curvature and the tower/podium relationship, this study attempts to capture the design implications of optimizing contemporary office building architecture.

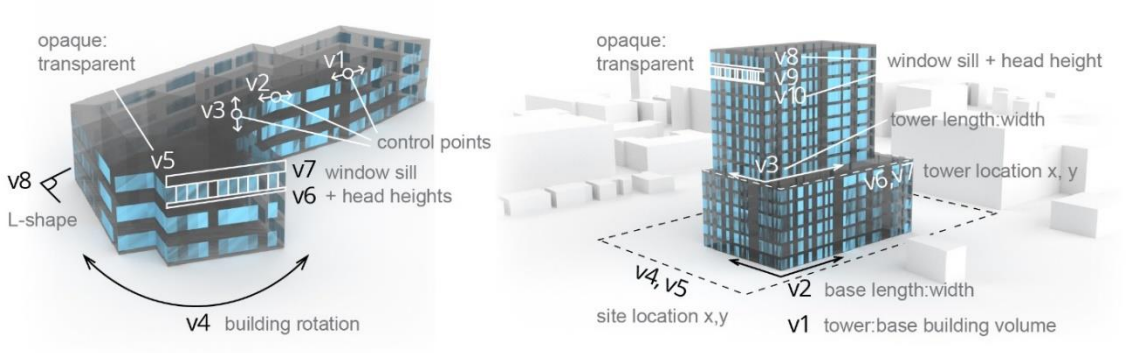

Figure **5-4**: Variables used to generate the design space, case study 1 (left) and 2 (right).

Table **5-3**: Case study 1 geometric variables.

	Variable	Minimum	Maximum	Range	Original Design
v1	Curve control point 1* (m)	0.50	0.75	0.25	0.65
v2	Curve control point 2* (m)	0.50	1.75	1.25	1.15
v3	Curve control point 3* (m)	0.01	0.49	0.48	0.25
v4	Site rotation (deg)	0.00	360.00	360.00	0.00
v5	Window fraction	0.01	0.98	0.97	0.15
v6	Window head height (m)	2.00	4.37	2.37	3.00
v7	Windowsill height (m)	0.20	1.00	0.80	0.65
v8	L-shape (deg)	0.00	25.00	25.00	0.00

*Moves control point with respect to the start of the defined façade curve

Table **5-4**: Case study 2 geometric variables.

	Variable	Minimum	Maximum	Range	Original Design
v1	Tower: base building volume fraction	0.20	0.60	0.40	0.40
v2	Base length-width aspect ratio	0.50	2.00	1.50	0.85
v3	Tower length-width aspect ratio	0.50	2.00	1.50	0.75
v4	Site location x	0.00	1.00	1.00	0.50
v5	Site location y	0.00	1.00	1.00	0.50
v6	Tower location x	0.25	0.75	0.50	0.50
v7	Tower location y	0.25	0.75	0.50	0.35
v8	Windowsill height (m)	0.20	1.00	0.80	0.60

v9	Window fraction	0.01	0.98	0.97	0.3
v10	Window head height (m)	2.00	4.37	2.37	3.5

Additional variables were established for the dynamic properties of both façades. Glazing properties were accessed through ClimateStudio's window component in Grasshopper. This component wraps the simple window component from EnergyPlus, which allows users to create custom glazing by specifying VT, SHGC, and U-value. The bounds of the glazing variables were established by surveying existing window products in the LBNL glazing database within Climate Studio's glazing component. The bounds for each glazing variable are provided in Table **5-5**.

Table **5-5**: Glazing variable bounds.

	Variable	Minimum	Maximum	Range	Original Design
v9/v11	U-value (W/ m^2-K)	0.67	5.82	5.15	*See Table 6*
v10/v12	VT	0.05	0.91	0.86	*See Table 6*

Window products that are commercially available abide by physical restrictions between VT and SHGC. In general, to decrease SHGC, VT must also decrease, which creates a tradeoff between building energy and daylight. Wang et al. [87] built multiple regression models to relate four main glazing properties: solar heat gain coefficient (SHGC), visible transmittance (VT), U-value (U), and emissivity (E). Using a database of existing window products, Equation 1 was identified as the most accurate model. As current glazing technologies largely follow this relationship, the dynamic glazing optimization included only U-value and VT as variables, and SHGC was calculated using Equation 1. Emissivity was held constant at E=0.84 per typical window construction.

$$SHGC = 0.023 + 0.44 * VT + 1.88 * E + 0.002 * U - 2.38 * E^2 + 0.28 * VT * E$$

(Equation 1) [87]

Performance evaluation

Energy model simulations were performed in Grasshopper using the energy components of ClimateStudio. ClimateStudio links geometry in Rhinoceros to the EnergyPlus simulation engine. The formal optimization objective was to minimize the site energy consumption due to heating, cooling, and lighting requirements, which represent the aspects of operational energy which are affected by geometry and the façade (Equation 2). The objective function was subject to the daylighting constraint, which depended on whether the run included geometric optimization (left) or dynamic glazing optimization (right) (Equation 2). The daylighting constraint is described in following section. The envelope assumptions were determined based on ASHRAE 90.1 2019 in the respective climate zones. Consistent with the DOE prototype for large office buildings, the case study models were mechanically zoned to have four perimeter zones with 4.57 m zone depth and a core zone on each level. All other model settings were also based on ASHRAE 2019 standards and are provided in Table **5-6**.

$$\min f(x) = \frac{\sum_{i=1}^{n}\left(COP \times Q_{cooling,i}\right) + \left(PF_1 \times Q_{heating,i}\right) + \left(PF_2 \times Q_{lighting,i}\right)}{GSF}$$

$$s.t.\, g(x) = \frac{\left(\frac{0.88 \cdot DF}{VT} \cdot \frac{90°}{\theta}\right) - WWR}{\left(\frac{0.88 \cdot DF}{VT} \cdot \frac{90°}{\theta}\right)} < 0 \;\; or \;\; \frac{\left(\frac{0.88 \cdot DF}{WWR} \cdot \frac{90°}{\theta}\right) - VT_{avg}}{\left(\frac{0.88 \cdot DF}{WWR} \cdot \frac{90°}{\theta}\right)} < 0$$

$where\ i\ is\ the\ load\ condition\ at\ a\ particular\ hour\ and\ n\ is\ the\ number\ of\ hours$ (Equation 2)

Table **5-6**: EnergyPlus settings accessed via Climate Studio.

	Case study 1	Case study 2	Units
Roof R-value*	5.28	4.40	K-m^2/W
Exterior Wall R-value*	2.01	1.00	K-m^2/W
Floor R-value*	2.57	1.11	K-m^2/W
Window SHGC*	0.38	0.25	
Window U-value*	2.04	2.55	W/ K-m^2
Window VT***	0.60	0.60	
Schedule*	Typical office occupancy, equipment, and lighting		
Occupancy*	0.05		p/m^2

Equipment*	8.07	W/m^2
Lighting power density*	6.89	W/m^2
Daylighting*	Continuous dimming, 500	lux
Heating set point*	21 (constant setpoint – all on)	°C
Cooling set point*	24 (constant setpoint – all on)	°C
Mechanical ventilation**	2.5	L/s/person
	0.3	L/s/zone area m^2
Heat recovery***	Sensible, 60% recovery effectiveness	
Infiltration**	0.5	ACH
Peak flow****	0.12	L/h/person
Supply temperature***	60	°C
Mains temperature***	10	°C

*ASHRAE 90.1, **ASHRAE 62.1, ***Industry standard, ****LEED spreadsheet

The ClimateStudio components output the idealized heating, cooling, and lighting energy in Joules (J). The idealized loads were converted to site energy requirements assuming the system efficiencies listed in Table **5-7**. To make direct comparisons as building geometry changed, building energy consumption was normalized by the gross building area (GSF).

Table **5-7**: Secondary energy conversion assumptions. Values from [5].

	Load	Assumption
PF_1	Heating	85% site efficient
COP	Cooling	COP = 3
PF_2	Lighting	100% site efficient

Optimization method

To find the best possible results for each case study and sequence, local derivative-free constrained optimization was performed on the building geometry and glazing properties. Specifically, COBYLA (Constrained Optimization BY Linear Approximations) was implemented through the Grasshopper component Radical, available with the Design Space Exploration (DSE) plug-in [130]. This algorithm models the objective and constraint functions by linear interpolation

[204]. A local derivative-free optimization approach led to shorter run times compared to evolutionary algorithms, since it constructs successive linear approximations of the objective function and constraints via a simplex of n+1 points (in n dimensions) and optimizes these approximations in a trust region at each step, leading to fewer evaluations [205]. For a starting point, all variables were set to the middle point. The convergence criterion was a 0.01 change in objective function.

While building geometry was optimized on an annual basis as a static characteristic, glazing properties were optimized on a monthly resolution. Previous electrochromic glazing studies identified monthly simulations as a sufficient starting point to estimate energy savings [17]. Once the optimal properties for each month were determined, the monthly building energy values were summed to represent annual building energy. Because the beginning of each monthly simulation begins a new environment in EnergyPlus, there is a small discrepancy between summing monthly values and the result of a single annual simulation. The authors determined this error was less than 1% for the case study models.

Reviewing previous related optimization studies revealed a tendency to reduce the glazing area and lower visible transmittance well below industry-accepted values. As the main arguments of this paper are based on the typical building design process at the conceptual design phase, it seemed inappropriate to deem the optimal solution as one with small windows with low visible transmittance. However, accurate daylighting simulations are computationally expensive. To counter the algorithm's tendency to minimize glazing area, a daylighting proxy constraint was implemented on window-to-wall ratio (WWR) and VT. The minimum WWR required to meet daylighting requirements was calculated using a rule of thumb-based design sequence for sidelit spaces by Reinhart and LoVerso [206].

This basic calculation, intended for early design, is given in Equation 3, which was used to formulate the constraints (Equations 4 and 5). The daylight factor (DF) was set to 2%

according to recommendations in the IES Handbook [207]. It was assumed there were no obstructions in case study 1, therefore the obstruction angle θ was set to 90°. The obstruction angle in case study 2 was dynamically calculated as an output of the parametric model (Figure **5-5**). During geometric optimization, the relative error between the calculated WWR ratio (Equation 4) and that of the actual design was entered as a formal constraint. Similarly, the relative error between the calculated VT and average VT among all orientations (Equation 5) was adopted as a formal constraint. Note that Equation 2 is an approximation and accounts only for diffuse daylight contribution. Further analysis would be required for glare considerations in later design, but these constraints help ensure realistic glazing requirements as determined by the architecture.

$$WWR > \frac{0.088 \cdot DF}{VT} \cdot \frac{90°}{\theta} \qquad \text{(Equation 3 [206])}$$

$$\frac{\left(\frac{0.088 \cdot DF}{VT} \cdot \frac{90°}{\theta}\right) - WWR}{\left(\frac{0.88 \cdot DF}{VT} \cdot \frac{90°}{\theta}\right)} < 0 \qquad \text{(Equation 4)}$$

$$\frac{\left(\frac{0.088 \cdot DF}{WWR} \cdot \frac{90°}{\theta}\right) - VT_{avg}}{\left(\frac{0.88 \cdot DF}{WWR} \cdot \frac{90°}{\theta}\right)} < 0 \qquad \text{(Equation 5)}$$

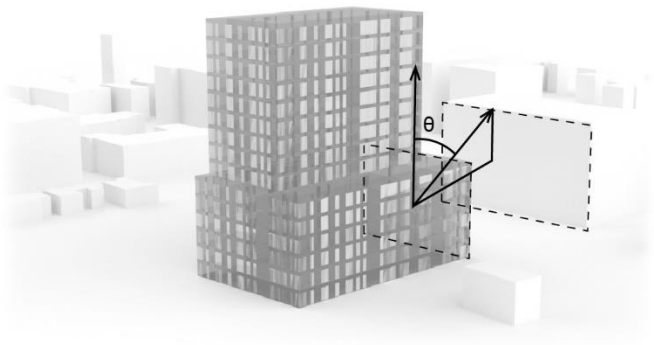

Figure **5-5**: Case study 2 obstruction angle diagram.

Results

In this section, the results of each constrained optimization run are first presented and analyzed to compare potential energy savings from manipulating different variable types. Then, sequentially designing with dynamic façades is evaluated. Finally, relative variable contributions are assessed directly.

Optimal geometry

The results of the simulated potential energy savings due to geometric optimization only are provided in Figure **5-6**, offering very little savings (1-2%). The design space was formulated to preserve original design intent, which may have limited savings slightly. However, this result confirms previous evidence that building form itself is not a good indicator of energy consumption [23]. Yet in some cases, 1-2% savings may still be desirable, and the designer must weigh architectural implications while deciding if altering the building geometry is worth it. Despite the small savings, both cases apparently responded to climate and context. Case study 1, located in a suburban setting, took advantage of its ability to fully rotate and oriented the façade with the greatest glazing area toward the south. It is likely that this geometric alteration, in addition to reducing glazing area within the daylight constraint, had the largest contribution to the energy savings. Case study 2 was more geometrically limited to account for the challenges of designing in an urban setting. While case study 1 leveraged solar gains to reduce the heating load, case study 2 attempted to block them. More square footage was distributed to the podium, rather than the tower since the podium receives shade from context. However, during optimization, the model moved away from adjacent buildings to satisfy the daylighting constraint.

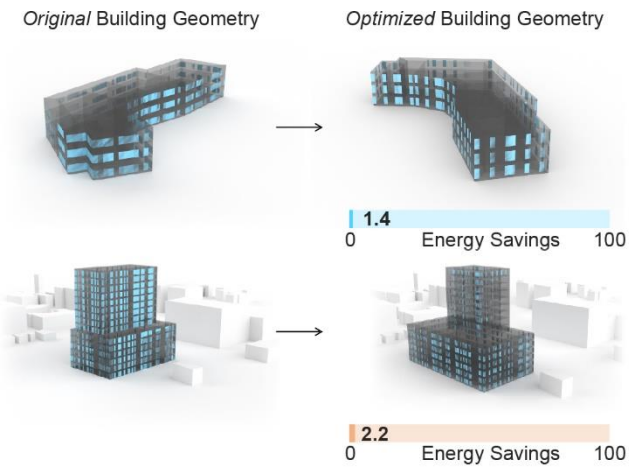

Figure **5-6**: Original vs. optimized building geometry for case study 1 (top) and case study 2 (bottom).

Optimal dynamic glazing properties

Results for optimization of the dynamic properties are shown in Figure **5-7**. A single dotted line follows the changing monthly setting for a glazing property on one side of the building. Overall savings for each constrained optimization run are provided at the bottom of each column.

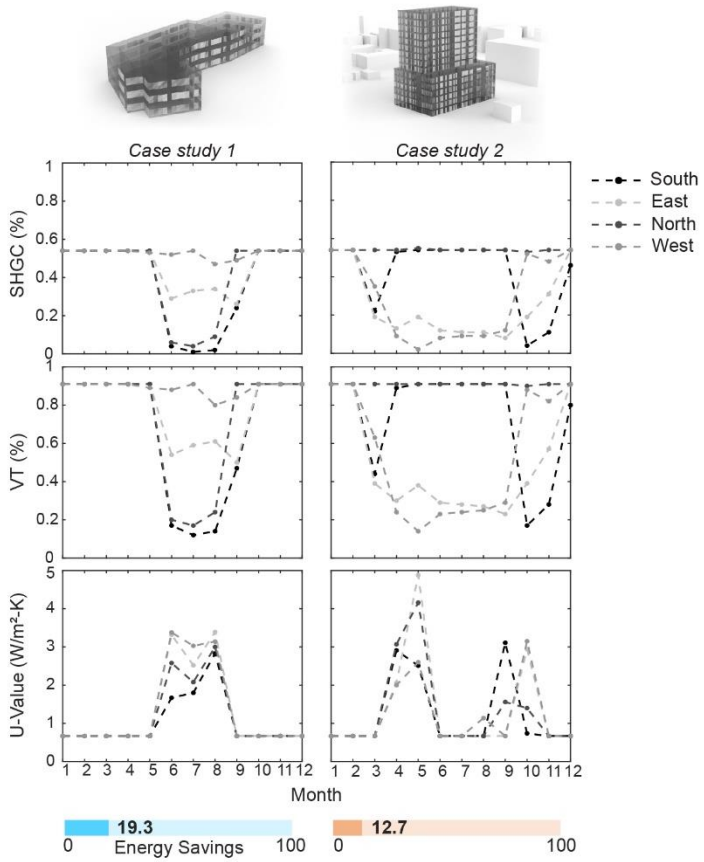

Figure **5-7**: Optimal glazing properties on a monthly resolution.

SHGC and VT

The existing constrained optimization results account for the relationship between SHGC, VT, and U-value, which was previously established using existing window product data [87]. Case study 1 optimization selected a higher SHGC in the winter months to accept solar gains and decrease the heating load and selected a lower SHGC in the summer months to block solar gains and decrease the cooling load. The case study 2 optimization instead opted for a lower SHGC the majority of the year. The optimal SHGC results are appropriate given case study 1 is located in ASHRAE climate zone 5 (heating-dominated), and case study 2 is located in ASHRAE climate

zone 2 (cooling-dominated). For case study 1, the south façade is dominated by the SHGC so it must be varied, whereas the north façade is constrained by the VT variation, which will be discussed in the next section. On the other hand, the east and west façades are varied more for case study 2 due to increased surface area. The north façade maintains a high VT, since it can afford a higher SHGC, with limited solar radiation.

Overall, the shapes of the existing SHGC graphs for both case studies mimic their respective existing VT graph. This clearly demonstrates the tradeoff between SHGC and VT in existing window products: in order to decrease SHGC, VT must also decrease. Due to this tradeoff, case study 1 existing was not able to achieve high SHGC values in the winter months. To the same effect, case study 2 existing only selected low SHGC in the summer for key façade orientations.

Additional investigation following these results present notable features in VT variations. With future technologies, it might be possible to slightly push the bounds towards products with both higher VT and SHGC than in the statistical models used above [87]. We experimented with giving VT more freedom in the simulation, and we expected that the maximum and constant VT would be most beneficial to the energy savings. However, window VT can influence heating and cooling loads as well due to the heat gains generated by the electrical lights. Even with standard-compliant lighting power density (LPD) in the simulations, the high lighting needs in commercial buildings may still enlarge the heat gain effects of electrical lights, which has been reported in other studies [208]. Future studies can test this relationship more rigorously.

In this work, in hot climates (case study 2), such heat gains are not beneficial to save heating and cooling energy, so the VT value was kept at or near the upper bound (~90%) on the south and north façades. Increasing the VT increased daylight levels and consequently reduced the electric lighting load. However, VT was not at 100% in the optimal scenario in heating seasons (case study 1), which is mainly constrained by the low U-value in the winter. To achieve a higher

insulating ability of windows, low-e coatings and/or additional window panes are required, which typically reduce the VT value. As mentioned previously, VT is sacrificed in both existing runs to achieve desirable SHGC values. This allows for a high light-to-solar gain (LSG) ratio, thus demonstrating the effectiveness of the algorithm.

U-value

It is widely known that highly insulating windows reduce heating and cooling loads consumption, and the results of the dynamic glazing optimization runs generally agree. For case study 1 and case study 2, the optimal U-value was the lower bound for nine and seven of twelve months, respectively. However, a higher U-value was selected for the summer months in climate zone 5 and shoulder months in climate zone 2. During these mild weather periods, strong solar heat gains may significantly enhance the building cooling loads. Such increased heat gains can be offset by the high U-value of the building window systems because the outdoor temperature conditions at most times are desirable or beneficial to the heat release from the interior. For window orientations with higher solar heat gains, a higher U-value was selected. Further, if the simulations were conducted on an hourly resolution, a lower U-value would be selected during the day, and a higher U-value would be selected during the night. While additional studies can investigate these phenomena in more detail, the optimization still largely gives intuitive results that would be helpful at the early stages of design.

Although U-value is not strongly correlated to SHGC and VT [87], there are still losses to address by manipulating this glazing property: to increase the thermal insulating ability of glazing systems, VT and SHGC will be somewhat reduced due to the addition of glazing layers or low-e coatings.

Since most months optimized to the lower bound, it was difficult to understand if modulating the U-value contributed to energy savings. To answer this question, a "high-performance" static baseline model was used to quantify the savings due to the dynamic aspect alone. The high-performance glazing adopted the lower bound of the U-value from the optimization and maintained the ASHRAE recommended SHGC value. The high-performance static model performed better than the baseline, but the dynamic model exceeded it by 5% and 3% respectively for case study 1 and case study 2. This suggests adopting dynamic glazing is a viable step in reducing building energy consumption. Energy savings comparisons are discussed further in the next section.

Comparing sequential optimization results

After determining potential savings from each category separately (runs 1, 2, 5, and 6), existing dynamic glazing properties were optimized using the optimal geometric configuration (runs 3 and 7) and an additional constrained optimization was conducted on the building geometry with the existing dynamic glazing optimal settings (runs 4 and 8). Figure **5-8** shows the results of these two design procedures. Case study 1 achieved 1% reduction in heating, cooling, and lighting load energy from the geometric optimization and up to 19% reduction from the dynamic glazing optimization. Similarly, case study 2 achieved 2% reduction in heating, cooling, and lighting load energy from the geometric optimization and up to 13% reduction from the dynamic glazing optimization.

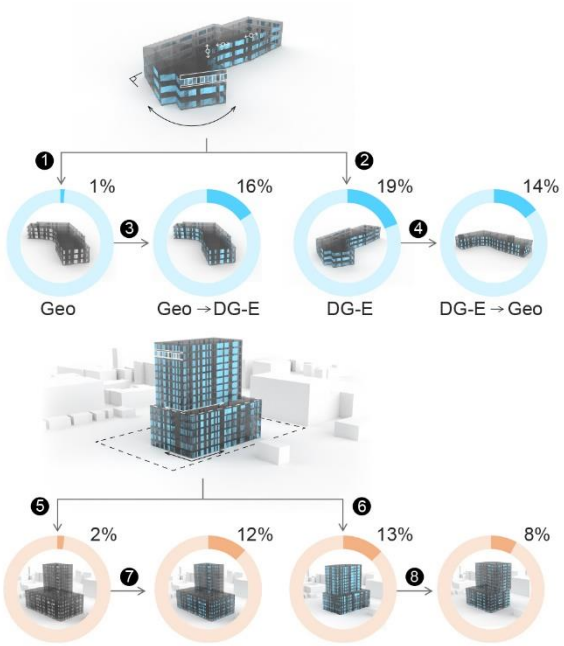

Figure **5-8**: Combining optimal settings for sequential optimization. Run numbers correspond with Table 5-1.

Designers might assume that combining the optimal variable settings from each constrained optimization run would yield the highest energy savings. However, because the geometric optimization altered the building orientation and form, thus altering many aspects of the fenestration, the combination did not lead to greater savings (runs 3 and 7). Compared to the existing dynamic glazing optimization, the energy savings values differed by 3% for case study 1. The relationship between dynamic glazing and building geometry is also demonstrated by the additional sequential optimization run (runs 4 and 8). For these runs, the optimal existing dynamic glazing settings were set, and the building geometry was optimized. For case study 1, optimizing the building geometry with the optimal existing glazing settings resulted in a loss of about 5% savings compared to the dynamic glazing optimization alone. This suggests the performance of dynamic glazing is not only dependent on the climate zone, but also the effects of window orientation, self-shading, and radiant heat exchange in relation the building shape. A direct comparison of the energy use reduction for each procedure is provided in Figure **5-9**.

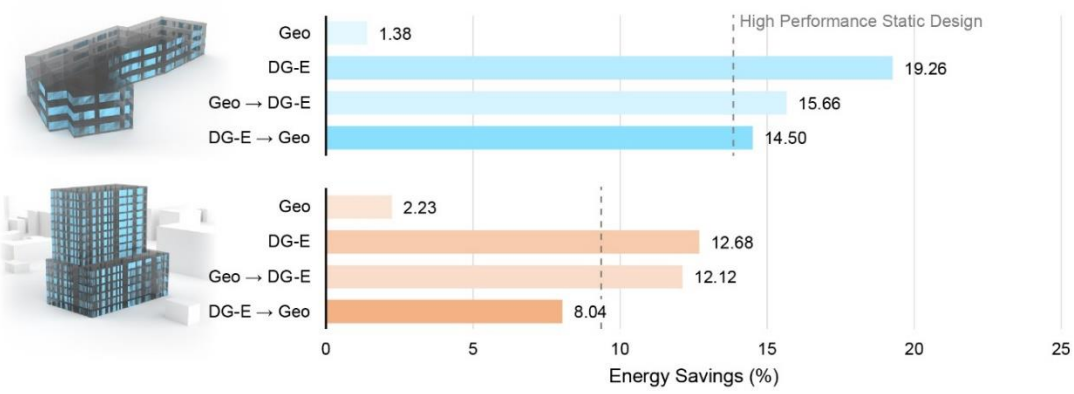

Figure **5-9**: Energy savings comparison.

The results show that making geometric adjustments warrants a new set of optimal dynamic glazing settings, and vice versa. Therefore, to truly understand the full potential of dynamic glazing in architect-designed buildings with atypical geometries, an additional optimization run would need to be conducted with all 16 variables and 18 variables for case studies 1 and 2, respectively. We predict that building geometry and dynamic façade materials must be considered simultaneously to achieve the optimal geometric-material combination for minimal energy consumption. Unfortunately, limitations in existing engineering software prevent exploration of complex geometry, and limitations in parametric environments prevent the full customization of dynamic materials. This suggests an avenue for extensive tool development and future research, towards a future in which designers use simulation to specify dynamic materials that can adapt to necessary conditions, along with building geometries that afford the most flexibility for achieving future energy savings through dynamic properties.

Considering variable importance directly

To analyze which individual variables were most influential in predicting building energy usage, a random forest regression model was built to first predict energy consumption and then calculate feature importance. This secondary analysis complements the findings of the overall optimization procedure by attempting to understand variables at a more granular level. To create this data model, case study 1 and case study 2 design spaces were sampled at a rate of n=1000 using the Latin Hypercube Sampling method. The dependent variable was the combined annual heating, cooling, and lighting load (converted to secondary energy) divided by the gross square footage. The training and validation data were split at a ratio of 0.6. The random forest module from scikit learn [135] was implemented and tuned before calculating feature importance, reaching an 87.2% accuracy on the case study 1 test set and an 83.6% accuracy on the test set for case study 2. Figure **5-10** shows the collective influence of the four main categories of variables: percentage of opaque panels variable, other window geometry variables (sill height and head height), and window performance (SHGC, VT, and U-value). Both case study 1 and case study 2 identified the single most important variable as the percentage of opaque panels, which most strongly influences WWR. Note that there were three variables affecting fenestration size: percentage of opaque panels, sill height, and head height. The collective influence of the three variables that together dictate WWR was the most important category in predicting building energy usage, followed by window performance.

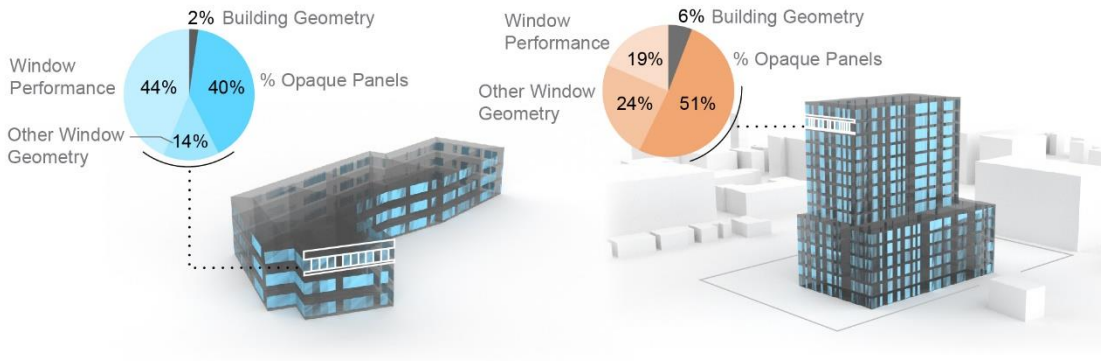

Figure **5-10**: Random forest variable importance.

It is noteworthy that control points from case study 1 (v_1, v_2, v_3) are not important features based on this model, reinforcing the notion that energy is not frequently "form-giving" for design. Likewise, the length: width aspect ratios in case study 2 (v_2 and v_3) were also deemed unimportant. However, because dynamic glazing does not yet outperform opaque construction, the amount and configuration of glazing matters most. This furthers the importance of exploring building geometry and façade materials in early design, as many geometric decisions are still relevant.

Discussion

The results demonstrate that a sequential design process is not necessarily fit for dynamic façade technologies. Because dynamic façades are sensitive to orientation, self-shading, and radiant heat exchange in relation to the building shape, simply applying the optimal values for the climate zone can lead to potential missed savings. Dynamic façade technologies introduce a unique opportunity to explore building geometry and envelope materials in early design to find the optimal geometric-material combination. However, it is currently difficult in conceptual design to structure an optimization problem with different resolutions using current design tools—building geometry is optimized on an annual basis, and dynamic façades are optimized on

a monthly or hourly resolution. At minimum, we conclude that to maximize the potential savings of dynamic glazing or dynamic building envelope materials in general, it is important to consider building geometry and orientation while developing proper control algorithms. Further, the design lessons learned here suggest fundamental changes in the early design process when working with dynamic façades and encourage further computational tool development. Given the cutting-edge and often open-source nature of digital design tools, it is likely that further modifications to existing software could make simultaneous optimization of geometry and façades increasingly accessible to designers in practice.

Furthermore, many previous studies on building energy optimization use rectangular buildings or prototypical models. This study provides an example of geometry optimization for more expressive architectural designs. While it is possible to achieve 2% energy savings in these examples, drastic geometric changes often influence performance in other engineering domains or substantially alter the original design intent. For example, the optimal geometric configuration for case study 1 required the building to rotate 117° clockwise. While this is a simple parametric adjustment, it would have huge implications for how the massing relates to the site. In case study 2, the shifting of the tower on the podium would likewise have considerable influence on the structural performance. Because decisions related to building geometry require consensus between architects and other engineering disciplines, implementing these changes may or may not be beneficial to the whole project. On the other hand, assuming dynamic envelope materials become more commercially available, the high energy savings potential from dynamic glazing creates a compelling argument for their importance in design.

There are several notable limitations to this study. Although a monthly resolution was sufficient to demonstrate the geometric-material relationship, future studies at a higher resolution (daily or hourly) across multiple climate zones would provide a more robust understanding of dynamic façade performance in various design settings. As advanced simulation tools and

advanced geometry tools are futher integrated, it will likely be possible in the future to conduct this framework in another platform and increase the resolution. Further, a simulation-based daylighting constraint could offer a more thorough treatment of daylight compared to the analytical constraint applied in this study. Nevertheless, the case studies were modeled with current, appropriate design variables and simulation resolution for early design, which reveals significant implications for both architecture and building performance.

Conclusion

In this study, we investigated the implications of automated sequential optimization while designing with dynamic glazing materials. While geometric optimization alone achieved only 2% energy savings, dynamic material optimization savings reached up to 19%. However, when combined in sequence, around 5% potential energy savings are lost. The paper also determines the relative importance of different decision categories in early design. The results are in accordance with previous findings or assumptions about the building design process established by studying these properties separately, such as the limits of geometric optimization on savings compared to façade materials [23] and the relative importance of WWR [209]. However, by using repeated constrained optimization runs that consider geometry, façades, and realistic design constraints altogether, the data in this paper provides a comprehensive analysis of these interrelated building features and how they are manipulated during design.

This study leaves several areas for further research. More extensive simulation of modern building geometries and types requires increasing access for designers and allowing for customization of dynamic components in parametric environments. Other issues to address include increasing the resolution of the simulation and allowing for continuous transitions, rather than state-to-state. Additionally, there are opportunities for multi-disciplinary optimization

(MDO) [112], [210], [211] and further studies with multi-objective methodologies, as opposed to constrained optimization. Such studies could provide new insight into early design strategies for balancing adjacent objectives in conjunction with operational energy use. As daylighting simulations become less computationally expensive, including a daylight objective such as spatial daylight autonomy (sDA) or a glare metric will also provide more detailed information. Finally, a more extensive treatment of simultaneous optimization for flexible geometric variables and façade characteristics should be conducted for geometries outside the typical rectilinear prototypes, once tools are developed to make this accessible within design software.

While dynamic façades show considerable promise for improving the sustainability of future buildings, several barriers remain to their frequent adoption in architecture, making them a topic of ongoing research. As the fundamental material and technological questions surrounding dynamic façades are being answered, it is critical that digital design approaches develop to make these technologies accessible for design practitioners. This paper hopes to stimulate further investigation into how dynamic façade considerations can be better incorporated into advanced design approaches, including parametric design and optimization.

Chapter 6

Conclusion

Summary of contributions

Surrogate model-based workflows

The first half of this dissertation focused on addressing two limitations of surrogate model-based workflows: *accessibility* and *flexibility*. Although the idea of generalizable design spaces was initially proposed in [33], new exploration methods were required to make the data useful during the early design stages and across multiple projects. In Chapter 2, a novel sensitivity analysis named dynamic subset sensitivity analysis was proposed. This method provides updated variable importance by interpolating regional surrogate models outputs from a tree-like model. The method was demonstrated across three domains, and a set of recommendations was developed for future implementation. Looking forward, in order for these models to be truly generalizable, climate information should be incorporated into the surrogate model. For example, the daylighting analysis developed for Pittsburgh, PA, US, cannot be used in Phoenix, AZ, US, since their sky conditions differ. Additionally, further work is required to identify and construct all repeated subproblems.

While dynamic subset sensitivity analysis works to filter a large generalizable design space, improving *accessibility*, the workflow in Chapter 3 allows for the expansion of a custom design space to improve *flexibility*. Chapter 3 proposes a new workflow that combines a tabular transfer learning method with random walks sampling to significantly reduce the number of additional samples required to update the surrogate model when new variables are added to the

parametric model. Through a unique façade case study, it was shown that far fewer simulations are needed to update the surrogate model and achieve adequate performance via this workflow. This enables greater flexibility in the early design stages, where changes are frequent. Future work is required to establish or adopt techniques for determining when transfer learning is effective for early building design models, as well as further testing on case studies from other building system domains.

To advance surrogate model-based workflows for building façade design, 'static' design decisions were included as variables in these two studies. However, the next two studies investigated 'dynamic' design improvements.

Dynamic façade design

The second half of this dissertation focused on dynamic façade design, optimizing dynamic glazing on a whole building basis, both as a component using prototypical buildings (Chapter 4) and as an integrated design decision in real-world building design scenarios (Chapter 5). Chapter 4 first finds the optimal two-state dynamic glazing configuration across multiple climates to determine the ideal relationship between SHGC and VT via parametric energy simulations. The results show that in order to maximize energy savings for cold and mixed climates, there must be a large range of SHGC, while modulating VT is less important. However, in hot climates, a much smaller range is required for SHGC modulations, and VT modulations have a greater impact on energy savings. In both situations, the analyses demonstrate the need to decouple solar heat and light to maximize energy savings, either as a static or dynamic window technology. It also established the energy savings potential by tuning SHGC and VT alone on a ten-minute resolution, which was up to 17.4% in ASHRAE climate zone 5a. This chapter focused on dynamic glazing on the component level, using prototypical buildings as case studies to

develop direction for future product development. Chapter 5 begins to combine ‘static’ and ‘dynamic’ design decisions in a constrained optimization workflow using real-world building examples.

In Chapter 5, a series of constrained optimization workflows were conducted to quantify the missed energy savings due to optimizing ‘static’ variables first and then ‘dynamic’ variables (in this case, dynamic glazing properties) according to traditional building design processes, and vice versa. The results showed that by following a sequential optimization approach, up to 5% of energy savings were missed, suggesting that dynamic façade variables should be considered in conjunction with ‘static’ variables that affect their control and operation. As new dynamic façade systems are developed and implemented, designers should consider adopting an integrated design approach.

Future work

The studies in this dissertation lay the foundation for a surrogate model-based workflow that incorporates both ‘static’ and ‘dynamic’ façade design decisions. There are two main considerations when accomplishing this, 1) whether the dynamic façade technology is already established or custom and actively designed during building design, and 2) the dimensionality of the design space. If the dynamic façade is already established, for example, electrochromic glazing, it can likely be considered in surrogate model-based workflows within the simulation itself (e.g., there is an electrochromic glazing object within EnergyPlus). However, if the dynamic façade is custom and there are variables related to it, more effort is required to develop a custom component. In both cases, but particularly in the latter, there is the potential to produce a very high-dimensional design space, which would require significant computational resources.

To mitigate this barrier, it would be best to consider only static design variables that significantly affect the control and operation of dynamic façade technologies. For example, the WWR has been shown to affect the effectiveness of dynamic glazing [212]. Additionally, other geometric variables such as room depth (which would influence illuminance distribution and sensor placement) or even categorical variables like space type (which would affect the operation) have the potential to interact with dynamic façade variables. However, dynamic glazing that is controlled based on solar radiation or outdoor air temperature may not be affected by all static design decisions. Further research is required to determine this and adopt appropriate dimensionality reduction methods to make this workflow feasible.

Another area of future research related to the workflows developed in this dissertation is the ability to translate early design surrogate models to later stages of design. It is possible that transfer learning techniques could be leveraged to transition the surrogate model from low-resolution information in early design stages to high resolution in the later stages. This would eliminate redundancies throughout the design process and continue to improve the accessibility and flexibility of surrogate model-based workflows.

References

[1] A. Wong, “Introduction to Model Trees from scratch,” *Towards Data Science*, 2018. https://towardsdatascience.com/introduction-to-model-trees-6e396259379a (accessed Mar. 14, 2022).

[2] IQRemix, “The National Art Center - Tokyo,” *flickr*, Accessed: Jan. 15, 2024. [Online]. Available: https://www.flickr.com/photos/iqremix/18111647225.

[3] J. Lin, “The National Art Center, Tokyo,” *flickr*. https://www.flickr.com/photos/jonolist/16103791833 (accessed Jan. 15, 2024).

[4] Z. Wang and J. Sun, “TransTab: Learning Transferable Tabular Transformers Across Tables,” *Advances in Neural Information Processing Systems*, vol. 35, pp. 2902–2915, Dec. 2022, Accessed: Dec. 28, 2023. [Online]. Available: https://transtab.readthedocs.io/en/latest/.

[5] D. Bourgeois, C. Reinhart, and I. Macdonald, “Adding advanced behavioural models in whole building energy simulation: A study on the total energy impact of manual and automated lighting control,” *Energy and Buildings*, vol. 38, no. 7, pp. 814–823, Jul. 2006, doi: 10.1016/j.enbuild.2006.03.002.

[6] U.S. Energy Information Administration, “Monthly Energy Review Table 2.1a and Table 2.1b,” 2022. [Online]. Available: https://www.eia.gov/totalenergy/data/monthly/pdf/sec2.pdf.

[7] A. Martinez and J.-H. Choi, “Exploring the potential use of building facade information to estimate energy performance A R T I C L E I N F O Keywords: Building energy performance Data mining Evidence-based design Best-practice buildings,” 2017, doi: 10.1016/j.scs.2017.07.022.

[8] S. Attia, E. Gratia, A. De Herde, and J. L. M. Hensen, "Simulation-based decision support tool for early stages of zero-energy building design," *Energy and Buildings*, vol. 49, pp. 2–15, 2012, doi: 10.1016/j.enbuild.2012.01.028.

[9] R. Oxman, "Performance-based Design: Current Practices and Research Issues."

[10] R. Balling, "Design by shopping: A new paradigm," in *Proceedings of the Third World Congress of structural and multidisciplinary optimization (WCSMO-3)*, 1999, pp. 295–297.

[11] G. Stump, T. W. Simpson, M. Yukish, and L. Bennett, "Multidimensional visualization and its application to a design by shopping paradigm," in *9th AIAA/ISSMO Symposium on Multidisciplinary Analysis and Optimization*, 2002, pp. 795–804, doi: 10.2514/6.2002-5622.

[12] P. Westermann and R. Evins, "Surrogate modelling for sustainable building design – A review," *Energy and Buildings*, vol. 198. Elsevier Ltd, pp. 170–186, Sep. 01, 2019, doi: 10.1016/j.enbuild.2019.05.057.

[13] M. Turrin, P. Von Buelow, and R. Stouffs, "Design explorations of performance driven geometry in architectural design using parametric modeling and genetic algorithms," *Advanced Engineering Informatics*, vol. 25, no. 4, pp. 656–675, Oct. 2011, doi: 10.1016/j.aei.2011.07.009.

[14] N. C. Brown and C. T. Mueller, "Design for structural and energy performance of long span buildings using geometric multi-objective optimization," *Energy and Buildings*, vol. 127, pp. 748–761, Sep. 2016, doi: 10.1016/j.enbuild.2016.05.090.

[15] A. de Gracia, "Dynamic building envelope with PCM for cooling purposes – Proof of concept," *Applied Energy*, vol. 235, pp. 1245–1253, Feb. 2019, doi: 10.1016/j.apenergy.2018.11.061.

[16] N. L. Sbar, L. Podbelski, H. M. Yang, and B. Pease, "Electrochromic dynamic windows

for office buildings," *International Journal of Sustainable Built Environment*, vol. 1, no. 1, pp. 125–139, 2012, doi: 10.1016/j.ijsbe.2012.09.001.

[17] F. Favoino, M. Overend, and Q. Jin, "The optimal thermo-optical properties and energy saving potential of adaptive glazing technologies," *Applied Energy*, vol. 156, pp. 1–15, Oct. 2015, doi: 10.1016/j.apenergy.2015.05.065.

[18] A. Jahid, J. Wang, E. Zhang, Q. Duan, and Y. Feng, "Energy savings potential of reversible photothermal windows with near infrared-selective plasmonic nanofilms," *Energy Conversion and Management*, vol. 263, p. 115705, 2022, doi: 10.1016/j.enconman.2022.115705.

[19] IEA, "Electricity 2024," Paris, 2024. [Online]. Available: https://www.iea.org/reports/electricity-2024.

[20] R. Oxman, "Thinking difference: Theories and models of parametric design thinking," *Design Studies*, vol. 52, pp. 4–39, Sep. 2017, doi: 10.1016/j.destud.2017.06.001.

[21] R. Oxman, "Performance-based design: current practices and research issues," *International Journal of Architectural Computing*, vol. 06, no. 01, pp. 1–17, 2008, doi: 10.1260/147807708784640090.

[22] Robert McNeel & Associates, "Grasshopper." 2007.

[23] H. Samuelson, S. Claussnitzer, A. Goyal, Y. Chen, and A. Romo-Castillo, "Parametric energy simulation in early design: High-rise residential buildings in urban contexts," *Building and Environment*, vol. 101, pp. 19–31, May 2016, doi: 10.1016/j.buildenv.2016.02.018.

[24] J. T. Jin and J. W. Jeong, "Optimization of a free-form building shape to minimize external thermal load using genetic algorithm," *Energy and Buildings*, vol. 85, pp. 473–482, Dec. 2014, doi: 10.1016/j.enbuild.2014.09.080.

[25] A. Wagdy and F. Fathy, "A parametric approach for achieving optimum daylighting

performance through solar screens in desert climates," *Journal of Building Engineering*, vol. 3, pp. 155–170, Sep. 2015, doi: 10.1016/J.JOBE.2015.07.007.

[26] R. Danhaive and C. T. Mueller, "Design subspace learning: Structural design space exploration using performance-conditioned generative modeling," *Automation in Construction*, vol. 127, Jul. 2021, doi: 10.1016/j.autcon.2021.103664.

[27] C. Mueller, "Combining parametric modeling and interactive optimization for high-performance and creative structural design," in *Proceedings of IASS Annual Symposia, IASS 2015 Amsterdam Symposium: Future Visions – Computational Design*, 2015, pp. 1–11, Accessed: Nov. 07, 2022. [Online]. Available: http://digitalstructures.mit.edu/files/2015-09/iass2015-524698.pdf.

[28] S. Wehrend and C. Lewis, "A problem-oriented classification of visualization techniques," in *VIS '90: Proceedings of the 1st conference on Visualization*, 1990, pp. 139–143, 46, doi: 10.1109/visual.1990.146375.

[29] T. Wortmann, "Surveying design spaces with performance maps: A multivariate visualization method for parametric design and architectural design optimization," *International Journal of Architectural Computing*, vol. 15, no. 1, pp. 38–53, 2017, doi: 10.1177/1478077117691600.

[30] S. P. Thole and P. Ramu, "Design space exploration and optimization using self-organizing maps," *Structural and Multidisciplinary Optimization*, vol. 62, no. 3, pp. 1071–1088, Jul. 2020, doi: 10.1007/s00158-020-02665-6.

[31] T. Østergård, R. L. Jensen, and S. E. Maagaard, "Interactive building design space exploration using regionalized sensitivity analysis," in *Building Simulation Conference Proceedings*, 2017, vol. 4, pp. 1997–2006, doi: 10.26868/25222708.2017.185.

[32] T. Wortmann, A. Costa, G. Nannicini, and T. Schroepfer, "Advantages of surrogate models for architectural design optimization," *Artificial Intelligence for Engineering*

Design, Analysis and Manufacturing: AIEDAM, vol. 29, no. 4, pp. 471–481, Oct. 2015, doi: 10.1017/S0890060415000451.

[33] B. Bass, L. Curtis, J. New, S. Sanborn, and P. McNally, "Universal design space exploration for building energy design," *Journal of Building Engineering*, vol. 68, Jun. 2023, doi: 10.1016/j.jobe.2023.105977.

[34] P. Westermann, M. Welzel, and R. Evins, "Using a deep temporal convolutional network as a building energy surrogate model that spans multiple climate zones," *Applied Energy*, vol. 278, Nov. 2020, doi: 10.1016/j.apenergy.2020.115563.

[35] I. Elzeyadi, "The impacts of dynamic façade shading typologies on building energy performance and occupant's multi-comfort," *Architectural Science Review*, vol. 60, no. 4, pp. 316–324, Jul. 2017, doi: 10.1080/00038628.2017.1337558.

[36] M. Aburas, V. Soebarto, T. Williamson, R. Liang, H. Ebendorff-Heidepriem, and Y. Wu, "Thermochromic smart window technologies for building application: A review," *Applied Energy*, vol. 255, Dec. 2019, doi: 10.1016/J.APENERGY.2019.113522.

[37] R. C. G. M. Loonen, S. Singaravel, M. Trčka, D. Cóstola, and J. L. M. Hensen, "Simulation-based support for product development of innovative building envelope components," 2014, doi: 10.1016/j.autcon.2014.05.008.

[38] L. Caldas, "Generation of energy-efficient architecture solutions applying GENE_ARCH: An evolution-based generative design system," *Advanced Engineering Informatics*, vol. 22, no. 1, pp. 59–70, Jan. 2008, doi: 10.1016/J.AEI.2007.08.012.

[39] Y. Wang and C. Wei, "Design optimization of office building envelope based on quantum genetic algorithm for energy conservation," *Journal of Building Engineering*, vol. 35, Mar. 2021, doi: 10.1016/J.JOBE.2020.102048.

[40] Y. Fang and S. Cho, "Design optimization of building geometry and fenestration for daylighting and energy performance," *Solar Energy*, vol. 191, pp. 7–18, Oct. 2019, doi:

10.1016/j.solener.2019.08.039.

[41] N. C. Brown and C. T. Mueller, “Gradient-based guidance for controlling performance in early design exploration,” 2018, [Online]. Available: https://www.ingentaconnect.com/contentone/iass/piass/2018/00002018/00000002/art00018?crawler=true&mimetype=application/pdf.

[42] C. T. Mueller and J. A. Ochsendorf, “Combining structural performance and designer preferences in evolutionary design space exploration,” *Automation in Construction*, vol. 52, pp. 70–82, Apr. 2015, doi: 10.1016/j.autcon.2015.02.011.

[43] N. Brown and C. Mueller, “Designing with data: Moving beyond the design space catalog,” in *Disciplines and Disruption - Proceedings Catalog of the 37th Annual Conference of the Association for Computer Aided Design in Architecture, ACADIA 2017*, 2017, pp. 154–163, Accessed: Feb. 22, 2021. [Online]. Available: https://papers.cumincad.org/cgi-bin/works/paper/acadia17_154.

[44] G. M. Stump, M. Yukish, T. W. Simpson, and E. N. Harris, “Design Space Visualization and Its Application to a Design by Shopping Paradigm,” in *ASME 2003 International Design Engineering Technical Conferences and Computers and Information in Engineering Conference*, Sep. 2003, pp. 795–804, doi: 10.1115/DETC2003/DAC-48785.

[45] S. Attia, E. Gratia, A. De Herde, and J. L. M. Hensen, “Simulation-based decision support tool for early stages of zero-energy building design,” *Energy and Buildings*, vol. 49. Elsevier, pp. 2–15, Jun. 01, 2012, doi: 10.1016/j.enbuild.2012.01.028.

[46] P. Pilechiha, M. Mahdavinejad, F. Pour Rahimian, P. Carnemolla, and S. Seyedzadeh, “Multi-objective optimisation framework for designing office windows: quality of view, daylight and energy efficiency,” *Applied Energy*, vol. 261, Mar. 2020, doi: 10.1016/J.APENERGY.2019.114356.

[47] N. C. Brown, “Design performance and designer preference in an interactive, data-driven

conceptual building design scenario," *Design Studies*, vol. 68, pp. 1–33, May 2020, doi: 10.1016/j.destud.2020.01.001.

[48] T. Yang, Y. Pan, J. Mao, Y. Wang, and Z. Huang, "An automated optimization method for calibrating building energy simulation models with measured data: Orientation and a case study," *Applied Energy*, vol. 179, pp. 1220–1231, Oct. 2016, doi: 10.1016/j.apenergy.2016.07.084.

[49] S. Gou, V. M. Nik, J.-L. Scartezzini, Q. Zhao, and Z. Li, "Passive design optimization of newly-built residential buildings in Shanghai for improving indoor thermal comfort while reducing building energy demand," *Energy & Buildings*, vol. 169, pp. 484–506, 2017, doi: 10.1016/j.enbuild.2017.09.095.

[50] J. Yang, "Convergence and uncertainty analyses in Monte-Carlo based sensitivity analysis," *Environmental Modelling & Software*, vol. 26, no. 4, pp. 444–457, 2011, doi: 10.1016/j.envsoft.2010.10.007.

[51] L. Hinkle, G. Pavlak, N. Brown, and L. Curtis, "Dynamic Subset Sensitivity Analysis For Design Exploration," *2022 Annual Modeling and Simulation Conference (ANNSIM)*, pp. 581–592, Jul. 2022, doi: 10.23919/ANNSIM55834.2022.9859293.

[52] N. C. Brown, "Design performance and designer preference in an interactive, data-driven conceptual building design scenario," *Design Studies*, vol. 68, pp. 1–33, 2020, doi: 10.1016/j.destud.2020.01.001.

[53] W. J. Doherty and R. P. Kelisky, "Managing VM/CMS systems for user effectiveness," *IBM Systems Journal*, vol. 18, no. 1, pp. 143–163, Mar. 1979, doi: 10.1147/SJ.181.0143.

[54] J. T. Brady, "A Theory of Productivity in the Creative Process," *IEEE Computer Graphics and Applications*, vol. 6, no. 5, pp. 25–34, 1986, doi: 10.1109/MCG.1986.276789.

[55] M. Csikszentmihalyi, *Creativity: Flow and the Psychology of Discovery and Invention*. New York: HarperPerennial, 1997.

[56] N. L. Jones, “Validated Interactive Daylighting Analysis for Architectural Design,” p. 154, 2017, [Online]. Available: https://dspace.mit.edu/handle/1721.1/111461?show=full.

[57] S. Tseranidis, N. C. Brown, and C. T. Mueller, “Data-driven approximation algorithms for rapid performance evaluation and optimization of civil structures,” *Automation in Construction*, 2016, doi: 10.1016/j.autcon.2016.02.002.

[58] A. I. J. Forrester, A. Sóbester, and A. J. Keane, *Engineering Design via Surrogate Modelling*. Wiley, 2008.

[59] Z. Romani, A. Draoui, and F. Allard, “Metamodeling the heating and cooling energy needs and simultaneous building envelope optimization for low energy building design in Morocco,” *Energy and Buildings*, vol. 102, pp. 139–148, 2015, doi: 10.1016/j.enbuild.2015.04.014.

[60] P. Geyer and A. Schlüter, “Automated metamodel generation for Design Space Exploration and decision-making - A novel method supporting performance-oriented building design and retrofitting,” *Applied Energy*, vol. 119, pp. 537–556, 2014, doi: 10.1016/j.apenergy.2013.12.064.

[61] S. Shamshirband *et al.*, “Predicting Standardized Streamflow index for hydrological drought using machine learning models,” *Engineering Applications of Computational Fluid Mechanics*, vol. 14, no. 1, pp. 339–350, Jan. 2020, doi: 10.1080/19942060.2020.1715844.

[62] A. Noulas, S. Scellato, N. Lathia, and C. Mascolo, “Mining user mobility features for next place prediction in location-based services,” *Proceedings - IEEE International Conference on Data Mining, ICDM*, pp. 1038–1043, 2012, doi: 10.1109/ICDM.2012.113.

[63] J. Golbeck, C. Robles, and K. Turner, “Predicting personality with social media,” in *Conference on Human Factors in Computing Systems - Proceedings*, 2011, pp. 253–262, doi: 10.1145/1979742.1979614.

[64] T. Wortmann, J. Cichocka, and C. Waibel, “Simulation-based optimization in architecture and building engineering—Results from an international user survey in practice and research,” *Energy and Buildings*, vol. 259, Mar. 2022, doi: 10.1016/j.enbuild.2022.111863.

[65] E. Whalen and C. Mueller, “Toward Reusable Surrogate Models: Graph-Based Transfer Learning on Trusses,” *Journal of Mechanical Design, Transactions of the ASME*, vol. 144, no. 2, Feb. 2022, doi: 10.1115/1.4052298/1119281.

[66] S. Xu, Y. Wang, Y. Wang, Z. O’neill, Q. Zhu, and Q. 2020 Zhu, “One for Many: Transfer Learning for Building HVAC Control,” in *BuildSys ’20: Proceedings of the 7th ACM International Conference on Systems for Energy-Efficient Buildings, Cities, and Transportation*, 2020, pp. 230–239, doi: 10.1145/3408308.3427617.

[67] A. Li, F. Xiao, C. Fan, and M. Hu, “Development of an ANN-based building energy model for information-poor buildings using transfer learning,” *Building Simulation*, vol. 14, no. 1, pp. 89–101, 2021, doi: 10.1007/s12273-020-0711-5.

[68] “Asterisk.” Thornton Tomasetti, Accessed: May 24, 2023. [Online]. Available: https://asterisk.thorntontomasetti.com/.

[69] K.-M. Mark TAM, T. Van Mele, and P. Block, “Trans-topological learning and optimisation of reticulated equilibrium shell structures with Automatic Differentiation and CW Complexes Message Passing,” in *Proceedings of the IASS 2022 Symposium affiliated with APCS 2022 conference*, 2022, pp. 1–13.

[70] H. Samuelson, S. Claussnitzer, A. Goyal, Y. Chen, and A. Romo-Castillo, “Parametric energy simulation in early design: High-rise residential buildings in urban contexts,” *Building and Environment*, vol. 101, pp. 19–31, May 2016, doi: 10.1016/J.BUILDENV.2016.02.018.

[71] E. Brembilla, C. J. Hopfe, and J. Mardaljevic, “Influence of input reflectance values on

climate-based daylight metrics using sensitivity analysis," *Journal of Building Performance Simulation*, vol. 11, no. 3, pp. 333–349, May 2018, doi: 10.1080/19401493.2017.1364786.

[72] A. T. Nguyen and S. Reiter, "A performance comparison of sensitivity analysis methods for building energy models," *Building Simulation*, vol. 8, no. 6, pp. 651–664, Dec. 2015, doi: 10.1007/s12273-015-0245-4.

[73] M. L. Pannier, P. Schalbart, and B. Peuportier, "Comprehensive assessment of sensitivity analysis methods for the identification of influential factors in building life cycle assessment," *Journal of Cleaner Production*, vol. 199, pp. 466–480, Oct. 2018, doi: 10.1016/j.jclepro.2018.07.070.

[74] S. De Wit and G. Augenbroe, "Analysis of uncertainty in building design evaluations and its implications," *Energy and Buildings*, vol. 34, no. 9, pp. 951–958, Oct. 2002, doi: 10.1016/S0378-7788(02)00070-1.

[75] S. Qiu, Z. Li, Z. Pang, W. Zhang, and Z. Li, "A quick auto-calibration approach based on normative energy models," *Energy and Buildings*, vol. 172, pp. 35–46, Aug. 2018, doi: 10.1016/J.ENBUILD.2018.04.053.

[76] X. Chen, H. Yang, and K. Sun, "Developing a meta-model for sensitivity analyses and prediction of building performance for passively designed high-rise residential buildings," *Applied Energy*, vol. 194, pp. 422–439, May 2017, doi: 10.1016/J.APENERGY.2016.08.180.

[77] Z. Yu, F. Haghighat, B. C. M. Fung, and H. Yoshino, "A decision tree method for building energy demand modeling," *Energy and Buildings*, vol. 42, no. 10, pp. 1637–1646, Oct. 2010, doi: 10.1016/J.ENBUILD.2010.04.006.

[78] Z. X. Conti and S. Kaijima, "Enabling inference in performance-driven design exploration," in *Humanizing Digital Reality: Design Modelling Symposium*, 2017, pp.

177–188, doi: 10.1007/978-981-10-6611-5_16.

[79] N. Delgarm, B. Sajadi, K. Azarbad, and S. Delgarm, "Sensitivity analysis of building energy performance: A simulation-based approach using OFAT and variance-based sensitivity analysis methods," *Journal of Building Engineering*, vol. 15, pp. 181–193, 2018, doi: 10.1016/j.jobe.2017.11.020.

[80] Y. Gao, M. Mae, and K. Taniguchi, "A new design exploring framework based on sensitivity analysis and Gaussian process regression in the early design stage," *Journal of Asian Architecture and Building Engineering*, pp. 1–14, 2020, doi: 10.1080/13467581.2020.1783271.

[81] A. Mohiuddin and R. Woodbury, "Interactive parallel coordinates for parametric design space exploration," in *Conference on Human Factors in Computing Systems - Proceedings*, 2020, pp. 1–9, doi: 10.1145/3334480.3383101.

[82] S. P. Thole and P. Ramu, "Design space exploration and optimization using self-organizing maps," *Structural and Multidisciplinary Optimization*, vol. 62, no. 3, pp. 1071–1088, Jul. 2020, doi: 10.1007/s00158-020-02665-6.

[83] J. Harding, "Dimensionality Reduction for Parametric Design Exploration," in *Advances in Architectural Geometry 2016 - Dimensionality Reduction for Parametric Design Exploration*, 2016, pp. 274–287, doi: 10.3218/3778-4_19.

[84] "LEED v4 for Building Design and Construction - current version | U.S. Green Building Council." https://www.usgbc.org/resources/leed-v4-building-design-and-construction-current-version (accessed May 21, 2023).

[85] The Daylight Metrics Committee, "Approved Method: IES Spatial Daylight Autonomy (sDA) and Annual Sunlight Exposure (ASE)," *Illuminating Engineering Society of North America*, 2012. https://store.ies.org/product/approved-method-ies-spatial-daylight-autonomy-sda-and-annual-sunlight-exposure-ase/?v=7516fd43adaa (accessed May 25,

2023).

[86] L. Gosselin and J. M. Dussault, “Correlations for glazing properties and representation of glazing types with continuous variables for daylight and energy simulations,” *Solar Energy*, vol. 141, pp. 159–165, 2017, doi: 10.1016/j.solener.2016.11.031.

[87] J. Wang, L. Caldas, L. Huo, and Y. Song, “Simulation-based optimization on window properties based on existing products,” 2016, [Online]. Available: http://www.ibpsa.org/proceedings/BSO2016/p1054.pdf.

[88] I. Hens, R. Solnosky, and N. C. Brown, “Design space exploration for comparing embodied carbon in tall timber structural systems,” *Energy and Buildings*, vol. 244, Aug. 2021, doi: 10.1016/j.enbuild.2021.110983.

[89] S. Zargar and N. C. Brown, “Deep learning in early-stage structural performance prediction: assessing morphological parameters for buildings,” in *Proceedings of the IASS Annual Symposium*, 2021, pp. 1–13, Accessed: May 21, 2023. [Online]. Available: https://www.ingentaconnect.com/contentone/iass/piass/2020/00002020/00000019/art00007.

[90] I. Hens, R. Solnosky, and N. Brown, “Parametric Framework for Early Evaluation of Prescriptive Fire Design and Structural Feasibility in Tall Timber,” *Journal of Architectural Engineering*, vol. 29, no. 1, Mar. 2023, doi: 10.1061/jaeied.aeeng-1455.

[91] L. Hinkle, G. Pavlak, N. Brown, and L. Curtis, “Dynamic Subset Sensitivity Analysis For Design Exploration,” *Proceedings of the 2022 Annual Modeling and Simulation Conference, ANNSIM 2022*, pp. 581–592, 2022, doi: 10.23919/ANNSIM55834.2022.9859293.

[92] S. Tseranidis, N. C. Brown, and C. T. Mueller, “Data-driven approximation algorithms for rapid performance evaluation and optimization of civil structures,” *Automation in Construction*, vol. 72, pp. 279–293, Dec. 2016, doi: 10.1016/J.AUTCON.2016.02.002.

[93] Z. O'Neill and F. Niu, "Uncertainty and sensitivity analysis of spatio-temporal occupant behaviors on residential building energy usage utilizing Karhunen-Loève expansion," *Building and Environment*, vol. 115, pp. 157–172, 2017, doi: 10.1016/j.buildenv.2017.01.025.

[94] N. C. Brown, V. Jusiega, and C. T. Mueller, "Implementing data-driven parametric building design with a flexible toolbox," *Automation in Construction*, vol. 118, Oct. 2020, doi: 10.1016/j.autcon.2020.103252.

[95] A. Raina, J. Cagan, and C. McComb, "Learning to Design Without Prior Data: Discovering Generalizable Design Strategies Using Deep Learning and Tree Search," *Journal of Mechanical Design*, vol. 145, no. 3, Mar. 2023, doi: 10.1115/1.4056221.

[96] B. F. Robertson and D. F. Radcliffe, "Impact of CAD tools on creative problem solving in engineering design," *CAD Computer Aided Design*, vol. 41, no. 3, pp. 136–146, 2009, doi: 10.1016/j.cad.2008.06.007.

[97] A. Häggman, G. Tsai, C. Elsen, T. Honda, and M. C. Yang, "Connections between the design tool, design attributes, and user preferences in early stage design," *Journal of Mechanical Design*, vol. 137, no. 7, Jul. 2015, doi: 10.1115/1.4030181/376282.

[98] F. Zhuang *et al.*, "A Comprehensive Survey on Transfer Learning," *Proceedings of the IEEE*, vol. 109, no. 1. Institute of Electrical and Electronics Engineers Inc., pp. 43–76, Jan. 01, 2021, doi: 10.1109/JPROC.2020.3004555.

[99] N. C. Brown and C. T. Mueller, "Design variable analysis and generation for performance-based parametric modeling in architecture," *International Journal of Architectural Computing*, vol. 17, no. 1, pp. 36–52, 2019, doi: 10.1177/1478077118799491.

[100] A. Eltaweel and Y. SU, "Parametric design and daylighting: A literature review," *Renewable and Sustainable Energy Reviews*, vol. 73. pp. 1086–1103, 2017, doi:

10.1016/j.rser.2017.02.011.

[101] Y. Xue and W. Liu, “A Study on Parametric Design Method for Optimization of Daylight in Commercial Building’s Atrium in Cold Regions,” *Sustainability (Switzerland)*, vol. 14, no. 13, p. 7667, Jul. 2022, doi: 10.3390/SU14137667/S1.

[102] A. Tabadkani, M. Valinejad Shoubi, F. Soflaei, and S. Banihashemi, “Integrated parametric design of adaptive facades for user’s visual comfort,” *Automation in Construction*, vol. 106, 2019, doi: 10.1016/j.autcon.2019.102857.

[103] P. Shiel, S. Tarantino, and M. Fischer, “Parametric analysis of design stage building energy performance simulation models,” *Energy and Buildings*, vol. 172, pp. 78–93, Aug. 2018, doi: 10.1016/j.enbuild.2018.04.045.

[104] Y. Wang, W. Yang, and Q. Wang, “Multi-objective parametric optimization of the composite external shading for the classroom based on lighting, energy consumption, and visual comfort,” *Energy and Buildings*, vol. 275, p. 112441, Nov. 2022, doi: 10.1016/J.ENBUILD.2022.112441.

[105] Y. Ibrahim, T. Kershaw, P. Shepherd, and I. Elwy, “A parametric optimisation study of urban geometry design to assess outdoor thermal comfort,” *Sustainable Cities and Society*, vol. 75, p. 103352, Dec. 2021, doi: 10.1016/J.SCS.2021.103352.

[106] A. Razmi, M. Rahbar, and M. Bemanian, “PCA-ANN integrated NSGA-III framework for dormitory building design optimization: Energy efficiency, daylight, and thermal comfort,” *Applied Energy*, vol. 305, 2022, doi: 10.1016/j.apenergy.2021.117828.

[107] A. Jayasinghe, J. Orr, T. Ibell, and W. P. Boshoff, “Minimising embodied carbon in reinforced concrete flat slabs through parametric design,” *Journal of Building Engineering*, vol. 50, p. 104136, 2022, doi: 10.1016/j.jobe.2022.104136.

[108] Y. Choi, D. Song, S. Yoon, and J. Koo, “Comparison of Factorial and Latin Hypercube Sampling Designs for Meta-Models of Building Heating and Cooling Loads,” *Energies*

2021, Vol. 14, Page 512, vol. 14, no. 2, p. 512, Jan. 2021, doi: 10.3390/EN14020512.

[109] R. Danhaive and C. T. Mueller, "Design subspace learning: Structural design space exploration using performance-conditioned generative modeling," *Automation in Construction*, vol. 127, 2021, doi: 10.1016/j.autcon.2021.103664.

[110] L. E. Hinkle, G. Pavlak, L. Curtis, and N. C. Brown, "Implementing dynamic subset sensitivity analysis for early design datasets," *Automation in Construction*, vol. 158, 2024, doi: 10.1016/j.autcon.2023.105198.

[111] Z. Jalali, E. Noorzai, and S. Heidari, "Design and optimization of form and facade of an office building using the genetic algorithm," *Science and Technology for the Built Environment*, vol. 26, no. 2, pp. 128–140, Feb. 2020, doi: 10.1080/23744731.2019.1624095.

[112] N. C. Brown and C. T. Mueller, "Design for structural and energy performance of long span buildings using geometric multi-objective optimization," *Energy and Buildings*, vol. 127, pp. 748–761, 2016, doi: 10.1016/j.enbuild.2016.05.090.

[113] S. Raschka, "Model Evaluation, Model Selection, and Algorithm Selection in Machine Learning," Nov. 2018, Accessed: Jan. 27, 2024. [Online]. Available: https://arxiv.org/abs/1811.12808v3.

[114] C. Molnar, "Interpretable Machine Learning A Guide for Making Black Box Models Explainable," Accessed: Jan. 09, 2024. [Online]. Available: www.dbooks.orghttp://leanpub.com/interpretable-machine-learning.

[115] T. Miller, "Explanation in artificial intelligence: Insights from the social sciences," *Artificial Intelligence*, vol. 267, pp. 1–38, 2019, doi: 10.1016/j.artint.2018.07.007.

[116] M. Zaker Esteghamati and M. M. Flint, "Developing data-driven surrogate models for holistic performance-based assessment of mid-rise RC frame buildings at early design," *Engineering Structures*, vol. 245, p. 112971, Oct. 2021, doi:

10.1016/J.ENGSTRUCT.2021.112971.

[117] M. W. Ahmad, M. Mourshed, and Y. Rezgui, “Trees vs Neurons: Comparison between random forest and ANN for high-resolution prediction of building energy consumption,” *Energy and Buildings*, vol. 147, pp. 77–89, Jul. 2017, doi: 10.1016/j.enbuild.2017.04.038.

[118] J. S. Gero and M. Lou Maher, “Mutation and Analogy to Support Creativity in Computer-Aided Design,” in *Computer Aided Architectural Design Futures: Education, Research, Applications*, 1991, pp. 261–270.

[119] B. F. Robertson and D. F. Radcliffe, “Impact of CAD tools on creative problem solving in engineering design,” *CAD Computer Aided Design*, vol. 41, no. 3, pp. 136–146, 2009, doi: 10.1016/j.cad.2008.06.007.

[120] J. Huang, A. J. Smola, A. Gretton, K. M. Borgwardt, and B. Schölkopf, “Correcting Sample Selection Bias by Unlabeled Data,” *Advances in Neural Information Processing Systems*, vol. 19, 2006.

[121] S. A. Sharif, A. Hammad, and P. Eshraghi, “Generation of whole building renovation scenarios using variational autoencoders,” *Energy and Buildings*, vol. 230, 2021, doi: 10.1016/j.enbuild.2020.110520.

[122] R. Levin *et al.*, “Transfer Learning with Deep Tabular Models,” Jun. 2022, Accessed: Dec. 30, 2023. [Online]. Available: http://arxiv.org/abs/2206.15306.

[123] X. Li, Y. Yuan, G. Liu, Z. Han, and R. Stouffs, “A predictive model for daylight performance based on multimodal generative adversarial networks at the early design stage,” *Energy & Buildings*, vol. 305, p. 113876, 2024, doi: 10.1016/j.enbuild.2023.113876.

[124] A. Li, F. Xiao, C. Fan, and M. Hu, “Development of an ANN-based building energy model for information-poor buildings using transfer learning,” *Building Simulation*, vol. 14, no. 1, pp. 89–101, Feb. 2021, doi: 10.1007/s12273-020-0711-5.

[125] C. Fan *et al.*, "Statistical investigations of transfer learning-based methodology for short-term building energy predictions," *Applied Energy*, vol. 262, 2020, doi: 10.1016/j.apenergy.2020.114499.

[126] M. Demianenko and C. I. De Gaetani, "A Procedure for Automating Energy Analyses in the BIM Context Exploiting Artificial Neural Networks and Transfer Learning Technique," *Energies 2021, Vol. 14, Page 2956*, vol. 14, no. 10, p. 2956, May 2021, doi: 10.3390/EN14102956.

[127] A. E. W. Johnson *et al.*, "MIMIC-IV, a freely accessible electronic health record dataset," *Scientific Data*, vol. 10, no. 1, p. 1, 2023, doi: 10.1038/s41597-022-01899-x.

[128] "Climate Studio." Solemma LLC.

[129] "Architecture | About The National Art Center, Tokyo." https://www.nact.jp/english/introduce/architecture.html (accessed Jan. 26, 2024).

[130] N. C. Brown, V. Jusiega, and C. T. Mueller, "Implementing data-driven parametric building design with a flexible toolbox," *Automation in Construction*, vol. 118, Oct. 2020, doi: 10.1016/j.autcon.2020.103252.

[131] A. Vaswani *et al.*, "Attention Is All You Need," *Advances in Neural Information Processing Systems*, vol. 2017-December, pp. 5999–6009, Jun. 2017, Accessed: Jan. 08, 2024. [Online]. Available: https://arxiv.org/abs/1706.03762v7.

[132] D. P. Kingma and J. L. Ba, "Adam: A method for stochastic optimization," 2015.

[133] G. James, D. Witten, T. Hastie, R. Tibshirani, and J. Taylor, "An Introduction to Statistical Learning," *Springer Texts in Statistics.*, pp. 289–329, 2023, Accessed: Jan. 14, 2024. [Online]. Available: https://doi.org/10.1007/978-3-031-38747-0_7.

[134] P. Xanthopoulos, P. M. Pardalos, and T. B. Trafalis, "Linear Discriminant Analysis," pp. 27–33, 2013, doi: 10.1007/978-1-4419-9878-1_4.

[135] F. Pedregosa *et al.*, "Scikit-learn: Machine Learning in Python," *Journal of Machine*

Learning Research, vol. 12, pp. 2825–2830, 2011.

[136] P. Flach, J. Hernández-Orallo, and C. Ferri, "A coherent interpretation of AUC as a measure of aggregated classification performance," in *Proceedings of the 28th International Conference on Machine Learning, ICML 2011*, 2011, pp. 657–664.

[137] G. Pinto, Z. Wang, A. Roy, T. Hong, and A. Capozzoli, "Transfer learning for smart buildings: A critical review of algorithms, applications, and future perspectives," *Advances in Applied Energy*, vol. 5, p. 100084, 2022, doi: 10.1016/j.adapen.2022.100084.

[138] M. Ayoub, "A review on machine learning algorithms to predict daylighting inside buildings," *Solar Energy*, vol. 202, pp. 249–275, May 2020, doi: 10.1016/j.solener.2020.03.104.

[139] J. D. Camba, M. Contero, and P. Company, "Parametric CAD modeling: An analysis of strategies for design reusability," *Computer-Aided Design*, vol. 74, pp. 18–31, May 2016, doi: 10.1016/J.CAD.2016.01.003.

[140] IEA and UNEP, "Global Status Report 2018: Towards a zero-emission, efficient and resilient buildings and construction sector," *Global Status Report*, p. 325, 2018.

[141] S. Somasundaram, A. Chong, Z. Wei, and S. R. Thangavelu, "Energy saving potential of low-e coating based retrofit double glazing for tropical climate," *Energy and Buildings*, vol. 206, p. 109570, Jan. 2020, doi: 10.1016/J.ENBUILD.2019.109570.

[142] M. Casini, "Active dynamic windows for buildings: A review," *Renewable Energy*, vol. 119. Elsevier Ltd, pp. 923–934, Apr. 01, 2018, doi: 10.1016/j.renene.2017.12.049.

[143] A. Shafaghat and A. Keyvanfar, "Dynamic façades design typologies, technologies, measurement techniques, and physical performances across thermal, optical, ventilation, and electricity generation outlooks," 2022, doi: 10.1016/j.rser.2022.112647.

[144] J. Hoon Lee, J. Jeong, and Y. Tae Chae, "Optimal control parameter for electrochromic glazing operation in commercial buildings under different climatic conditions," *Applied*

Energy, vol. 260, p. 114338, Feb. 2020, doi: 10.1016/j.apenergy.2019.114338.

[145] N. Deforest, A. Shehabi, S. Selkowitz, and D. J. Milliron, "A comparative energy analysis of three electrochromic glazing technologies in commercial and residential buildings," 2017, doi: 10.1016/j.apenergy.2017.02.007.

[146] Y. Li, K. W. Shah, W. Li, and T. Xiong, "Experimental investigation on indoor thermal environment improvement and energy-saving of electrochromic window under Singapore's tropical climate," *Journal of Building Engineering*, vol. 73, p. 106779, Aug. 2023, doi: 10.1016/J.JOBE.2023.106779.

[147] W. Lu, "Dynamic Shading and Glazing Technologies: Improve Energy, Visual, and Thermal Performance," *Energy and Built Environment*, vol. 5, no. 2, pp. 211–229, Apr. 2024, doi: 10.1016/J.ENBENV.2022.09.004.

[148] L. Giovannini, F. Favoino, A. Pellegrino, V. R. M. Lo Verso, V. Serra, and M. Zinzi, "Thermochromic glazing performance: From component experimental characterisation to whole building performance evaluation," *Applied Energy*, vol. 251, p. 113335, Oct. 2019, doi: 10.1016/j.apenergy.2019.113335.

[149] A. Ghosh and B. Norton, "Durability of switching behaviour after outdoor exposure for a suspended particle device switchable glazing," *Solar Energy Materials and Solar Cells*, vol. 163, pp. 178–184, Apr. 2017, doi: 10.1016/J.SOLMAT.2017.01.036.

[150] S. Nundy and A. Ghosh, "Thermal and visual comfort analysis of adaptive vacuum integrated switchable suspended particle device window for temperate climate," 2019, doi: 10.1016/j.renene.2019.12.004.

[151] S. Park and J. Who Hong, "Polymer dispersed liquid crystal film for variable-transparency glazing," 2008, doi: 10.1016/j.tsf.2008.11.115.

[152] W. Shen and G. Li, "Recent Progress in Liquid Crystal-Based Smart Windows: Materials, Structures, and Design," *Laser & Photonics Reviews*, vol. 17, no. 1, p. 2200207, Jan.

2023, doi: 10.1002/LPOR.202200207.

[153] A. Piccolo, C. Marino, A. Nucara, and M. Pietrafesa, “Energy performance of an electrochromic switchable glazing: Experimental and computational assessments,” *Energy and Buildings*, vol. 165, pp. 390–398, Apr. 2018, doi: 10.1016/j.enbuild.2017.12.049.

[154] J. Chambers *et al.*, “Evaluating the electricity saving potential of electrochromic glazing for cooling and lighting at the scale of the Swiss non-residential national building stock using a Monte Carlo model,” 2019, doi: 10.1016/j.energy.2019.07.037.

[155] P. F. Tavares, A. R. Gaspar, A. G. Martins, and F. Frontini, “Evaluation of electrochromic windows impact in the energy performance of buildings in Mediterranean climates,” 2013, doi: 10.1016/j.enpol.2013.07.038.

[156] M. E. A. Warwick, I. Ridley, and R. Binions, “Variation of Thermochromic Glazing Systems Transition Temperature, Hysteresis Gradient and Width Effect on Energy Efficiency,” *Buildings 2016, Vol. 6, Page 22*, vol. 6, no. 2, p. 22, Jun. 2016, doi: 10.3390/BUILDINGS6020022.

[157] A. Cannavale, U. Ayr, F. Fiorito, and F. Martellotta, “Smart electrochromic windows to enhance building energy efficiency and visual comfort,” *Energies*, vol. 13, no. 6, 2020, doi: 10.3390/en13061449.

[158] A. Malekafzali Ardakan, E. Sok, and J. Niemasz, “Electrochromic glass vs. fritted glass: An analysis of glare control performance,” in *Energy Procedia*, 2017, vol. 122, pp. 343–348, doi: 10.1016/j.egypro.2017.07.334.

[159] A. Aldawoud, “Conventional fixed shading devices in comparison to an electrochromic glazing system in hot, dry climate,” *Energy and Buildings*, vol. 59, pp. 104–110, 2013, doi: 10.1016/j.enbuild.2012.12.031.

[160] B. Petter Jelle, “Solar radiation glazing factors for window panes, glass structures and electrochromic windows in buildings-Measurement and calculation,” 2013, doi:

10.1016/j.solmat.2013.04.032.

[161] N. G. Ardabili, Y. Feng, and J. Wang, “Design and optimization of thermally responsive autonomous dynamic glazed attachment systems for building solar heat gain control,” 2023, doi: 10.1007/s12273-023-0993-5.

[162] H. Ye, X. Meng, L. Long, and B. Xu, “The route to a perfect window,” *Renewable Energy*, vol. 55, pp. 448–455, Jul. 2013, doi: 10.1016/J.RENENE.2013.01.003.

[163] J. Pu, C. Shen, J. Wang, Y. Zhang, C. Zhang, and S. A. Kalogirou, “Near-infrared absorbing glazing for energy-efficient windows: A critical review and performance assessments from the building requirements,” *Nano Energy*, vol. 110, 2023, doi: 10.1016/j.nanoen.2023.108334.

[164] S. Philip, “eppy.” 2020, [Online]. Available: https://eppy.readthedocs.io/en/latest/readme.html.

[165] J. Pu, C. Shen, S. Yang, C. Zhang, D. Chwieduk, and S. A. Kalogirou, “Feasibility investigation on using silver nanorods in energy saving windows for light/heat decoupling,” *Energy*, vol. 245, p. 123289, Apr. 2022, doi: 10.1016/J.ENERGY.2022.123289.

[166] J. Pu, M. Han, L. Lu, C. Shen, and F. Wang, “Spectrally selective design and energy-saving demonstration of a novel liquid-filled window in hot and humid region,” *Energy*, vol. 297, p. 131090, Jun. 2024, doi: 10.1016/J.ENERGY.2024.131090.

[167] V. Costanzo, G. Evola, and L. Marletta, “Thermal and visual performance of real and theoretical thermochromic glazing solutions for office buildings,” *Solar Energy Materials and Solar Cells*, vol. 149, pp. 110–120, May 2016, doi: 10.1016/j.solmat.2016.01.008.

[168] I. Lahmar, A. Cannavale, F. Martellotta, and N. Zemmouri, “The Impact of Building Orientation and Window-to-Wall Ratio on the Performance of Electrochromic Glazing in Hot Arid Climates: A Parametric Assessment,” *Buildings 2022, Vol. 12, Page 724*, vol.

12, no. 6, p. 724, May 2022, doi: 10.3390/BUILDINGS12060724.

[169] R. Evins, “A review of computational optimisation methods applied to sustainable building design,” *Renewable and Sustainable Energy Reviews*, vol. 22. Pergamon, pp. 230–245, Jun. 01, 2013, doi: 10.1016/j.rser.2013.02.004.

[170] H. Teixeira, M. Glória Gomes, A. Moret Rodrigues, and D. Aelenei, “Assessment of the visual, thermal and energy performance of static vs thermochromic double-glazing under different European climates,” *Building and Environment*, vol. 217, p. 109115, Jun. 2022, doi: 10.1016/J.BUILDENV.2022.109115.

[171] M. Salamati, P. Mathur, G. Kamyabjou, and K. Taghizade, “Daylight performance analysis of TiO2@W-VO2 thermochromic smart glazing in office buildings,” *Building and Environment*, vol. 186, p. 107351, Dec. 2020, doi: 10.1016/J.BUILDENV.2020.107351.

[172] J. Bohórquez-Órdenes, A. Tapia-Calderón, D. A. Vasco, O. Estuardo-Flores, and A. N. Haddad, “Methodology to reduce cooling energy consumption by incorporating PCM envelopes: A case study of a dwelling in Chile,” *Building and Environment*, vol. 206, p. 108373, Dec. 2021, doi: 10.1016/J.BUILDENV.2021.108373.

[173] M. Vanags, K. Lebedeva, A. Snegirjovs, G. Kashkarova, and P. Shipkovs, “Optical Properties of New Type of Glazing Unit Modified by Phase Change Material (Theoretical Approach),” *Latvian Journal of Physics and Technical Sciences*, 2019, doi: 10.2478/lpts-2019-0002.

[174] Z. Fan, M. Liu, and S. Tang, “A multi-objective optimization design method for gymnasium facade shading ratio integrating energy load and daylight comfort,” *Building and Environment*, vol. 207, p. 108527, Jan. 2022, doi: 10.1016/J.BUILDENV.2021.108527.

[175] M. K. Bracht, A. P. Melo, and R. Lamberts, “A metamodel for building information

modeling-building energy modeling integration in early design stage," *Automation in Construction*, vol. 121, p. 103422, Jan. 2021, doi: 10.1016/J.AUTCON.2020.103422.

[176] Chartered Institution of Building Services Engineers, *Energy efficiency in buildings : CIBSE guide F*, Third. London: CIBSE, 2012.

[177] W. Jabi, *Parametric Design for Architecture*. Laurence King Publishing Ltd, 2013.

[178] Autodesk, "Dynamo." 2011.

[179] T. Wortmann, "Efficient, Visual, and Interactive Architectural Design Optimization with Model-based Methods Opossum-Surrogate-based Optimization for Architectural Design View project Informed Design Group View project," 2018, doi: 10.13140/RG.2.2.15380.55685.

[180] C. Wang, S. Lu, H. Chen, Z. Li, and B. Lin, "Effectiveness of one-click feedback of building energy efficiency in supporting early-stage architecture design: An experimental study," *Building and Environment*, vol. 196, p. 107780, Jun. 2021, doi: 10.1016/J.BUILDENV.2021.107780.

[181] M. Perino and V. Serra, "Switching from static to adaptable and dynamic building envelopes: A paradigm shift for the energy efficiency in buildings," *Journal of Facade Design and Engineering*, vol. 3, no. 2, pp. 143–163, Nov. 2015, doi: 10.3233/fde-150039.

[182] D. Aelenei, L. Aelenei, and C. P. Vieira, "Adaptive Façade: Concept, Applications, Research Questions," in *Energy Procedia*, 2016, vol. 91, pp. 269–275, doi: 10.1016/j.egypro.2016.06.218.

[183] J. Li, Q. Duan, E. Zhang, and J. Wang, "Applications of shape memory polymers in kinetic buildings," *Advances in Materials Science and Engineering*, vol. 2018. Hindawi Limited, 2018, doi: 10.1155/2018/7453698.

[184] A. Ghosh and B. Norton, "Advances in switchable and highly insulating autonomous (self-powered) glazing systems for adaptive low energy buildings," *Renewable Energy*,

vol. 126. Elsevier Ltd, pp. 1003–1031, Oct. 01, 2018, doi: 10.1016/j.renene.2018.04.038.

[185] R. A. Kishore, M. V. A. Bianchi, C. Booten, J. Vidal, and R. Jackson, "Enhancing building energy performance by effectively using phase change material and dynamic insulation in walls," *Applied Energy*, vol. 283, p. 116306, Feb. 2021, doi: 10.1016/j.apenergy.2020.116306.

[186] L. Le-Thanh, T. Le-Duc, H. Ngo-Minh, Q. H. Nguyen, and H. Nguyen-Xuan, "Optimal design of an Origami-inspired kinetic façade by balancing composite motion optimization for improving daylight performance and energy efficiency," *Energy*, vol. 219, p. 119557, Mar. 2021, doi: 10.1016/J.ENERGY.2020.119557.

[187] D.-S. Lee, S.-H. Koo, Y.-B. Seong, and J.-H. Jo, "Evaluating Thermal and Lighting Energy Performance of Shading Devices on Kinetic Façades," *Sustainability*, vol. 8, no. 9, p. 883, Sep. 2016, doi: 10.3390/su8090883.

[188] J. Wang and L. Beltran, "A Method of Energy Simulation For Dynamic Building Envelopes," in *ASHRAE and IBPSA-USA SimBuild 2016, Building Performance Modeling Conference*, Aug. 2016, vol. 6, no. 1, pp. 298–303.

[189] C. Kasinalis, R. C. G. M. Loonen, D. Cóstola, and J. L. M. Hensen, "Framework for assessing the performance potential of seasonally adaptable facades using multi-objective optimization," *Energy and Buildings*, vol. 79, pp. 106–113, Aug. 2014, doi: 10.1016/j.enbuild.2014.04.045.

[190] J. J. Wang and L. Beltran, "Energy Performance Of Future Dynamic Building Envelopes," 2016.

[191] T. Pflug, T. E. Kuhn, R. Nörenberg, A. Glück, N. Nestle, and C. Maurer, "Closed translucent façade elements with switchable U-value—A novel option for energy management via the facade," *Energy and Buildings*, vol. 86, pp. 66–73, Jan. 2015, doi: 10.1016/J.ENBUILD.2014.09.082.

[192] S. Wang, Y. Zhou, T. Jiang, R. Yang, G. Tan, and Y. Long, "Thermochromic smart windows with highly regulated radiative cooling and solar transmission," *Nano Energy*, vol. 89, p. 106440, Nov. 2021, doi: 10.1016/j.nanoen.2021.106440.

[193] P. Tavares, H. Bernardo, A. Gaspar, and A. Martins, "Control criteria of electrochromic glasses for energy savings in mediterranean buildings refurbishment," *Solar Energy*, vol. 134, pp. 236–250, Sep. 2016, doi: 10.1016/j.solener.2016.04.022.

[194] J. Mäkitalo, "Simulating control strategies of electrochromic windows : Impacts on indoor climate and energy use in an office building.," 2013.

[195] H. Yan, K. Yan, and G. Ji, "Optimization and prediction in the early design stage of office buildings using genetic and XGBoost algorithms," *Building and Environment*, vol. 218, p. 109081, Jun. 2022, doi: 10.1016/J.BUILDENV.2022.109081.

[196] G. Z. Brown and M. DeKay, *Sun, Wind & Light: Architectural Design Strategies*, 2nd ed. New York: John Wiley & Sons, 2001.

[197] V. Granadeiro, J. P. Duarte, J. R. Correia, and V. M. S. Leal, "Building envelope shape design in early stages of the design process: Integrating architectural design systems and energy simulation," *Automation in Construction*, vol. 32, pp. 196–209, Jul. 2013, doi: 10.1016/j.autcon.2012.12.003.

[198] P. Depecker, C. Menezo, J. Virgone, and S. Lepers, "Design of buildings shape and energetic consumption," *Building and Environment*, vol. 36, no. 5, pp. 627–635, Jun. 2001, doi: 10.1016/S0360-1323(00)00044-5.

[199] NREL, "EnergyPlus." U.S. Department of Energy.

[200] I. Korolija, L. Marjanovic-Halburd, Y. Zhang, and V. I. Hanby, "UK office buildings archetypal model as methodological approach in development of regression models for predicting building energy consumption from heating and cooling demands," *Energy and Buildings*, vol. 60, pp. 152–162, May 2013, doi: 10.1016/j.enbuild.2012.12.032.

[201] “Lake Trust Credit Union Headquarters | SmithGroup.” https://www.smithgroup.com/projects/lake-trust-credit-union-headquarters.

[202] “Construction on GrayStreet’s Broadway tower estimated to begin Feb. 1 - San Antonio Heron.” https://saheron.com/construction-on-graystreets-broadway-tower-estimated-to-begin-feb-1/.

[203] T. Logan, “Elk.” Feb. 01, 2016, Accessed: Jun. 21, 2021. [Online]. Available: https://www.food4rhino.com/en/app/elk.

[204] M. J. D. Powell, “A Direct Search Optimization Method That Models the Objective and Constraint Functions by Linear Interpolation,” in *Advances in Optimization and Numerical Analysis*, Springer Netherlands, 1994, pp. 51–67.

[205] “NLopt Algorithms.” NLopt.

[206] C. Reinhart and V. LoVerso, “A rules of thumb-based design sequence for diffuse daylight,” *Lighting Research & Technology*, vol. 42, no. 1, pp. 7–31, Mar. 2010, doi: 10.1177/1477153509104765.

[207] D. DiLaura, K. Houser, R. Mistrick, and G. Steffy, *The IES Lighting Handbook*, Tenth. Illuminating Engineering Society, 2011.

[208] B. L. Ahn, C. Y. Jang, S. B. Leigh, S. Yoo, and H. Jeong, “Effect of LED lighting on the cooling and heating loads in office buildings,” *Applied Energy*, vol. 113, pp. 1484–1489, Jan. 2014, doi: 10.1016/j.apenergy.2013.08.050.

[209] J. C. Lam, K. K. W. Wan, D. Liu, and C. L. Tsang, “Multiple regression models for energy use in air-conditioned office buildings in different climates,” *Energy Conversion and Management*, vol. 51, no. 12, pp. 2692–2697, Dec. 2010, doi: 10.1016/j.enconman.2010.06.004.

[210] F. Kheiri, “A review on optimization methods applied in energy-efficient building geometry and envelope design,” *Renewable and Sustainable Energy Reviews*, vol. 92.

Elsevier Ltd, pp. 897–920, Sep. 01, 2018, doi: 10.1016/j.rser.2018.04.080.

[211] T. Wortmann, “Model-based Optimization for Architectural Design: Optimizing Daylight and Glare in Grasshopper,” *Technology|Architecture + Design*, vol. 1, no. 2, pp. 176–185, Nov. 2017, doi: 10.1080/24751448.2017.1354615.

[212] M. Krarti, “Energy performance of control strategies for smart glazed windows applied to office buildings,” *Journal of Building Engineering*, vol. 45, pp. 2352–7102, 2022, doi: 10.1016/j.jobe.2021.103462.

VITA

LAURA HINKLE

EDUCATION

Doctor of Philosophy in Architectural Engineering 2024
Pennsylvania State University, University Park, PA
Dissertation: Flexible, data-driven parametric design for building façades
Co-advisors: Nathan Brown and Julian Wang

Master of Architectural Engineering 2020
Pennsylvania State University, University Park, PA

Bachelor of Architectural Engineering 2020
Pennsylvania State University, University Park, PA

PUBLICATIONS

PEER-REVIEWED JOURNAL ARTICLES

- **L. E. Hinkle**, G. Pavlak, L. Curtis, and N. C. Brown, "Implementing dynamic subset sensitivity analysis for early design datasets," *Automation in Construction*, vol. 158, 2024, doi: 10.1016/j.autcon.2023.105198.
- **L. E. Hinkle**, J. Wang, and N. C. Brown, "Quantifying potential dynamic façade energy savings in early design using constrained optimization," *Building and Environment*, vol. 221, Aug. 2022, doi: 10.1016/J.BUILDENV.2022.109265.
- Q. Duan, **L. Hinkle**, J. Wang, E. Zhang, and A. Memari, "Condensation effects on energy performance of building window systems," *Energy Reports*, vol. 7, pp. 7345–7357, Nov. 2021, doi: 10.1016/j.egyr.2021.10.096.
- X. Liu, H. Yang, C. Wang, C. Shen, R. Bo, **L. Hinkle**, J. Wang, Semi-experimental investigation on the energy performance of photovoltaic double skin façade with different façade materials, *Energy*. 295 (2024) 131049. https://doi.org/10.1016/J.ENERGY.2024.131049.